World Spine Day 2019

16th October

Videos online
OOT OPEN OPERATING THEATRE

Posterior foraminotomy for lateral cervical disc herniation

Thoracoscopic technique of anterior discectomy and interbody fusion (ATIF)

Surgical correction in AIS

Access the online contents and videos:

http://collections.medengine.com/orthopedics/world-spine-day/

Springer Healthcare Education

Pfizer Limited: The Capital – A Wing 1802, 18th Floor, Plot No. C-70, G-Block, Bandra – Kurla Complex, Bandra (East), Mumbai - 400051.

For the use only of a Registered Medical Practitioner or a Hospital or a Laboratory.

World Spine Day 2019

Springer Healthcare Education

October 2019

Springer Healthcare

This edition is published by Springer Nature India Private Limited.
Registered Office: 7th Floor, Vijaya Building, 17, Barakhamba Road, New Delhi 110 001, India.
T: +91 (0) 11 4575 5888
www.springerhealthcare.com

Part of the Springer Nature group

Contents

Case Reports

1. **Traumatic posterior atlantoaxial dislocation with associated C1 Jefferson fracture and bilateral vertebral artery occlusion without odontoid process fracture or neurological deficit 1**
   Mark Nowell, Richard Nelson

2. **Revision strategy and follow-up for implant failure in a case of combined anterior and posterior reconstruction after three-level en bloc vertebral body replacement and replacement of the aorta for chondrosarcoma of the thoracic spine 5**
   T. Graulich, C. Krettek, C. W. Müller

3. **Designing patient-specific solutions using biomodelling and 3D-printing for revision lumbar spine surgery 10**
   Ganesha K. Thayaparan, Mark G. Owbridge, Robert G. Thompson, Paul S. D'Urso

4. **Huge myxoid chondrosarcoma expanded into the thoracic cavity with spinal involvement 17**
   Ming Lu, Zhongxin Zhou, Zixiong Lei, Haomiao Li, Stefano Boriani

5. **Rescue Nuss procedure for inferior vena cava compression syndrome following posterior scoliosis surgery in Marfan syndrome 23**
   M. Löhnhardt, A. Hättich, A. Andresen, *et al.*

6. **Posterior atlantoaxial dislocation without fracture or neurological symptoms treated by transoral–posterior approach surgery: a case report and literature review 29**
   Shenghua Ning, Sidong Yang, Wenyuan Ding, Tianxiao Ma, Zhanyong Wu

7. **Lung metastases regression with increased CD8+ T lymphocyte infiltration following preoperative spinal embolization and total en bloc spondylectomy using tumor-bearing frozen autograft in a patient with spinal metastatic leiomyosarcoma 33**
   Noritaka Yonezawa, Hideki Murakami, Apiruk Sangsin, Eishiro Mizukoshi, Hiroyuki Tsuchiya

8. **Neurological impairment in a patient with concurrent cervical disc herniation and POEMS syndrome 43**
   Tingxian Ling, Limin Liu, Yueming Song, Shilian Zhou, Chunguang Zhou

9. A novel fixation technique using anterior C1 screw in a pediatric solitary cervical spinal juvenile xanthogranuloma **48**
Rekhapalli Rajasekhar, Madhivanan Karthigeyan, Pravin Salunke, Kirti Gupta

10. Chylous fistula: management of a rare complication following right anterior cervical spine approach **53**
Federica Novegno, Pierluigi Granaroli, Luigi Ciccoritti, Pierpaolo Lunardi, Mario Francesco Fraioli

11. Delayed presentation of infected common iliac artery pseudoaneurysm caused by malpositioned pedicle screw after minimally invasive scoliosis surgery **60**
Seung-Woo Suh, Gang-Un Kim, Hoon-Nyun Lee, Jae Hyuk Yang, Dong-Gune Chang

Open Operating Theatre (OOT)

12. Posterior foraminotomy for lateral cervical disc herniation **65**
C. Mehren, L. Wanke-Jellinek

13. Thoracoscopic technique of anterior discectomy and interbody fusion (ATIF) **67**
Daniel Sauer, Franziska C. Heider, Christoph Mehren, Christoph J. Siepe

14. Surgical correction in AIS **70**
Cesare Faldini, Fabrizio Perna, Alberto Ruffilli, *et al.*

Step by step procedure for online viewing:

1. Go to http://collections.medengine.com/orthopedics/world-spine-day/ or scan QR code.
2. Web page of the issue will open on the screen.
3. View and read the PDF version and watch the videos online.
4. The PDF file can be downloaded too for offline reading.

European Spine Journal (2019) 28 (Suppl 2):S9–S12
https://doi.org/10.1007/s00586-018-5678-x

CASE REPORT

Traumatic posterior atlantoaxial dislocation with associated C1 Jefferson fracture and bilateral vertebral artery occlusion without odontoid process fracture or neurological deficit

Mark Nowell[1] · **Richard Nelson**[1]

Received: 28 November 2017 / Revised: 19 June 2018 / Accepted: 20 June 2018 / Published online: 2 July 2018

Abstract

Purpose Traumatic atlantoaxial dislocation (AAD) is usually associated with fatal high-velocity road traffic accidents (Xu et al. in Medicine (Baltimore) 94:e1768, 2015). There are few reports of survival following posterior AAD without odontoid fracture (Xu et al. 2015; Zhen et al. in Arch Orthop Trauma Surg 131:681–685, 2011; de Carvalho and Swash in Handb Clin Neurol 119:435–448, 2014).

Method We present a previously undescribed case of posterior AAD associated with a C1 Jefferson fracture but no odontoid fracture and bilateral vertebral artery occlusion without neurological deficit.

Conclusion The presence of bilateral vertebral artery occlusion raised challenges in the surgical management. Survival was only possible due to the presence of robust cerebral collateral circulation.

Keywords Posterior atlantoaxial dislocation · C1 Jefferson fracture · Vertebral artery occlusion

Case report

A 71-year helmeted horse rider was admitted to the emergency department having been struck by a car and thrown to the ground, sustaining an axial compression and hyperextension injury of the spine. There was no loss of consciousness. He was able to stand following the impact, but complained of neck pain and a transitory sensory disturbance affecting the right upper and lower limbs and left upper limb. There was no reported weakness. He was immobilised at the scene with full spinal precautions by paramedics. Apart from mild rheumatoid arthritis, he was previously fit and well.

His primary advanced trauma and life support (ATLS) survey revealed high cervical spine tenderness with no bruising or palpable deformity. Neurological examination was normal. Secondary survey revealed tenderness in the mid thoracic spine and facial abrasions.

A CT trauma study as per the major trauma centre protocol demonstrated a fracture of the anterior arch of C1 with anterior displacement of the intact odontoid process ventral to the ring and associated soft tissue swelling to the upper cervical spine. There were bilateral displaced fractures of the posterior arch of C1 (Fig. 1). There was a T3 compression fracture with no disruption of the posterior elements. There was no significant injury to the head, chest, abdomen or pelvis.

The patient was admitted to the intensive care unit for close monitoring. After 4 h, he deteriorated with upper airway obstruction due to retropharyngeal soft tissue swelling necessitating intubation and ventilation. The next day an MRI/MRA study demonstrated normal craniocervical alignment, which was attributed to spontaneous reduction under general anaesthesia, with no evidence of cord compression. There were signs of cord signal change and significant ligamentous injury associated with bilateral VAO at the level of C2 with retrograde filling of the vertebro-basilar circulation via posterior communicating arteries (Fig. 2).

The following day an instrumented C1–2 stabilisation was undertaken using C1 lateral mass screws, C2 pedicle screws and intraarticular autologous bone grafting. After prone positioning, lateral fluoroscopy confirmed spontaneous reduction in the AAD so that exploration of the vertebral arteries was considered unnecessary.

✉ Mark Nowell
mnowell@gmail.com

[1] Department of Neurosurgery, Southmead Hospital, Bristol, UK

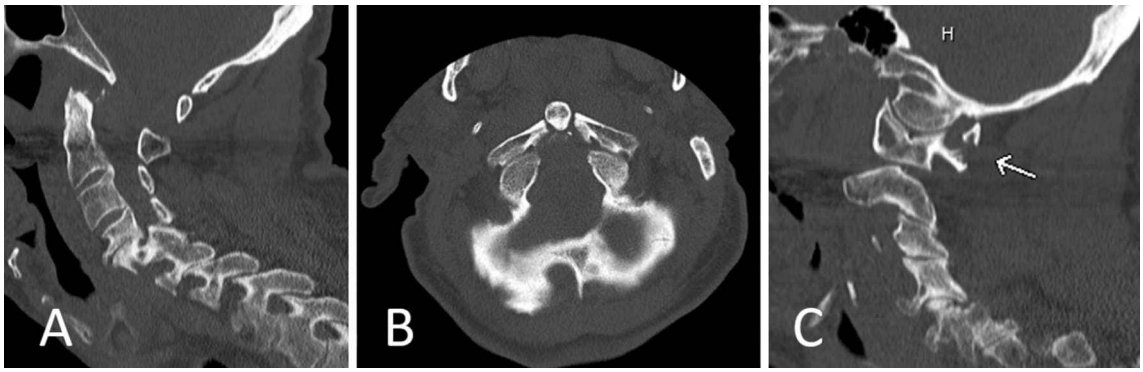

Fig. 1 CT Cervical spine, mid-sagittal (**a**), axial (**b**) and parasagittal (**c**). The intact odontoid process has displaced through the anterior arch of atlas. There is posterior displacement of C1 on C2, consistent with a type IV atlantoaxial subluxation. There is also a fracture to the posterior ring of the atlas

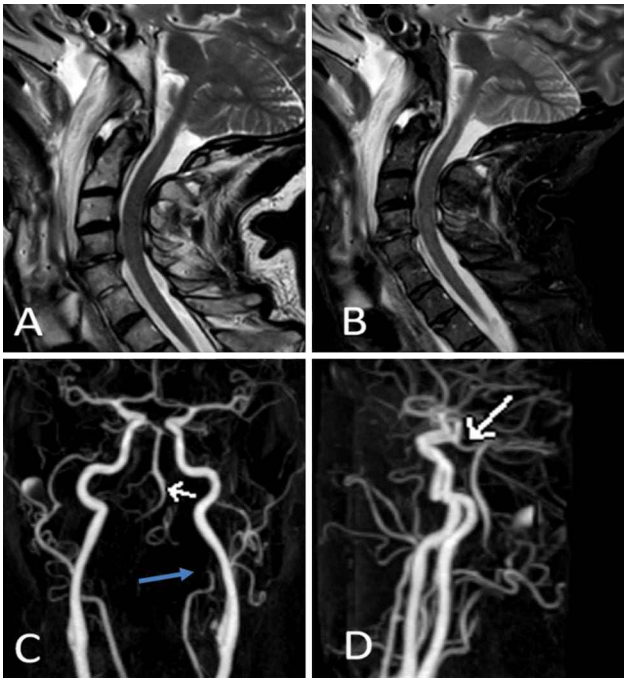

Fig. 2 MRI cervical spine, mid-sagittal T2 weighted (**a**), mid-sagittal short tau inversion recovery (STIR) (**b**), anteroposterior view of 3D MR angiography (**c**), and lateral view of 3D MR angiography (**d**). There has been spontaneous reduction in the atlantoaxial dislocation. There is high signal within the cervical spinal cord as it passes posterior to the odontoid process and through the foramen magnum extending as far as C7, in keeping with contusion. There is no ongoing spinal cord compression. In (**c**) there is bilateral occlusion of the vertebral arteries at the level of C2 (blue arrow) with retrograde filling of the basilar and posterior inferior cerebellar arteries (white arrow). In (**d**) there is good collateral circulation via robust posterior communicating arteries (white arrow)

The patient made an uncomplicated recovery from the operation. Post-operative CT scanning confirmed good craniocervical alignment with satisfactory instrumentation (Fig. 3). He was commenced on 75 mg aspirin for 3 months to reduce the risk of a posterior circulation thromboembolic event. He was mobilised wearing a suboccipito-mental collar.

The patient's post-operative course was complicated by dysphagia, caused by the soft tissue swelling, vagal neuropraxia and muscular deconditioning. This improved with regular speech and language therapy. He suffered two transient episodes of sudden onset dysarthria, with no associated weakness or dysphasia. MRI head showed no evidence of cerebral infarction. A diagnosis of transient ischaemia was made, and he was commenced on 75 mg once a day clopidogrel for 3 months.

Discussion

There are several unusual features of this case including the injury pattern, the associated vascular injury with no neurological deficit and the surgical strategy to restore alignment and stability and avoid thromboembolic events.

Injury pattern

AAD is an uncommon but clinically important condition due to the severity of neurological deficits [1, 2]. The stability of the atlantoaxial complex is provided by the articular processes of C1 and C2, and the osteoligamentous ring that encircles the odontoid process. Conditions that predispose to AAD by weakening these structures include Downs syndrome, rheumatoid arthritis, Paget's disease and other metabolic bone disorders [3].

Traumatic AAD is usually a result of distraction injuries with superimposed hyperflexion or hyperextension. The typical pattern is anterior displacement of the atlas on the intact axis, with or without fracture to the process depending on integrity of the transverse ligament. There are 19 reported cases in the literature of posterior traumatic AAD without

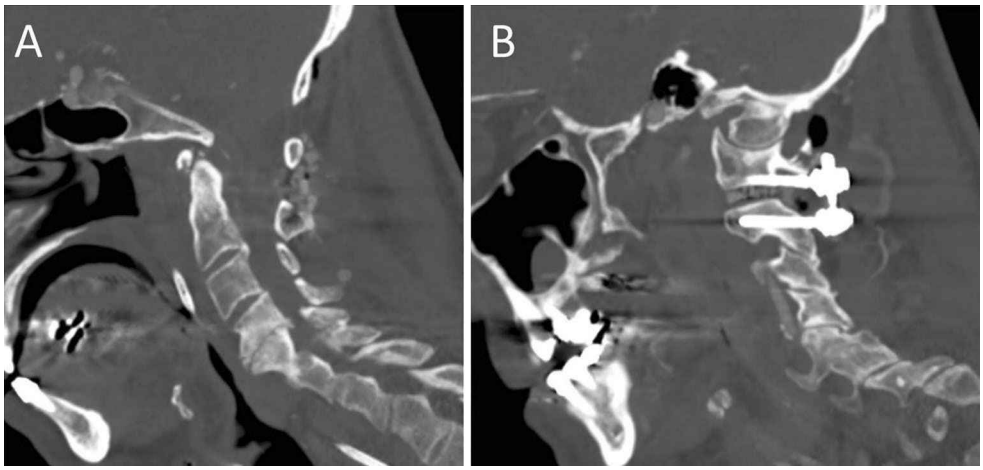

Fig. 3 Post-operative CT cervical spine, mid-sagittal (**a**) and lateral sagittal (**b**). There is reduction in the posterior atlantoaxial dislocation, with lateral mass screws to C1 and pedicle screws to C2. There is autologous bone grafting to the interfacet space

odontoid process fracture [4]. These have typically been the result of distraction hyperextension injuries with associated facial injuries and are not associated with significant neurological deficit. It is postulated that posterior ADD without odontoid fracture may be more common but normally leads to immediate death. In cases that do survive, there is little or no damage to the spinal cord, as the remaining ligamentous structures lock the axis and prevent further displacement, reducing the spinal canal area to approximately 36% [5].

In this case, we speculate the background inflammatory condition predisposed to weakening of the C1 arch and apical and alar ligaments, with relative preservation of the integrity of the odontoid process and transverse ligament. Thus, the craniocervical junction was particularly susceptible to an axial loading and hyperextension injury, generating this atypical form of posterior AAD comprising anterior C1 arch and Jefferson fractures. To our knowledge, this is the first report of this unusual injury pattern.

Associated vascular injury with no neurological deficit

VAO is a rare complication of blunt trauma to the craniocervical junction. It has also been observed following chiropractic manoeuvres [6, 7] and cervical spine surgery. VAO may result in immediate ischaemia and also lead to thromboembolic events causing posterior circulation and spinal cord infarction of varying severity. The prevalence of asymptomatic VAO and clinical sequelae following VAO are not known. Risk factors for ischaemic stroke in the presence of VAO include increasing age and bilateral VAO. Corrective cervical spine surgery potentially decreases the risk by reducing motion across the occluded segments [8].

There is a case report of a patient sustaining a traumatic AAD with associated bilateral VAO and carotid artery injuries [9]. This patient had a type IIA traumatic spondylolisthesis at C2 and C1/2 distraction. The vascular injury was managed by anticoagulation 48 h after surgical treatment. The patient made a reasonable neurological recovery.

In our case the patient remained neurologically intact due to the presence of robust collateral circulation via the posterior communicating arteries. Without this, the injury would have been fatal. Acute post-traumatic VAO presents an ongoing risk of thromboembolic stroke. Antiplatelet treatment and/or anticoagulation following surgery is advocated, but the duration of medical treatment and the role of follow-up vascular imaging are controversial. Our patient has been followed up for a year and remains well with no further episodes of dysarthria.

Surgical strategy

Most cases of posterior AAD have successfully been managed with closed reduction, although it is technically challenging to relocate the odontoid process back into osteoligamentous ring. On-table fluoroscopy, with spinal cord monitoring if the patient is under a general anaesthesia, is recommended. The procedure is terminated if there are any signs of spinal cord compromise due to over-distraction. Of the 19 previously described cases, successful closed reduction was followed by internal fixation in five patients and conservative management in 6. The remaining eight patients were treated by open reduction and internal fixation, including 4 that developed neurological deficits during attempts at closed reduction [4]. Most cases were stabilised posteriorly with wiring, transarticular screw fixation or lateral mass and pedicle screw fixation. Anterior approaches include transoral

odontoidectomy and the anterior retropharyngeal approach. They have the advantage of avoiding prone position and the possibility of further craniocervical displacement [10].

In this case, we initially considered that early operative reduction in the posterior AAD would be associated with a high risk of vertebral reperfusion and distal thromboembolism. Our intended strategy was to isolate and temporarily clip the vertebral arteries before reducing the fracture. Spontaneous reduction in the AAD under general anaesthesia preoperatively made this unnecessary. At operation, the vertebral arteries were insonated with a microvascular Doppler to confirm persisting occlusion. A standard posterior C1–C2 fusion was preferred over an occipito-cervical fixation as there was normal occipital-C1 articulation.

Conclusion

We describe a case of traumatic posterior AAD with associated Jefferson fracture and bilateral VAO without odontoid process fracture or neurological deficit. This variation of AAD has not previously been reported in the literature. We postulate that this injury pattern would usually be fatal and our patient survived due to excellent collateral circulation. Challenges to management include surgical approach and timing, and management of the associated vascular injury.

Compliance with ethical standards

Conflict of interest None of the authors has any potential conflict of interest.

Informed consent Informed consent was obtained from all individual participants in this case report.

References

1. Xu Y, Li F, Guan H, Xiong W (2015) Traumatic posterior atlantoaxial dislocation without associated fracture but with neurological deficit: a case report and literature review. Medicine (Baltimore) 94:e1768
2. Zhen P, Lan X, Yang LW (2011) Traumatic posterior atlantoaxial dislocation without associated fracture and neurological deficit. Arch Orthop Trauma Surg 131:681–685
3. de Carvalho M, Swash M (2014) Neurologic complications of craniovertebral dislocation. Handb Clin Neurol 119:435–448
4. Hu D, Yang X, Wang J (2015) Traumatic posterior atlantoaxial dislocation without fracture of odontoid process: a case report and systematic analysis of 19 cases. J Orthop Trauma 29:e342–e345
5. Tucker SK, Taylor BA (1998) Spinal canal capacity in simulated displacements of the atlantoaxial segment: a skeletal study. J Bone Joint Surg Br 80:1073–1078
6. Ke JQ, Yin B, Fu FW, Shao SM, Lin Y, Dong QQ et al (2016) A case report of locked-in syndrome due to bilateral vertebral artery dissection after cervical spine manipulation treated by arterial embolectomy. Medicine (Baltimore) 95:e2693
7. Preul C, Joachimski F, Witte OW, Isenmann S (2010) Bilateral vertebral artery dissection after chiropractic maneuver. Clin Neuroradiol 20:255–259
8. Foreman PM, Griessenauer CJ, Chua M, Hadley MN, Harrigan MR (2015) Corrective spinal surgery may be protective against stroke in patients with blunt traumatic vertebral artery occlusion. J Neurosurg Spine. https://doi.org/10.3171/2015.1.SPINE141174
9. Leach JC, Malham GM (2009) Complete recovery following atlantoaxial fracture-dislocation with bilateral carotid and vertebral artery injury. Br J Neurosurg 23:92–94
10. Jiang LS, Shen L, Wang W, Wu H, Dai LY (2010) Posterior atlantoaxial dislocation without fracture and neurologic deficit: a case report and the review of literature. Eur Spine J 19(Suppl 2):S118–S123

European Spine Journal (2019) 28 (Suppl 2):S13–S17
https://doi.org/10.1007/s00586-018-5682-1

CASE REPORT

Revision strategy and follow-up for implant failure in a case of combined anterior and posterior reconstruction after three-level en bloc vertebral body replacement and replacement of the aorta for chondrosarcoma of the thoracic spine

T. Graulich[1] · C. Krettek[1] · C. W. Müller[1]

Received: 17 November 2017 / Revised: 20 March 2018 / Accepted: 24 June 2018 / Published online: 28 June 2018

Abstract

Objective In 2013, we reported a case of combined anterior and posterior reconstruction after three-level en bloc vertebral body replacement and replacement of the aorta for chondrosarcoma of the thoracic spine. Eight years after, we observed an implant failure and now report on revision strategy and 2-year follow-up (f/u) after revision.

Methods We report about the 2-year f/u of the same now 51-year-old gravedigger who needed to undergo revision surgery after implant failure. We did a combined anterior and posterior correction vertebral interbody fusion by (1) removal of broken screws in Th9 and L2, removal of broken titanium bars, correction of kyphosis, enhancement of the vertebral interbody fusion from Th8 to L4 using monoaxial titanium screws and cancellous bone transplantation and (2) removal of the broken plate and the loose cage, implantation of a novel expandable PEEK cage from Th11 to L1 and anterior stabilization from Th9/10 to L2/3, as well as autologous and allogeneic cancellous bone transplantation.

Results Two years after revision surgery, the patient presented fully reintegrated without any complains. No painkillers needed to be taken. Pain was reported with 2 out of 10 on the VAS.

Conclusion Both procedures offer a good primary stabilization with excellent pain reduction and good return to life. Limited information on long-term survivors is known. Therefore, the theoretical advantage of a biological solution needs to be checked in the long-term f/u for consistency.

Keywords Correction vertebral interbody fusion · Three-level en bloc vertebral body replacement · Chondrosarcoma · Spine

Introduction

Multilevel vertebral body replacement and vertebral interbody fusion were first described by Stener in 1971 and became a well-established technique which, however, remains a rare situation with very limited indications [9, 11, 13, 15, 19, 21]. The common principle is a posterior vertebral interbody fusion with tension band and anterior cage interposition for load transmission [11]. We recently reported the first case of a 51-year-old gravedigger who underwent three-level en bloc vertebral body replacement with combined replacement of the aorta after chondrosarcoma (G2, R0) in 2007 [9]. We performed constant at least yearly f/u during which the patient showed himself fully reintegrated to daily life. Between 2014 and 2015, a successive screw pullout and implant failure was observed, and we therefore saw the indication for revision surgery. We now want to report about the 2-year f/u with special emphasis on the different vertebral interbody fusion procedure.

Case

This case is a 9-year f/u after initial wide en bloc resection of Th11 to L1 with partial replacement of the aorta, cage interposition, cement augmentation and anterior–posterior stabilization and 2 years after revision surgery with

✉ T. Graulich
graulich.tilman@mh-hannover.de

[1] Trauma Department, Hannover Medical School, Carl-Neuberg-Str. 1, 30625 Hannover, Germany

two-stage anterior–posterior correction vertebral interbody fusion by (1) posterior removal of broken screws in Th9 and L2, removal of broken titanium bars, correction of kyphosis, enlargement of the vertebral interbody fusion from Th8 to L4 with monoaxial titan screws and cancellous bone transplantation and (2) anterior removal of the broken plate and the loosened cage, implantation of an expandable PEEK cage from Th11 to L1 and anterior stabilization from Th9/10 to L2/3 as well as autologous and allogeneic cancellous bone transplantation (Figs. 1, 2, 3, 4).

Initially after 1-year back pain, MRI showed a histologically confirmed chondrosarcoma (G2) surrounding the Th11 to L1 vertebral bodies which embraced more than 50% of the aorta. The tumor was classified as Tomita type 6, and en bloc resection was performed [7, 9, 21].

Postoperatively local radiation with 54 grays of Th9 to L2 was performed. Nearly half a year after operation, the patient could start rehabilitation and was fully reintegrated. Eight years after the operation, we observed a successive screw pullout and implant failure and we therefore saw the indication for revision surgery (Fig. 2). Operation time was (1) 301 min and (2) 598 min, and intraoperative blood transfusion was 0 ml and 1370 ml (5 EK), respectively. Total time in hospital was 22 days with 1 day on the ICU after the posterior stabilization and 2 days after the anterior stabilization. The patient could be discharged without neurovascular deficit and only limited pain on the visual analogous scale (VAS) 2/10.

Two years after revision surgery, the patient presented fully reintegrated without any complains (Fig. 5). No painkillers needed to be taken. Pain was reported with 2 out of 10 on the VAS. He reported free walking distance. The patient reported that he is able to work as a gravedigger and regularly carries coffins although we insistently urged him to avoid heavy weight carrying. Neurological evaluation showed no neurovascular deficit with full power for both lower extremities. F/u CT scan of the thoracolumbar spine showed no hint for implant failure (Fig. 3). The preoperative kyphosis was corrected as shown in Fig. 6.

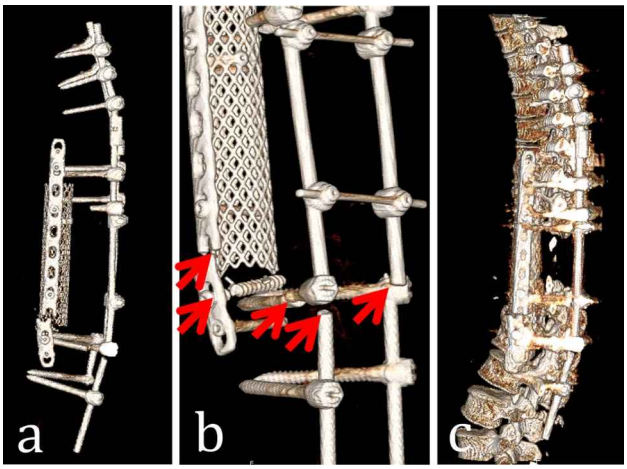

Fig. 2 F/u 04/2015 3D CT scan of the spine. A situation after anterior–posterior stabilization during the 2015 control. The patient has back pain. Red arrows: indicating the location of implant failure, **a** lateral few on the 3D spin. Only the implants are shown. Distal screws, bars and the plate are broken, **b** detailed few in the implant failure, the distal part is fully separated from the proximal part, and **c** implants are shown in relation to the spine

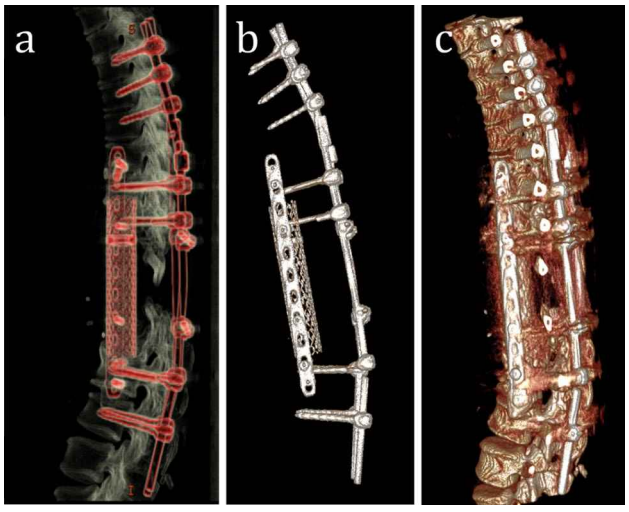

Fig. 1 F/u 02/2015 3D CT scan of the spine. A situation after anterior–posterior stabilization during the 2015 control. The patient has no complains. **a** Lateral few on the 3D spin with implants in slight red: **b** only the implants are reformatted, and **c** implants are well integrated. No hint for implant failure. No fracture

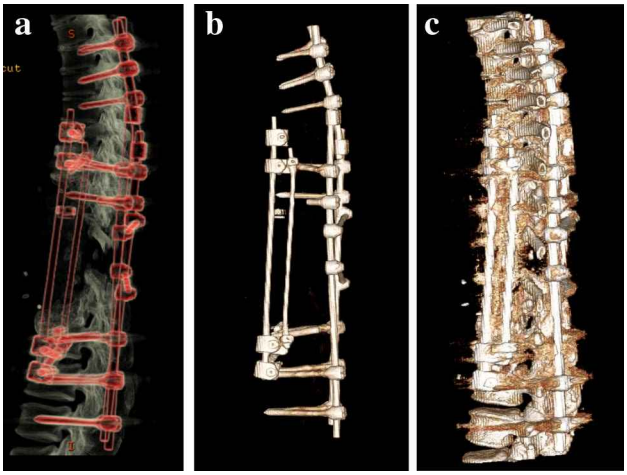

Fig. 3 F/u 05/2016 3D CT scan of the spine. A situation 1 year after anterior–posterior revision surgery in 2015. **a** Overview of the situs during the anterior: **b** only the implants are reformatted, and **c** implants are well integrated. No hint for implant failure. No fracture

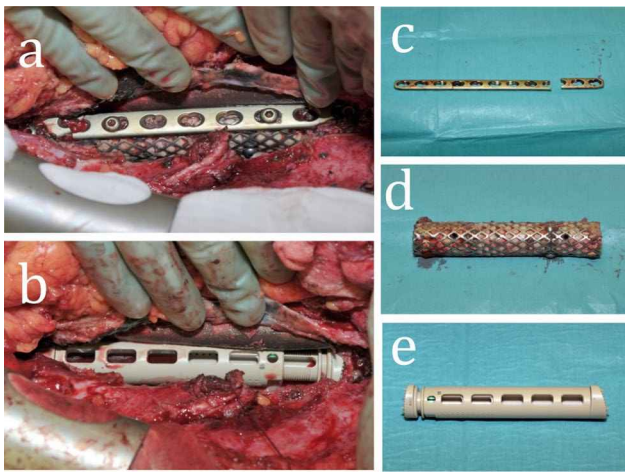

Fig. 4 Intraoperative documentation of revision surgery in 2015 with posterior correction vertebral interbody fusion, anterior replacement of the titanium cage and insertion of the PEEK cage. **a** Situs with broken anterior bar and loosened cage before removal, **b** detailed look at the PEEK cage in situ, **c** close-up on the broken plate, **d** removed cage, **e** PEEK cage

Discussion

We would like to discuss the following two aspects. First, the tumor expansion determines the type of resection and is strongly associated with the long-term outcome. In this case, en bloc resection was performed which was a hazardous procedure but was necessary to be curative according to the long-term survival [2, 4, 5, 11, 13–15].

However, limited experience on reconstruction techniques in long-term-survivors is known. Therefore, secondly, we would like to discuss the stabilization as in this case two different procedures have been used with failure of the initial surgery. Both in common is the anterior–posterior procedure and the combination of a posterior tension wiring like stabilization as well as the anterior space-filling load-holding column. In this case, the mechanical axis could be restored and the thoracolumbar angle (Th10-L2) as a parameter of the kyphosis was corrected from 22° before the first operation and 19° before the second operation, respectively, to 12° and 2° after the first and second operation, respectively. The pelvic incidence is a fundamental parameter for regulation of spinal sagittal curve. It equals the sum of pelvic tilt and sacral slope and is a constant individual parameter with a mean of 53 ± 10 in adult men [3]. The lordosis is largely related to the orientation of the pelvis expressed by the sacral slope with a mean of 41 ± 8 in adult men.

As the anterior fusion limits the overall result, with high nonunion rates up to 70% even after single-level anterior lumbar interbody fusion, we reconsidered the anterior fusion strategy after implant failure [1, 16, 20], whereas during the first operation, a cement augmented rigid cage was used, and during the second operation, an expandable PEEK cage with autologous and allogeneic cancellous bone transplantation was used. The major difference between both procedures was the time, following radiation and the resulting bone quality. After the first operation, an adjuvant radiation was planed. As radiation leads to loss of bone mass, a high risk of secondary loosening was anticipated and tried to be avoided. Therefore, we used a rigid cage with cement augmentation, which gives high primary stability. We added an anterior plate to give further stabilization [5, 10]. A biological situation would have been highly questionable, as during the radiation healing would have been prolonged or even impossible. The danger of an enlarged stress shielding at the bone implant interface by a too rigid fixation was accepted to reduce the risk of an early implant failure by screw cutout as a result of the osteoporotic bone. At the time of the revision surgery, we expected good, healthy, not osteoporotic bone which enabled us to use an expandable PEEK cage which is closer to the normal oscillation behavior of the spine and added cancellous bone for a biological reconstruction [5, 8]. An adequate solution between rigidity and stability needed

Fig. 5 Clinical F/u in 2016. The patient has no complains and only little pain VAS 2/10. **a–c** Inspection of the chest and abdomen with completely healed scars. Straight alignment of the spine

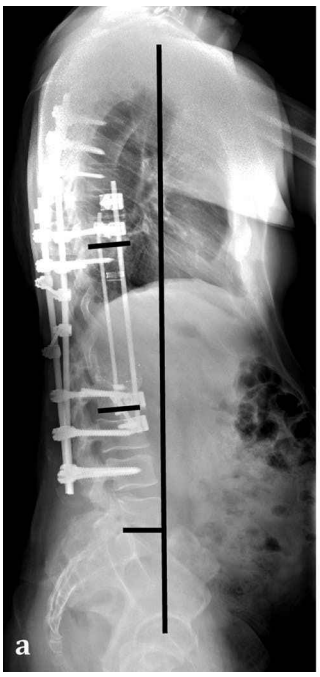

Time	PI [°]	SS [°]	PT [°]	C7Lot-S1 Distance [cm]	TLA [°]
Pre OP I	44	37	7	8.8	22
Post OP I	*51*	*40*	*11*	*3.6*	*12.6*
Pre OP II	43	41	2	3.3	19
One Year F/up	*56*	*42*	*14*	*5.0*	*2*

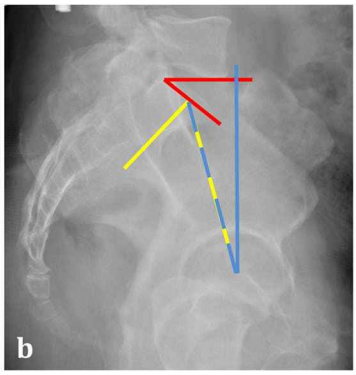

Fig. 6 One year postoperatively after revision surgery: **a** sagittal image with the C7 lot and the distance from the posterior edge of S1 to the lot with 5 cm indicating compensated imbalance. The thoracolumbar angle (TLA) with 2° is within the normal range. **b** Showing in red the sacral slope (SS), in yellow the pelvic incidence (PI) and in blue the pelvic tilt (PT), all values are within normal range. The table shows the measurements of the f/up with each time preoperative decompensation, with enlarged TLA, and reduced PI. After the initial surgery and, respectively, after the revision surgery, both the TLA and the PI were corrected

to be found as initial rigidity enlarges stress shielding at the bone implant interface [5]. As the PEEK cage has a higher primary, better adaptable stability, there was no need for the anterolateral plate [5, 6]. During the initial operation due to the anticipated loss of bone mass, it was important to get further stabilization by the anterior plate. Although over the time and additional regain of bone mass to a stable fixation certainly led to an implant failure due to the not physiological oscillation behavior [8, 10]. Therefore, we decided to use a more elastic anterior wire-stabilization system, which was additionally necessary as only a four-point anterior stabilization results in sufficient stability [5, 18]. An initially advantage in case of stress shielding by a strong fixation in the osteoporotic bone is accompanied by a higher risk of stress shielding and implant failure in the healthy bone [5]. Finally, the enlargement of the posterior fixation defines and increases the primary stabilization and is furthermore the tool for an adequate kyphosis correction [5].

However, according to Pumberger et al., osseous integration even in biological reconstructions was not observed in any of the patients after anterior fusion of multilevel vertebral body replacement. They could show that after biological reconstruction of the load-bearing anterior column in the PET-CT control, no spinal fusion could be seen. The general problem of multilevel en bloc vertebral body replacement and stabilization is, however, the anterior spinal fusion [17]. As the initial strategy was certainly non-biological without any chance of anterior fusion, our aim during revision surgery was the anterior fusion and mechanical stable reconstruction. Alternative reconstruction options like fibula or rib autografts from rather small case series show only limited and very heterogeneous results [12, 22].

The situation described by Pumberger et al. is different to our revision surgery. They discuss that in all their cases a postoperative radiation or chemotherapy reduced the osseous integration as we expected before initial surgery. We nevertheless did expect a normal healthy situation and adequate anterior fusion during revision surgery as no postoperative adjacent therapy was performed. In our case, the rather short follow-up with this excellent clinical function and stability after revision surgery might mask an ongoing micromovement without osseous integration, fusion and prolonged reimplant failure. Therefore, more satisfying data on the long-term survival of anterior–posterior spinal fusion need to be collected to hint at future stabilization strategies.

Conclusion

We conclude reconstruction strategies following column resections of tumors in the thoracic spine have to be balanced between optimal anti-tumor and biomechanical goals. Although an implant failure with a non-biological solution had to be expected after initial surgery on the long run, the long-term outcome and osseous integration after revision surgery with a biological reconstruction are unclear, too. Both procedures offered a good primary stabilization with excellent pain reduction and good return to life. We expect better long-term results with the now more biological solution.

Compliance with ethical standards

Conflict of interest The authors declare that they have no conflict of interest.

References

1. Blumenthal SL, Gill K (1993) Can lumbar spine radiographs accurately determine fusion in postoperative patients? Correlation of routine radiographs with a second surgical look at lumbar fusion. Spine 18:1186–1189
2. Boriani S, Biagini R, De Iure F, Bertoni F, Malaguti MC, Di Fiore M, Zanoni A (1996) En bloc resection of bone tumors of the thoracolumbar spine. A preliminary report on 29 patients. Spine 21:1927–1932
3. Duval-Beaupère G, Schmidt C, Cosson P (1992) A barycentremetric study of the sagittal shape of spine and pelvis: the conditions required for an economic standing position. Ann Biomed Eng 20:451–462
4. Disch A, Pumberger M, Schmoelz W, Melcher I, Druschel C, Schaser KD (2012) Biomechanische Aspekte radikaler Resektionen und deren Rekonstruktion an der thorakolumbalen Wirbelsäule. Orthopäde 41:647–658
5. Disch AC, Schaser KD, Melcher I, Luzzati A, Feraboli F, Schmoelz W (2008) En bloc spondylectomy reconstructions in a biomechanical in vitro study. Eur Spine J 17:715–725
6. Disch AC, Schaser KD, Melcher I, Luzzati A, Feraboli F, Schmoelz W, Druschel C, Luzzati A (2011) Oncosurgical results of multilevel thoracolumbar en-bloc spondylectomy and reconstruction with a carbon composite vertebral body replacement system. Spine 36:647–655
7. Enneking WF, Spanier SS, Goodman MA (1980) A system for surgical staging of musculoskeletal sarcoma. CORR 153:106–120
8. Ferguson SJ, Winkler F, Nolte LP (2002) Anterior fixation in the osteoporotic spine: cut-out and pullout characteristics of implants. Eur Spine J 11:527–534
9. Gösling T, Pichlmaier MA, Länger F, Krettek C, Hüfner T (2013) Two-stage multilevel en bloc spondylectomy with resection and replacement of the aorta. Eur Spine J 22(Suppl 3):363–368
10. Haas N, Blauth M, Tscherne H (1991) Anterior plating in thoracolumbar spine injuries. Indication, technique and results. Spine 16:S100–S111
11. Halm H, Richter A, Lerner T, Liljenqvist U (2008) En-bloc spondylectomy and reconstruction for primary tumors and solitary metastasis of the spine. Orthopade 37(4):356–366
12. Iwai C, Taneichi H, Inami S, Namikawa T, Takeuchi D, Kato N, Lida T, Shimizu K, Nohara Y (2012) Clinical outcomes of combined anterior and posterior spinal fusion for dystropic thoracolumbar spinal deformities of neurofibromatosis-1. Spine 38:44–50
13. Liljenqvist U, Lerner T, Halm H, Buerger H, Gosheger G, Winkelmann W (2008) En bloc spondylectomy in malignant tumors of the spine. Eur Spine J 17(4):600–609
14. Luzzati AD, Shah S, Gagliano F, Perrucchini G, Scotto G, Alloisio M (2015) Multilevel en bloc spondylectomy for tumors of the thoracic and lumbar spine is challenging but rewarding. CORR 473:858–867
15. Melcher I, Disch AC, Khodadadyan-Klostermann C, Tohtz S, Smolny M, Stöckle U, Haas NP, Schaser KD (2007) Primary malignant bone tumors and solitary metastases of the thoracolumbar spine: results by management with total en bloc spondylectomy. Eur Spine J 16(8):1193–1202
16. Pallisè F, Puig O, Rivas A et al (2003) Low fusion rate after L5-S1 laparoscopic anterior lumbar interbody fusion using twin stand-alone carbon fiber cages. Spine 28:520–521
17. Pumberger M, Prasad V, Druschel C, Disch AC, Brenner W, Schaser KD (2016) Quantitative in vivo fusion assessment by ^{18}F-fluoride PET/CT following en bloc spondylectomy. Eur Spine J 25:836–842
18. Schultheiss M, Hartwig E, Sarker M (2006) Biomechanical in vitro comparison of different mono- and bisegmental anterior procedures with regard to the strategy for fracture stabilization using minimally invasive techniques. Eur Spine J 15(82):89
19. Stener B (1971) Total spondylectomy in chondrosarcoma arising from the seventh thoracic vertebra. J Bone Joint Surg Br 53(2):288–295
20. Strube P, Hoff E, Hartwig T, Perka CF, Gross C, Putzier M (2012) Stand-alone anterior versus posterior lumbar interbody single-level fusion after a mean follow-up of month. J Spinal Disord Tech 25:362–369
21. Tomita K, Kawahara N, Baba H, Tsuchiya H, Fujita T, Toribatake Y (1997) Total en bloc spondylectomy. A new surgical technique for primary malignant vertebral tumors. Spine (Phila Pa 1976) 22(3):324–333
22. Yanamadala V, Rozman PA, Kumar JI, Schwab JH, Lee S-G, Hornicek FJ, Curry WT Jr (2017) Vascularized fibular strut autografts in spinal reconstruction after resection of vertebral chordoma or chondrosarcoma: a retrospective series. Neurosurgery 81:156–164

European Spine Journal (2019) 28 (Suppl 2):S18–S24
https://doi.org/10.1007/s00586-018-5684-z

CASE REPORT

Designing patient-specific solutions using biomodelling and 3D-printing for revision lumbar spine surgery

Ganesha K. Thayaparan[1,2] · Mark G. Owbridge[3] · Robert G. Thompson[3] · Paul S. D'Urso[1,3]

Received: 21 November 2017 / Accepted: 24 June 2018 / Published online: 10 July 2018

Abstract

Purpose Despite the variety of "off-the-shelf" implants and instrumentation, outcomes following revision lumbosacral surgery are inconstant. Revision fusion surgery presents a unique set of patient-specific challenges that may not be adequately addressed using universal kits. This study aims to describe how patient-specific factors, surgeon requirements, and healthcare efficiencies were integrated to design and manufacture anatomically matched surgical tools and implants to complement a minimally invasive posterior approach for revision lumbar fusion surgery.

Methods A 72-year-old woman presented with sciatica and a complex L5–S1 pseudoarthrosis 12 months after L2–S1 fixation surgery for symptomatic degenerative scoliosis. Patient computed tomography data were used to develop 1:1 scale biomodels of the bony lumbosacral spine for pre-operative planning, patient education, and intraoperative reference. The surgeon collaborated with engineers and developed a patient-specific 3D-printed titanium lumbosacral fixation implant secured by L2–L5, S2, and iliac screws. Sizes and trajectories for the S2 and iliac screws were simulated using biomodelling to develop a stereotactic 3D-printed drill guide. Self-docking 3D-printed nylon tubular retractors specific to patient tissue depth and bony anatomy at L5–S1 were developed for a minimally invasive transforaminal approach. The pre-selected screws were separately sourced, bundled with the patient-specific devices, and supplied as a kit to the hospital before surgery.

Results At 6-month follow-up, the patient reported resolution of symptoms. No evidence of implant dysfunction was observed on radiography.

Conclusion Pre-operative planning combined with biomodelling and 3D printing is a viable process that enables surgical techniques, equipment, and implants to meet patient and surgeon-specific requirements for revision lumbar fusion surgery.

Keywords Biomodelling · Lumbosacral · Patient specific · Revision · 3D printing

Introduction

Lumbar fusion procedures have evolved to treat the neurological symptoms caused by degenerative disease of the lumbar spine. Current surgical techniques, with open and minimally invasive variations, allow near-circumferential access to the lumbar spine [1, 2]. Each surgical technique and implant for lumbosacral stabilization require a set of device-specific tools for instrumentation. This expansion of surgical tools and implants has partly contributed to a considerable increase in the rates of lumbar fusion surgery over the last two decades with a proportional increase in lumbar revision rates [3, 4].

Meticulous pre-operative planning is paramount to determine a revision strategy from a variety of approaches, techniques, and equipment. Subsequently, the decision to offer surgical correction is influenced by the suitability of the patient to a particular surgical technique, which may exclude a patient from surgery.

Recently, the adaptability of additive manufacturing techniques combined with biomodelling and pre-operative planning allows the development of implants and surgical tools to complement, adapt, or replace existing surgical methods to suit patient and surgeon-specific requirements [5, 6]. In this report, we present a process where patient-specific

✉ Ganesha K. Thayaparan
ganesha.thayaparan@gmail.com

[1] Department of Neurosciences Epworth Healthcare, Richmond, Victoria, Australia

[2] The Epworth Centre, Suite 7, Level 8, 32 Erin Street, Richmond, Victoria 3121, Australia

[3] Anatomics Pty Ltd, St Kilda, Victoria, Australia

implants and surgical tools were designed and manufactured using biomodelling and 3D printing (3DP) for a patient requiring revision lumbosacral fusion surgery.

Case history

A 72-year-old lady initially presented with a history of chronic lower back pain, left sciatica, and abnormal gait. Her history was significant for osteoarthritis with bilateral knee replacements, osteopenia with previous stress fractures in her right ankle, previous C4–6 anterior cervical discectomy and fusion, hysterectomy, and hypertension. Lumbar imaging revealed a scoliotic spine with grade 1 degenerative spondylolisthesis with severe canal stenosis at L4–5 and L3–4, disc prolapse at L2–3 with severe canal stenosis, and severe left L5 nerve root compression.

A two-stage operation was performed to correct scoliosis with interbody cages implanted at L2–3, L3–4, and L4–5 using a lateral technique (XLIF, Nuvasive, San Diego, CA, USA). A polyether ether ketone (PEEK) interbody cage combining autologous bone with bone morphogenic protein (Infuse Medtronic, Memphis, TN, USA) was implanted at L5–S1 using a minimally invasive left-sided transforaminal approach (MIS TLIF). Minimally invasive laminectomies and rhizolysis were performed on the right at L3–4 and bilaterally at L4–5. Pedicle screws and rods were inserted to connect L2 to S1.

Post-operative radiographs at 1 and 4 months were satisfactory. Despite the resolution of lower back pain, her left sciatica persisted. At 12 months, a computed tomography (CT) scan demonstrated a pseudoarthrosis and coronal collapse at L5–S1 with a loose S1 screw trapping and irritating the left L5 nerve root (Fig. 1). The sacral promontory had collapsed underneath a grade 1 spondylolisthesis of the L5 vertebra (Fig. 2). Revision surgery was proposed to decompress the L5 nerve root, to minimize movement across the L5–S1 segment without instrumenting S1, and to promote bony fusion across the L5–S1 segment.

Fig. 1 Coronal computed tomography image demonstrating a pseudoarthrosis at L5–S1, loosening of the left S1 screw, and coronal imbalance

Materials and methods

The design process is summarized in Fig. 3.

Biomodelling

The patient underwent a helical CT scan. Digital Imaging and Communications in Medicine (DICOM) data were transferred to a workstation running AnatomicsPro software (Anatomics, St Kilda, Australia) for processing prior to manufacture of a 1:1 stereolithographic biomodel of the osseous spine (Fig. 4) from polymerized transparent layers of ultraviolet light-cured acrylic resin. The biomodel allowed the treating surgeon to examine patient anatomy, appreciate surgical pathology, rehearse the surgical procedure, and formulate a surgical plan in conjunction with standard clinical imaging.

Pre-operative planning

Using AnatomicsC3D software (Anatomics, St Kilda, Australia), the surgeon collaborated with biomedical engineers to formulate a list of design specifications for the patient-specific posterior fixation construct (Table 1). The specifications allowed engineers to develop a software model of the fixation construct by simulating the required pedicle screws, connecting rods, and interbody cage. In this case, a patient-specific contoured iliolumbar implant spanning L2 to pelvis with a pelvic anchor was designed to provide stabilization (Fig. 4). The porous ventral surface of the anchor was contoured to complement the ilium.

Suitable entry points, sizes, and trajectories for the S2 and iliac screws were simulated in software. An interbody cage was sized and selected using the software and biomodel. Stereotactic drill guides were designed using planned pedicle screw positions for intraoperative use with fluoroscopy (Fig. 5). A self-docking tubular retractor specific to patient tissue depth and bony anatomy at L5–S1 was designed for a MIS TLIF technique (Fig. 6).

Fig. 2 Sagittal computed tomography image demonstrating a pseudoarthrosis at L5–S1 with a grade 1 spondylolisthesis

Verification

Technical specifications for the proposed fixation construct using the pre-selected implants were provided as a report to the surgeon.

The surgeon simulated the proposed solution using AnatomicsC3D software and specified design modifications to the engineers. A revised solution was communicated to the surgeon for verification. This process iterated until the surgeon confirmed the design and implant selection.

Additive manufacturing

After surgeon approval, the drill guides and tubular retractors were manufactured from nylon particles (PA-12) using an Eosint selective laser sintering printer (EOS GmbH, Krailling, Germany) at Anatomics (Anatomics, St Kilda, Australia). The patient-specific rods were fabricated from titanium alloy powder (Ti64) using an Arcam A1 EBM printer (Arcam AB, Mölndal, Sweden) at CSIRO Lab 22 (CSIRO, Clayton, Australia).

The printed equipment was post-processed at Anatomics where the parts were cleaned, polished, sterilized, and packaged for delivery to the hospital. The pre-selected screws and interbody cage were separately supplied. We chose an EIT Cellular Titanium® (Emerging Implant Technologies GmbH, Wurmlingen, Germany) interbody cage to replace the existing PEEK interbody cage at L5–S1.

Surgery

All pedicle screws and rods were removed via the previous para-median keyhole incisions. The patient-specific tubular retractor was secured to the spine using a temporary cannulated screw along the previous S1 screw trajectory. The existing L5–S1 interbody cage was replaced by the pre-selected 3DP titanium cage, and BMP (Infuse, Medtronic) was implanted. New pedicle screws were inserted at L2 to L5.

A 4-centimetre incision was made over each ilium to expose the bony surface. The sacroiliac drill guide was introduced to place two S2 screws and iliac pilot holes bilaterally under fluoroscopic guidance. The tulip of the lower left iliac bolt stretched the overlying skin and was removed. Consequently, the left iliolumbar rod was shortened intraoperatively (Figs. 5, 7). Operative and clinical performances are listed in Table 2. Our patient recovered well reflected by a reduction in her visual analogue score (VAS) and satisfactory post-operative radiographs (Fig. 7).

Discussion

Pathologies such as infection, stenosis, fractures, painful instrumentation, pseudoarthrosis, adjacent segment disease, post-operative deformity, or non-spinal causes may be individually or collectively responsible for late complications following instrumented lumbar fusion surgery. Depending on the patient-specific indications for revision surgery, a surgeon's plan for corrective surgery may be limited by available equipment and implants. The issues specific to this revision case are listed in Table 1.

"Off-the-shelf" kits for spinal instrumentation are designed for specific indications and can be adapted for revision surgery. For example, anterior approaches to the lumbar spine have been used to achieve a bony fusion after the development of a pseudoarthrosis following posterior lumbar fusion surgery [7]. However, an indirect decompression via an anterior approach may not relieve severe stenosis. Additionally, an anterior interbody cage is not suitable for this patient at L5–S1 due to a collapsed sacral promontory. Further, the patient's age, comorbidity, and previous abdominal surgery may complicate an anterior approach to the anterior vertebral surface.

Posterior approaches using "off-the-shelf" kits are suitable but may not entirely address patient-specific factors,

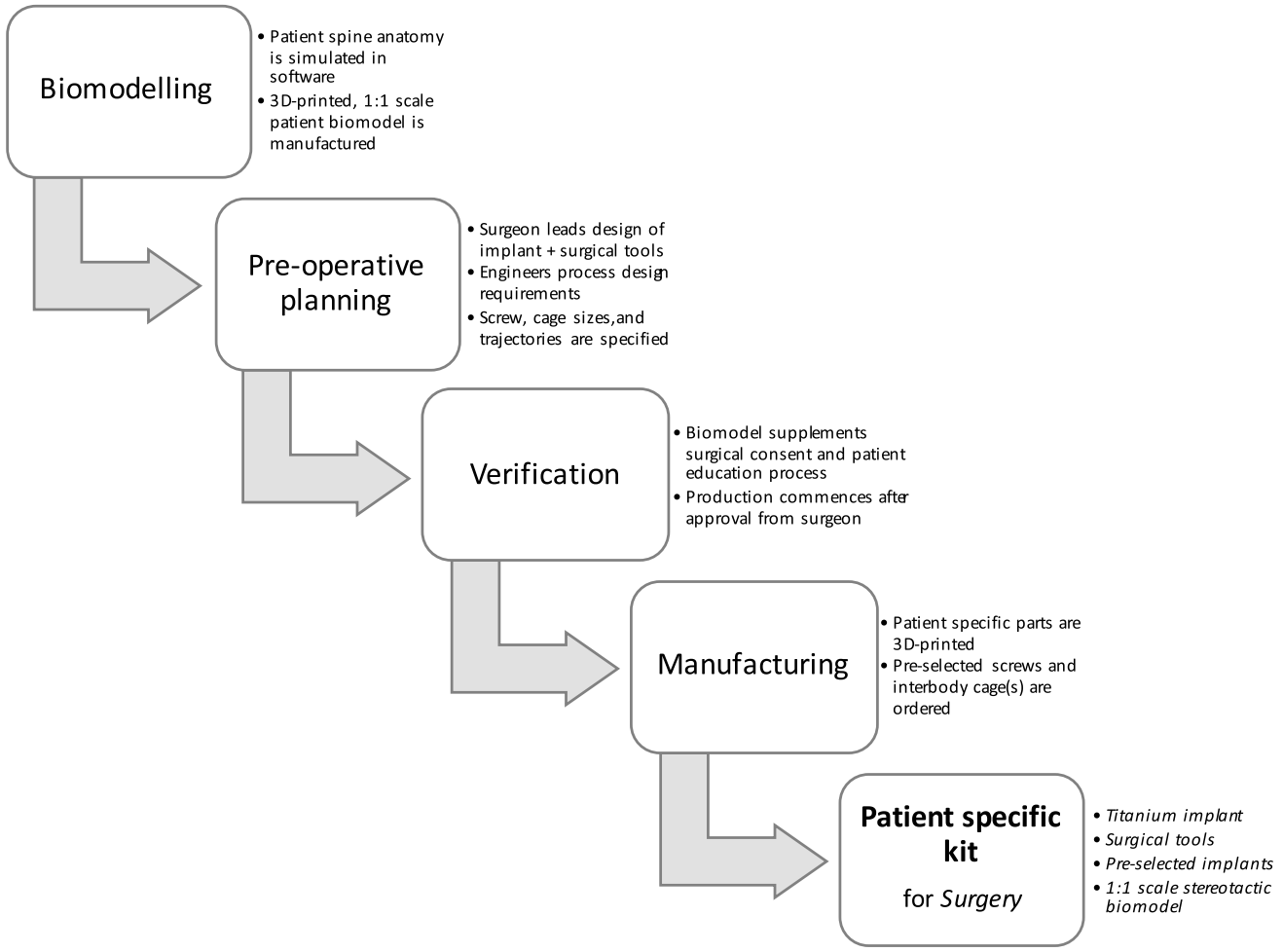

Fig. 3 Process flow diagram demonstrating the key steps in the design process

thereby compromising healthcare efficiencies [8, 9]. Several posterior techniques can adequately correct a pseudoarthrosis at L5–S1 and decompress the left L5 nerve root; we chose to use a minimally invasive transforaminal technique. However, this patient additionally needed the L2–S1 segments stabilized without re-instrumenting S1 as it was predicted replacement S1 pedicle screws would not find adequate purchase.

Consequently, a pelvic anchor was required to secure a long patient-specific rod and provide the necessary stability for bony fusion. An open posterior approach may provide adequate visualization to contour rods but may cost the patient in terms of blood loss, post-operative pain, hospital stay, and rehabilitation time [10, 11]. Further, intraoperative rod contouring significantly reduces the fatigue life [12], especially when biomechanical cadaveric studies show increased strain in rods and S1 screws for long lumbosacral constructs [13]. Additional fixation by way of cross-linkages or "outrigger rods" [14] may overcompensate for biomechanical stability while potentially increasing complexity, operating time, and cost.

Alternatively, a surgeon's pre-operative plan can be combined with biomodelling and rapid manufacturing methods to design, test, and implant patient-specific solutions that address all issues indicating revision lumbar surgery. Biomodelling was used for pre-operative planning, patient education, and intraoperative reference [15] and allows stereotactic guides to be developed for intraoperative use to percutaneously place iliac bolts and S2 screws along predefined trajectories using only 2D fluoroscopy (Fig. 5).

Fig. 4 1:1 scale biomodel of patient's spine with patient-specific 3D-printed titanium implants contoured to match the bony anatomy of the pelvis and desired spinal curvature for revision surgery

Fig. 5 1:1 scale biomodel of patient's spine with patient-specific drill guide designed to contour match the bony pelvis and guide placement of iliac bolts and S2 screws

Table 1 Patient- and surgeon-specific issues guiding design cues

Issue	Design cue
Osteoporosis; collapsed sacral promontory; previous abdominal surgery; L5 foraminal stenosis; L5–S1 pseudoarthrosis	*Approach*: Posterior MIS TLIF *Structural*: No pedicle screw to be placed in S1
Revise L5–S1 interbody cage Decompress S1 nerve root	*Exposure*: Custom self-docking tubular retractors specific to patient tissue depth to aid MIS S1 rhizolysis
Revise L2–S1 posterior fixation	*Structural*: MIS pedicle screw revision at L2, L3, L4, L5 bilaterally
Preserve scoliotic correction and anchor long segment construct to the pelvis	*Structural*: Connecting rods manufactured to planned curvature and continuous with a pelvic anchor
Reinforce long segment construct with a pelvic anchor	*Structural*: Custom pelvic contour matched anchor secured with bilateral S2 and iliac screws
MIS pelvic fixation	*Exposure*: MIS S2 and iliac screw drill trajectory guide

MIS minimally invasive surgery, *TLIF* transforaminal lumbar interbody fusion

The authors found the 3D-printed patient-specific biomodel, tubular retractor, and stereotactic drill guide particularly useful. Minimally invasive techniques typically limit visible patient anatomy. However, the biomodel improved our understanding of surgical anatomy by providing a scale visual and tactile frame of reference. The design of the tubular retractor matched the bony contours of the patient's spine and docked onto the bone, which removed the need for externally braced retraction systems to declutter the intraoperative workspace. Likewise, the contoured surface of the drill guide matched the patient's bony pelvic anatomy to simplify template positioning with minimal tissue dissection. The pre-planned trajectories were easily replicated intraoperatively to assist implantation of S2 screws and iliac bolts without the need for intraoperative image guidance systems.

The performance of this process is measured by an operating time of 291 min, 59 s of fluoroscope screening time, no complications, no blood transfusions, and length of stay of 5 days with a reduction in patient-reported pain scores. In a retrospective review of 112 patients for posterior instrumented revision surgery, the operating time was 280 ± 62 min, 1.04 ± 1.17 units transfused, and a length of stay of 6 ± 2.4 days [16]. Radiation exposure was not reported in this series. However, another series of 40 patients undergoing first-time single-level MIS TLIF reported on average 55.2 ± 11.3 s of fluoroscopic screening [17]. The number of sterile trays used and waste generated is reported to benchmark this process so that healthcare resource allocation is also incorporated into the pre-operative planning process.

Fig. 6 A patient-specific tubular retractor for a minimally invasive transforaminal lumbar interbody approach that is designed to match the tissue depth and contours of this patient's posterior L5–S1 bony anatomy. The retractor is secured to the spine using a cannulated bone screw along the trajectory of the existing S1 pedicle screw

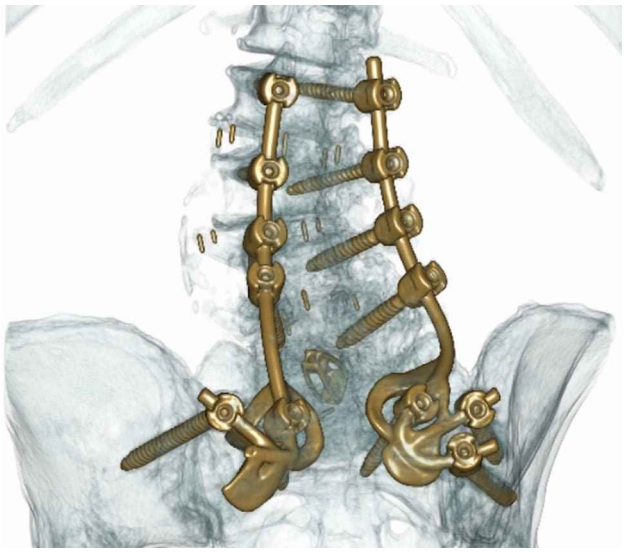

Fig. 7 3D reconstruction using post-operative computed tomography data demonstrating implant position. A second left-sided iliac bolt was not implanted as the tulip may have caused a pressure area. The respective segment of the patient-specific rod was intraoperatively shortened

Conclusion

For revision lumbar fusion surgery, "off-the-shelf" kits limit surgical solutions to a particular set of techniques, surgical tools, and implants, which can potentially compromise patient, surgeon, and healthcare-specific needs. As this single case history highlights, pre-operative planning combined with biomodelling and 3D printing is a viable process that enables the development of patient-specific implants and surgical tools suited to the needs of this clinical presentation. The next patient requiring lumbar revision surgery will present a different set of challenges. However, additive manufacturing techniques are adaptable, and so there is potential to tailor surgical solutions to optimally meet the needs of every patient needing revision lumbar fusion

Table 2 Patient characteristics and operative performance

Age (years)	72
BMI (kg/m^2)	25.4
Operative time (min)	291
Operative aids	Neural monitoring
Sterile trays	18
Contaminated OW (bags)[a]	0.5
Uncontaminated OW (bags)[a]	0.75
Fluoroscope screening time (s)	59
Total complications	0
Blood transfusion	0
Length of stay (days)	5
Pre-operative leg pain VAS	8
Post-operative leg pain VAS	5
Six-month follow-up leg pain VAS	2

BMI body mass index (kilograms per square metre), *OW* operative waste, *VAS* visual analogue score

[a]1 bag = 800 × 500 millimetres of 50 l capacity

surgery. Consequently, a patient's chance of resolving their chief complaint by revision surgery need not be dependent on their suitability to a limited set of techniques and implants.

Acknowledgements The authors would like to thank Dr Philip M. Lewis for providing academic support.

Compliance with ethical standards

Conflict of interest Mark Owbridge is an employee at Anatomics Pty Ltd. Robert Thompson is an employee at Anatomics Pty Ltd. Paul D'Urso is a director and shareholder at Anatomics Pty Ltd and has received funding from Stryker Corporation, Epworth Healthcare, and Anatomics Pty Ltd.

Ethical standards All procedures performed in studies involving human participants were in accordance with the ethical standards of the institutional and national research committee and with the 1964 Helsinki declaration and its later amendments or comparable ethical standards. Ethical approval for this study was obtained from Epworth Healthcare Human Research Ethics and Research Governance Committees (HREC2017-254).

Human and animal rights This article does not contain any studies with animals performed by any of the authors.

Informed consent Informed consent for surgery was obtained from all individual participants included in the study.

References

1. Kaiser MG, Eck JC, Groff MW, Watters WC 3rd, Dailey AT, Resnick DK, Choudhri TF, Sharan A, Wang JC, Mummaneni PV, Dhall SS, Ghogawala Z (2014) Guideline update for the performance of fusion procedures for degenerative disease of the lumbar spine. Part 1: introduction and methodology. J Neurosurg Spine 21:2–6. https://doi.org/10.3171/2014.4.SPINE14257
2. Foley KT, Holly LT, Schwender JD (2003) Minimally invasive lumbar fusion. Spine 28:S26–S35. https://doi.org/10.1097/01.BRS.0000076895.52418.5E
3. Rajaee SS, Bae HW, Kanim LE, Delamarter RB (2012) Spinal fusion in the United States: analysis of trends from 1998 to 2008. Spine 37:67–76. https://doi.org/10.1097/BRS.0b013e31820cccfb
4. Martin BI, Mirza SK, Comstock BA, Gray DT, Kreuter W, Deyo RA (2007) Are lumbar spine reoperation rates falling with greater use of fusion surgery and new surgical technology? Spine 32:2119–2126. https://doi.org/10.1097/BRS.0b013e318145a56a
5. D'Urso PS, Askin G, Earwaker JS, Merry GS, Thompson RG, Barker TM, Effeney DJ (1999) Spinal biomodeling. Spine 24:1247–1251
6. Mobbs RJ, Coughlan M, Thompson R, Sutterlin CE 3rd, Phan K (2017) The utility of 3D printing for surgical planning and patient-specific implant design for complex spinal pathologies: case report. J Neurosurg Spine 26:513–518. https://doi.org/10.3171/2016.9.SPINE16371
7. Mobbs RJ, Phan K, Thayaparan GK, Rao PJ (2016) Anterior lumbar interbody fusion as a salvage technique for pseudarthrosis following posterior lumbar fusion surgery. Glob Spine J 6:14–20. https://doi.org/10.1055/s-0035-1555656
8. Adogwa O, Parker SL, Shau D, Mendelhall SK, Aaronson O, Cheng J, Devin CJ, McGirt MJ (2015) Cost per quality-adjusted life year gained of revision fusion for lumbar pseudoarthrosis: defining the value of surgery. J Spinal Disord Tech 28:101–105. https://doi.org/10.1097/BSD.0b013e318269cc4a
9. Vertuani S, Nilsson J, Borgman B, Buseghin G, Leonard C, Assietti R, Quraishi NA (2015) A cost-effectiveness analysis of minimally invasive versus open surgery techniques for lumbar spinal fusion in Italy and the United Kingdom. Value Health 18:810–816. https://doi.org/10.1016/j.jval.2015.05.002
10. Goldstein CL, Macwan K, Sundararajan K, Rampersaud YR (2016) Perioperative outcomes and adverse events of minimally invasive versus open posterior lumbar fusion: meta-analysis and systematic review. J Neurosurg Spine 24:416–427. https://doi.org/10.3171/2015.2.SPINE14973
11. Goldstein CL, Phillips FM, Rampersaud YR (2016) Comparative effectiveness and economic evaluations of open versus minimally invasive posterior or transforaminal lumbar interbody fusion: a systematic review. Spine 41(Suppl 8):S74–S89. https://doi.org/10.1097/BRS.0000000000001462
12. Lindsey C, Deviren V, Xu Z, Yeh RF, Puttlitz CM (2006) The effects of rod contouring on spinal construct fatigue strength. Spine 31:1680–1687. https://doi.org/10.1097/01.brs.0000224177.97846.00
13. Kleck CJ, Illing D, Lindley EM, Noshchenko A, Patel VV, Barton C, Baldini T, Cain CM, Burger EL (2017) Strain in posterior instrumentation resulted by different combinations of posterior and anterior devices for long spine fusion constructs. Spine Deform 5:27–36. https://doi.org/10.1016/j.jspd.2016.09.045
14. Palumbo MA, Shah KN, Eberson CP, Hart RA, Daniels AH (2015) Outrigger rod technique for supplemental support of posterior spinal arthrodesis. Spine J 15:1409–1414. https://doi.org/10.1016/j.spinee.2015.03.004
15. D'Urso PS, Williamson OD, Thompson RG (2005) Biomodeling as an aid to spinal instrumentation. Spine 30:2841–2845
16. Zheng F, Cammisa FP Jr, Sandhu HS, Girardi FP, Khan SN (2002) Factors predicting hospital stay, operative time, blood loss, and transfusion in patients undergoing revision posterior lumbar spine decompression, fusion, and segmental instrumentation. Spine 27:818–824
17. Seng C, Siddiqui MA, Wong KP, Zhang K, Yeo W, Tan SB, Yue WM (2013) Five-year outcomes of minimally invasive versus open transforaminal lumbar interbody fusion: a matched-pair comparison study. Spine 38:2049–2055. https://doi.org/10.1097/BRS.0b013e3182a8212d

European Spine Journal (2019) 28 (Suppl 2):S25–S30
https://doi.org/10.1007/s00586-018-5689-7

CASE REPORT

Huge myxoid chondrosarcoma expanded into the thoracic cavity with spinal involvement

Ming Lu[1,2] · Zhongxin Zhou[3] · Zixiong Lei[1,2] · Haomiao Li[1,2] · Stefano Boriani[4]

Received: 22 February 2018 / Revised: 20 May 2018 / Accepted: 26 June 2018 / Published online: 4 July 2018

Abstract

Purpose En bloc resection is the treatment of choice of myxoid chondrosarcoma. These tumors can produce huge masses. Anatomical constraints limit the possibility to perform en bloc resection in the spine.

Methods A very huge myxoid chondrosarcoma (14.2 × 10.8 × 11.4 cm) arising from T2 to T5 and invading the whole higher left pleural cavity was observed. Surgical planning according to WBB staging system was performed.

Results The tumor was successfully submitted to en bloc resection achieving a tumor-free margin as demonstrated by the pathologist's report.

Conclusions A careful planning and a multidisciplinary collaboration make possible to perform en bloc resection even in apparently impossible cases.

Keywords En bloc spondylectomy · Spinal myxoid chondrosarcoma · WBB staging system · Multidisciplinary collaboration

Introduction

Myxoid variety of chondrosarcoma is known to produce huge masses [1–3]. This low-malignant tumor is radioresistent [4] and has a very high tendency to recurrence when submitted to intralesional excision [5–9, 13]. Chemotherapy has been proved ineffective and hence not recommended [10–12]. Its tendency to progress to higher level of malignancy at recurrence is also known. En bloc resection is therefore the treatment of choice [2, 3, 13–15]. Regional constraints and the dimension of some spine tumor can make impossible to perform en bloc resection [16–20].

This case is reported to demonstrate that careful planning, including multidisciplinary competences, makes possible to perform en bloc resection even in huge tumors.

Case report

A 34-year-old female was admitted to our department presenting with complains of increasing pain at the back, with a mass on the left back and complete paralysis of the lower extremities for 1 month. The patient initially presented to another hospital 3 months prior to this with a mass on the left back. An open incisional biopsy was performed at the left back in her primary hospital prior to our workup, and the diagnosis from histopathological analysis was of a low-grade myxoid chondrosarcoma.

A physical examination showed that there was complete paralysis of the lower extremities and decreased sensation below the trunk, with dysfunction of the bladder and bowel movement (ASIA impairment scale: B). Plain radiography, computed tomography and magnetic resonance imaging demonstrated an expansive mediastinal mass lesion with thoracic vertebral bodies and ribs involved (Fig. 1). Further

Ming Lu, Zhongxin Zhou and Zixiong Lei have contributed equally to this work.

✉ Haomiao Li
lihaomiao1977@hotmail.com

[1] Department of Orthopedic, The Third Affiliated Hospital of Southern Medical University, Guangzhou 510630, China

[2] Academy of Orthopaedics, Guangdong Province, Guangzhou 510630, China

[3] Department of Interventional Vascular Surgery, The Third Affiliated Hospital of Southern Medical University, Guangzhou 510630, China

[4] GSpine4 Spine Surgery Unit, IRCCS Galeazzi Orthopaedic Institute, Milan, Italy

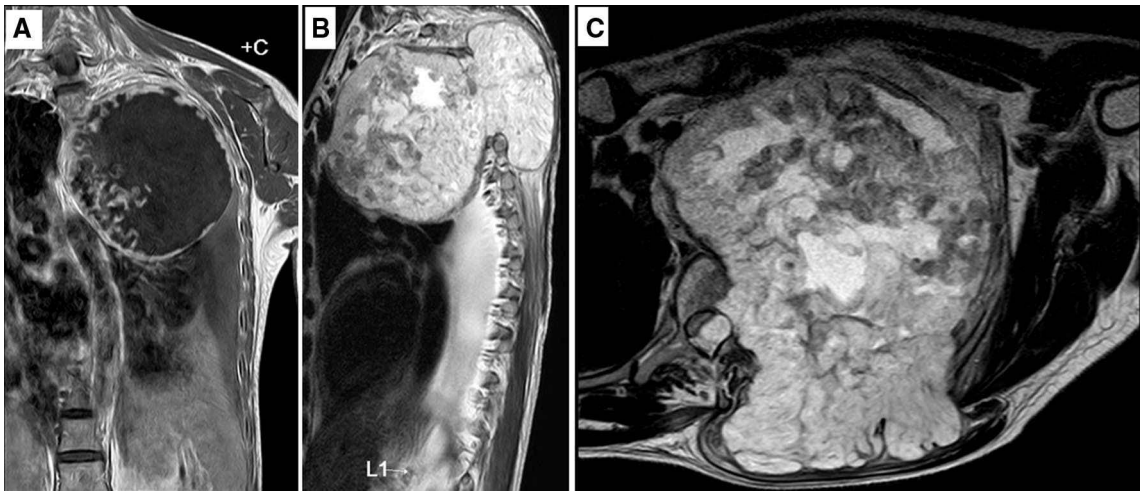

Fig. 1 **a** Coronal, **b** sagittal and **c** axial MRI images showing a huge expansive mediastinal mass lesion (14.2 × 10.8 × 11.4 cm) invading the thoracic vertebral bodies and ribs and spinal cord compression are demonstrated

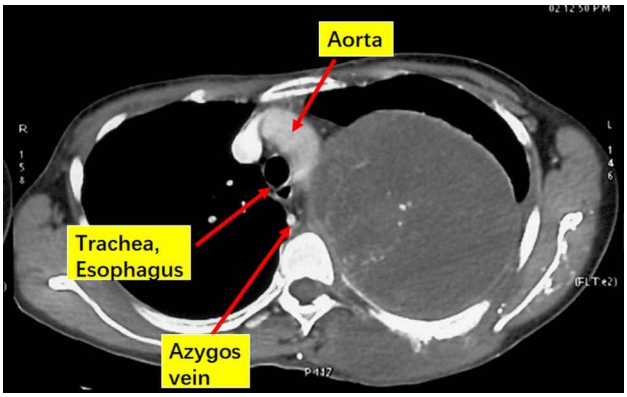

Fig. 2 Chest CT scan, showing the adjacent important structures of the mediastinum. There is a large soft tissue mass within the mottled calcification

investigation revealed no other tumor lesions existed. In the present case, the mass had become involved with the spinal canal and adhered to the aorta, trachea and esophagus (Figs. 2, 3) (Enneking stage IB and WBB stage 1-7/A-D). Selective arterial embolization was performed 1 day prior to the surgery. En bloc resection with a tumor-free margin by one-stage posterior approach was carefully designed by a multidisciplinary team.

Surgical planning by posterior approach (WBB-based en bloc resection type 2a, Fig. 4) [21] and detachment of the spinal muscles from the posterior elements from T2 to T5 were performed. The whole procedure was carried out in the prone position. First, the right pleural cavity was opened by section of the T2–T5 ribs, ligation of the azygos, release of the aortic arch and the esophagus. A dissection of the mass was performed by section of the T2–T6 left ribs and the left scapula. Lateral mass screws were implanted at C6, C7. Pedicle screws were implanted at the levels of T1, T6, T7 and T8. A wide right semi-laminectomy was performed by ultrasonic osteotome from T2 to T5, and the T2–T5 right nerve roots were sacrificed. Then, sectors 8-9-10 were piecemeal excised by high-speed burr to approach the spinal canal at levels T2–T5. A rod was connected on the right side, and osteotomy was performed by Tomita saw at T1/T2 and T5/T6 disk levels. At this time, the huge mass can be rotated on the longitudinal axis, allowing to separate the thecal sac from the mass in the spinal canal under direct vision. The T2–T5 left nerve roots are sectioned after ligation. Then, the whole mass is finally removed without any apparent surgical violation of the margins (Fig. 5a, c, d). The reconstruction was performed by four rods connection at bilateral C6, C7, T6 and T1, T7, T8, respectively. A titanium cage was inserted between the T1–T6 vertebral body, and two vertebral body screws were implanted at T1 and T6 to reinforce the fixation of the titanium cage. Reconstruction of the ribs defect was performed by using two rods connecting the screws and the defect ends in the left side (Figs. 5b, 6d). A chest tube was placed to re-expand the lung.

The operation took 15 h in total, with a total of 5500 mL of bleeding. Ventilator-assisted ventilation was used for 17 days after operation in intensive care unit. After respiratory function exercise for 1 month, she can breathe normally without hypoxic symptoms. Pulmonary infection occurred postoperatively, and etiological examination suggested Acinetobacter Bauman infection. Chest drainage sustained for 64 days. Anti-infective treatment regimen was based on the results of bacterial susceptibility. Imipenem combined with cefoperazone was used for the first month and then cefoperazone only until chest drainage was removed. A slowly skin sensation recovery was observed on the trunk postoperatively. No improvement in muscle

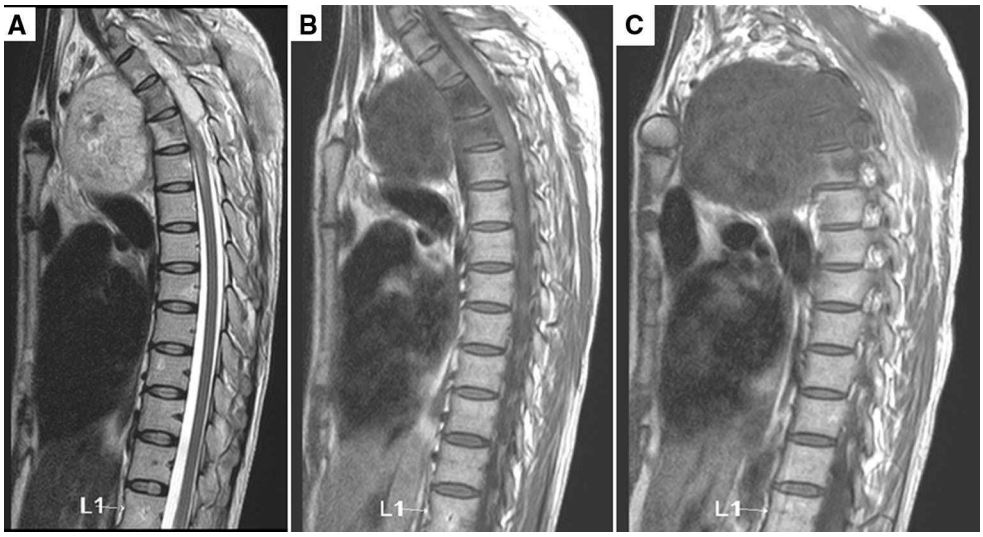

Fig. 3 **a** The sagittal T2-weighted MRI image demonstrates the epidural mass and spinal cord compression. **b**, **c** The sagittal T1-weighted MRI images show low signal intensity in the T2–T5 vertebral bodies and tumor mass

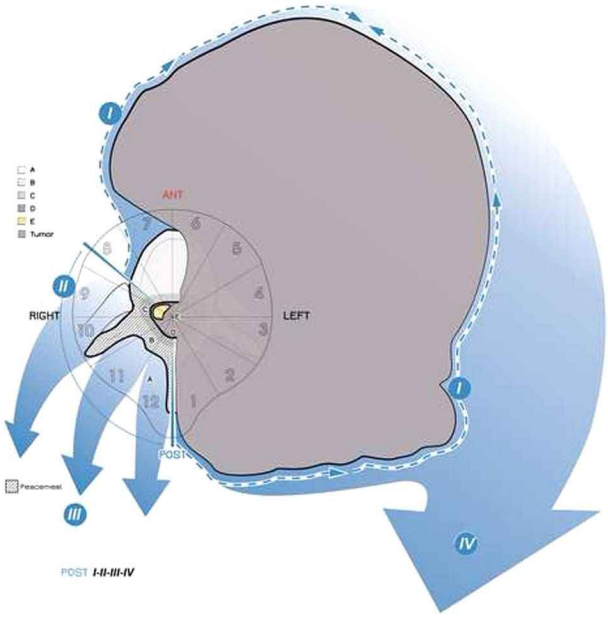

Fig. 4 WBB-based planning of the en bloc resection. Posterior approach only, patient in prone position (type 2b). Step I: completely release of the tumor mass from left and from right. Step II: definition of the approach to the canal: sectors 8–12. Step III piecemeal excision of sectors 8–12, release of the dural sac after section of the nerve roots. Step IV: En bloc tumor removal by careful clockwise rotation along the longitudinal axis

strength of the lower extremities and defecation functions was observed at 3 months postoperatively. Reconstructed postoperative CT scan at 3 months showed no signs of tumor recurrence and well-united bone at the reconstruction site (Fig. 6).

Discussion

From the earliest report by Lievre [22], Hamdi [23] and Stener [24, 25], en bloc resection was later on popularized by Roy Camille [26] and Tomita [27, 28] till more recent attempt to standardize the surgical planning according to the WBB staging system [21, 29]. En bloc resection with tumor-free margins remains the best oncological management of the spine, which aims to a better local control and longer survival rate.

Recurrence of chondrosarcoma usually occurs in 3–5 years postoperatively, and the relapse tends to be faster if an intralesional excision was performed [5, 30]. Thus, a worse prognosis could be achieved. These results were proved to be related to the inadvertent intraoperative contamination [5, 31]. Regional anatomical constraints and huge volumes remain, however, a severe limit to perform an oncological appropriate en bloc resection (it means resulting in tumor-free margins without any tumor contamination), and some reports in the literature of procedures including the separation of the tumor in two or more pieces with intralesional margins [16–20]. A long-term survival rate has only been observed in low-grade spinal chondrosarcoma patients after repeated intralesional excision surgeries, combined with radiotherapy [32].

Here, a case of en bloc resection of a huge myxoid chondrosarcoma is reported, resulting in a fully tumor-free margin resection. To our knowledge, this is one of the largest tumors ever resected by this technique. The peculiar steps were: the ligation of the azygos, the release of the aortic arch and of the esophagus, the opening of a window in the posterolateral vertebrae (T2–T5 in sectors

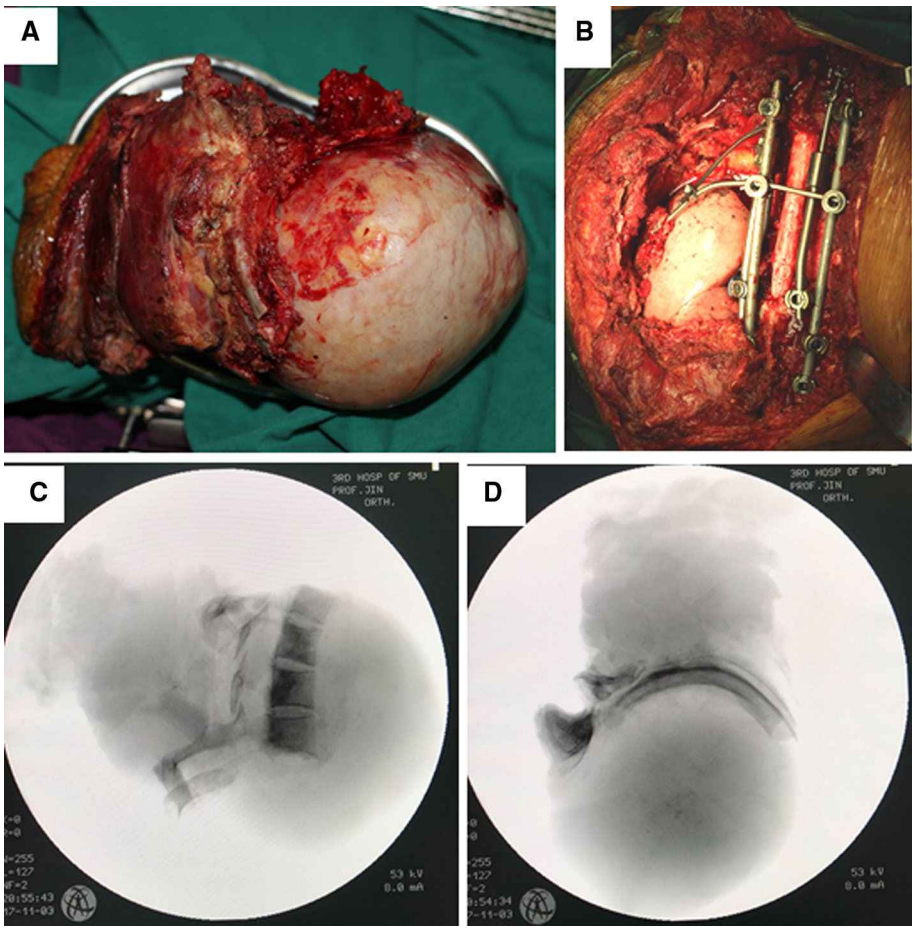

Fig. 5 **a** Photograph of the en bloc resected specimen. **b** Photograph demonstrates the reconstruction of the chest wall defect and spinal stability by screws and rods. **c**, **d** The X-ray images of the en bloc resected specimen

8-9-10) in order to release the dural sac. Once the osteotomies of the spine at the T1/T2 and T5/T6 disk levels were performed, the specimen could rotate, allowing to finalize the resection.

The goal of this surgical procedure was to remove the tumor en bloc with macroscopically healthy margins. Owing to its huge dimension and proximity to vital neurovascular structures, the surgical morbidity and functional impairment must be seriously considered. In the present case, multiple ribs and partial chest wall tissues were excised combined with the mass. The chest wall has both a protective structural around the vital organs of the body and functional role of respiratory movement. Large chest wall defects can cause devastating respiratory and circulatory functional consequences [33, 34]. Reconstruction of the chest wall defect was performed to recreate a stable chest wall with adequate functional capacity. Fadel et al. [35] reported an incidence of pneumonia of 35.3%: 6 patients suffered from pneumonia postoperatively in 17 patients following tumor resection involving the pleura and ribs. The use of sensitive antibiotics in the treatment of pulmonary infection and appropriate ventilator-assisted respiratory is critical for postoperative recovery.

Conclusions

The purpose of this article is to remark the role of preoperative planning in the surgical technique of en bloc resection. However, a careful follow-up will be mandatory for detecting local recurrence, whose risk—due to the histologically proven appropriate margin—is low but not negligible. The procedure

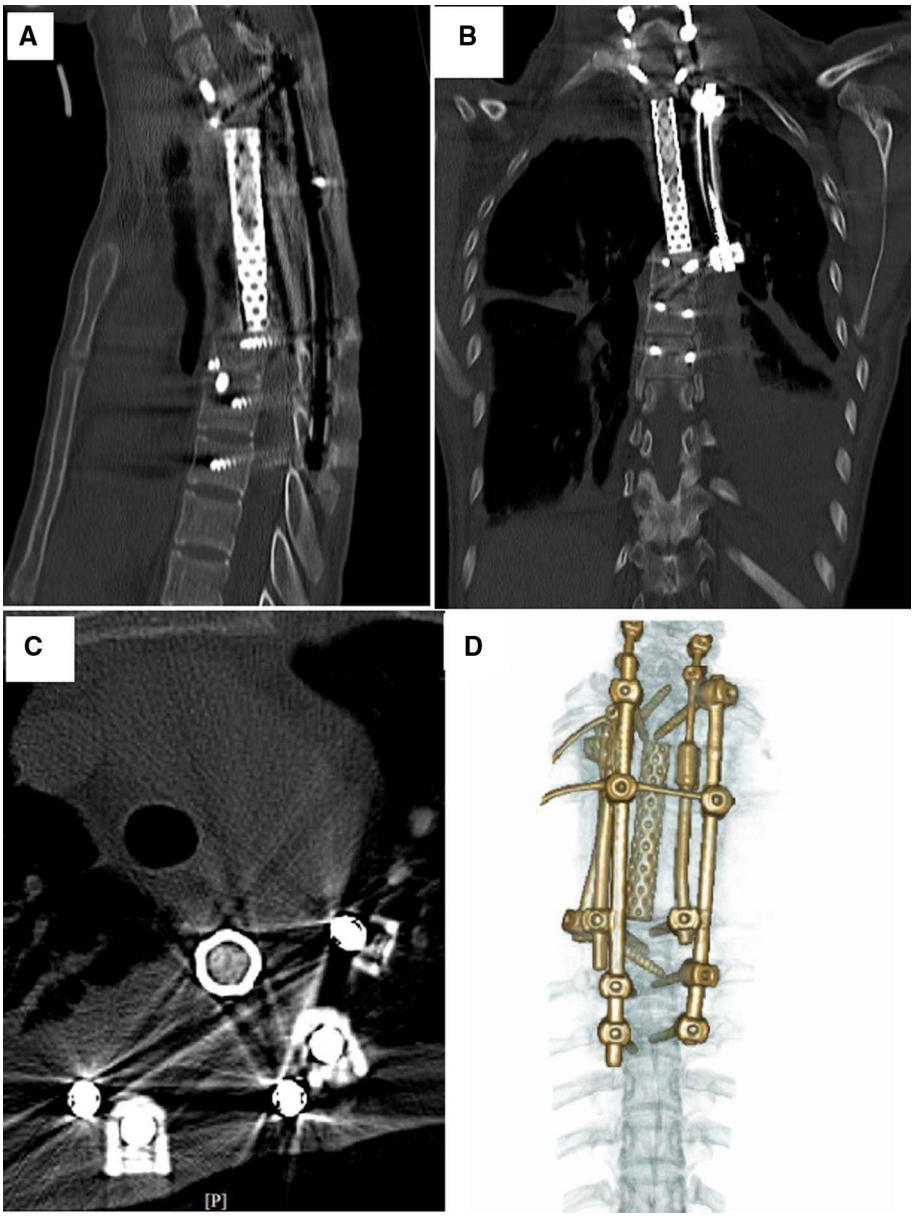

Fig. 6 Reconstructed **a** sagittal, **b** coronal, **c** axial and **d** three-dimensional computed tomography scan 3 months postoperatively

was successfully performed thanks to a very careful preoperative planning and to a multidisciplinary collaboration.

Acknowledgements The authors are indebted to Mr. Carlo Piovani for his excellent drawing interpretation of our surgical planning.

Compliance with ethical standards

Conflict of interest statement None of the authors has any potential conflict of interest.

References

1. Liu G, Wu G, Ghimire P, Pang H, Zhang Z (2013) Primary spinal chondrosarcoma: radiological manifestations with histopathological correlation in eight patients and literature review. Clin Imaging 37(1):124–133. https://doi.org/10.1016/j.clinimag.2012.02.010 **Epub 2012 Jun 8**
2. Quiriny M, Gebhart M (2008) Chondrosarcoma of the spine: a report of three cases and literature review. Acta Orthop Belg 74(6):885–890
3. Casadei R, Ricci M, Ruggieri P, Biagini R, Benassi S, Picci P, Campanacci M (1991) Chondrosarcoma of the soft tissues. Two different sub-groups. J Bone Joint Surg Br 73(1):162–168
4. Gelderblom H, Hogendoorn PCW, Dijkstra SD et al (2008) The clinical approach towards Chondrosarcoma. Oncologist 13:320–329

5. Boriani S, De Iure F, Bandiera S, Campanacci L et al (2000) Chondrosarcoma of the mobile spine: report on 22 cases. Spine (Phila Pa 1976) 25:804–812
6. Schoenfeld AJ, Hornicek FJ, Pedlow FX et al (2012) Chondrosarcoma of the mobile spine: a review of 21 cases treated at a single center. Spine (Phila Pa 1976) 37:119–126
7. Yang X, Wu Z, Xiao J et al (2012) Chondrosarcomas of the cervical and cervicothoracic spine: surgical management and long-term clinical outcome. J Spinal Disord Tech 25:1–9
8. Bergh P, Gunterberg B, Meis-Kindblom JM, Kindblom LG (2001) Prognostic factors and outcome of pelvic, sacral, and spinal chondrosarcomas: a center-based study of 69 cases. Cancer 91:1201–1212
9. Boriani S, Saravanja D, Yamada Y et al (2009) Challenges of local recurrence and cure in low grade malignant tumors of the spine. Spine (Phila Pa 1976) 34(22 Suppl):S48–S57
10. D'Ambrosio FG, Shiu MH, Brennan MF (1986) Intrapulmonary presentation of extraskeletal myxoid chondrosarcoma of the extremity: report of two cases. Cancer 58:1144
11. Saleh G, Evans HL, Ro JY, Ayala AG (1992) Extraskeletal myxoid chondrosarcoma: a clinicopathologic study of ten patients with long-term followup. Cancer 70:2827
12. Patel SR, Burgess MA, Papadopoulos NE, Linke KA, Benjamin RS (1995) Extraskeletal myxoid chondrosarcoma: long-term experience with chemotherapy. Am J Clin Oncol 18:161
13. Boriani S, Bandiera C, Biagini DF et al (2000) Chondrosarcoma of the Mobile Spine: report on 22 Cases. Spine 25(7):804–812
14. Prevedello DM, Cordiero JG, Koerbel A, Ditzel LF, Araujo JC (2004) Management of primary spinal chondrosarcoma: report of two cases causing cord compression. Arq Neuropsiquiatr 63(3):875–878
15. Xinghai Y, Zhipeng W, Jianru DF, Quan H, Wei Z et al (2012) Chondrosarcomas of the cervical and cervicothoracic spine: surgical management and long-term clinical outcome. J Spinal Disord Tech 25(1):1–9
16. Demura S, Kawahara N, Murakami H, Akamaru T, Kato S, Oda M et al (2012) Giant cell tumor expanded into the thoracic cavity with spinal involvement. Orthopedics 35(3):e453–e456
17. Rena O, Davoli F, Allegra G, Casadio C, Turello D (2014) Giant chordoma of the upper thoracic spine with mediastinal involvement: a surgical challenge. Asian Spine J. 8(3):353–356. https://doi.org/10.4184/asj.2014.8.3.353 **Epub 2014 Jun 9**
18. Selvaraj A, Wood AJ (2003) Superior mediastinal chordoma presenting as a bilobed paravertebral mass. Eur J Cardiothorac Surg 23:248–250
19. Topsakal C, Bulut S, Erol FS, Ozercan I, Yildirim H (2002) Chordoma of the thoracic spine: case report. Neurol Med Chir (Tokyo) 42:175–180
20. Chen B, Yang Y, Chen L, Zhou F, Yang H (2014) Unilateral lateral mass fixation of cervical spinal low-grade chondrosarcoma with intralesional resection: a case report. Oncol Lett 7(5):1515–1518 **Epub 2014 Mar 7**
21. Boriani S, Bandiera S, Colangeli S, Ghermandi R, Gasbarrini A (2014) En bloc resection of primary tumors of the thoracic spine: indications, planning, morbidity. Neurol Res 36:566–576
22. Lièvre JA, Darcy M, Pradat P, Camus JP, Bénichou C, Attali P, Joublin M (1968) Giant cell tumor of the lumbar spine; total spondylectomy in 2 states. Rev Rhum Mal Osteoartic 35(3):125–130
23. Hamdi FA (1969) Prosthesis for an excised lumbar vertebra: a preliminary report. Can Med Assoc J 100(12):576–580
24. Stener B, Johnsen OE (1971) Complete removal of three vertebrae for giant-cell tumour. J Bone Joint Surg Br 53(2):278–287
25. Stener B (1971) Total spondylectomy in chondrosarcoma arising from the seventh thoracic vertebra. J Bone Joint Surg Br 53(2):288–295
26. Roy-Camille R, Saillant G, Bisserie M, Judet TH, Hautefort E, Mamoudy P (1981) Resection vertebrale totale dans la chirurgie tumorale au niveau du rachis dorsal par voie posterieure pure. Rev Chir Orthop 67:421–430
27. Tomita K, Kawahara N, Baba H, Tsuchiya H, Nagata S, Toribatake Y (1994) Total en bloc spondylectomy for solitary spinal metastasis. Int Orthop 18:291–298
28. Tomita K, Kawahara N, Baba H, Tsuchiya H, Fujita T, Toribatake Y (1997) Total en bloc spondylectomy: a new surgical technique for primary malignant vertebral tumors. Spine 22:324–333
29. Boriani S, Weinstein JN, Biagini R (1997) Primary bone tumors of the spine. Terminology and surgical staging. Spine (Phila Pa 1976) 22(9):1036–1044
30. York JE, Berk RH, Fuller GN, Rao JS, Abi-Said D, Wildrick DM, Gokaslan ZL (1999) Chondrosarcoma of the spine: 1954 to 1997. J Neurosurg 90(1 Suppl):73–78
31. Matsumoto Y, Takahashi Y, Harimaya K et al (2013) Dedifferentiated chondrosarcoma of the cervical spine: a case report. World J Surg Oncol 11:32
32. Ozaki T, Lindner N, Hillmann A et al (1996) Influence of intralesional surgery on treatment outcome of chondrosarcoma. Cancer 77:1292–1297
33. Bennett DT, Weyant MJ (2014) Extended chest wall resection and reconstruction in the setting of lung cancer. Thorac Surg Clin 24(4):383–390
34. Yang H, Tantai J, Zhao H (2015) Clinical experience with titanium mesh in reconstruction of massive chest wall defects following oncological resection. J Thorac Dis. 7(7):1227–1234
35. Fadel E, Missenard G, Chapelier A, Mussot S, Leroy-Ladurie F, Cerrina J, Dartevelle P (2002) En bloc resection of non-small cell lung cancer invading the thoracic inlet and intervertebral foramina. J Thorac Cardiovasc Surg 123(4):676–685

European Spine Journal (2019) 28 (Suppl 2):S31–S36
https://doi.org/10.1007/s00586-018-5772-0

CASE REPORT

Rescue Nuss procedure for inferior vena cava compression syndrome following posterior scoliosis surgery in Marfan syndrome

M. Löhnhardt[1] · A. Hättich[1] · A. Andresen[1] · M. Stangenberg[1] · T. S. Mir[2] · K. Reinshagen[3] · M. Dreimann[1]

Received: 3 June 2018 / Revised: 4 September 2018 / Accepted: 25 September 2018 / Published online: 5 October 2018

Abstract

Purpose Scoliosis surgery in Marfan syndrome is common, even in the presence of a funnel chest. However, to date, no case has been reported with acute intra-/postoperative decompensation caused by vena cava compression following posterior spinal derotation and fusion.

Methods A 15-year-old male patient with Marfan syndrome, a funnel chest and severe scoliosis was treated with surgery for the spinal deformity. Intraoperatively, the patient developed a clinically relevant compression of the inferior vena cava with severe circular depression. Postoperatively, a cava compression syndrome with severe pleural effusion, ascites and enormous swelling of the lower limbs was developed. A conservative treatment of the symptoms, consisting of thoracic drainage and negative fluid balance, failed. Subsequently, the patient was transferred to pediatric intensive care unit for further treatment. Echocardiography and a CT scan demonstrated cava compression syndrome. A rescue Nuss procedure of the funnel chest deformity was performed since conservative treatment failed. The clinical course proceeded without complications and with a decrease in clinical symptoms of inferior inflow congestion. The patient was discharged after almost 3 weeks.

Conclusion The problem of congenital stenosis of the inferior vena cava in Marfan syndrome has not yet been investigated. In the case of simultaneously existing funnel chest and scoliosis in Marfan syndrome, an interdisciplinary discussion is required to decide whether a repair of the funnel chest should be performed first in order to prevent a clinically relevant compression syndrome. For the detection of a preoperatively relevant stenosis of the inferior vena cava, an MRI or thoracic/abdominal CT should be used preoperatively.

Keywords Marfan syndrome · Funnel chest · Posterior spinal fusion · Nuss procedure · Inferior vena cava syndrome · Inferior inflow congestion

Introduction

Scoliosis surgery in Marfan syndrome is common with the presence of a funnel chest (pectus excavatum). However, to date, no case of a postoperative decompensation following posterior spinal correction caused by vena cava compression has been described in the literature. In particular, a consequential Nuss procedure to repair the funnel chest in order to reduce pressure on the vein has not yet been analyzed.

The funnel chest is the most common morphological abnormality of the ventral chest wall, with an incidence of 1–8 per 1000 live births [1]. A high incidence is observed in male patients with Marfan syndrome. It typically results in an asymmetrical pectus excavatum and is used as a diagnostic criterion for Marfan syndrome [2].

The Nuss procedure (according to Nuss, 1998) [3] is a minimally invasive technique that can be described as the gold standard for correcting a funnel chest, due to its good cosmetic results and technical effectiveness. In the past, the procedure has mainly been used in children with symmetrical chest wall configurations; however, with modifications, it is now also used for asymmetrical repairs in adult patients.

✉ M. Dreimann
m.dreimann@uke.de

M. Löhnhardt
m.loehnhardt@uke.de

[1] Department of Trauma, Hand and Reconstructive Surgery, University Medical Center Hamburg-Eppendorf, Martinistrasse 52, 20246 Hamburg, Germany

[2] Department of Pediatric Cardiology, University Heart Center Hamburg-Eppendorf, Hamburg, Germany

[3] Department of Pediatric Surgery, University Medical Center Hamburg-Eppendorf, Hamburg, Germany

This surgery is considered an elective and should only be carried out after thorough planning and preparation [4, 5]. The presented case study is the first to describe Nuss surgery being performed as a rescue procedure. A posterior revision and reduction of the scoliosis correction had previously been discussed; however, due to the patient's wishes and a resulting of balance syndrome, this avenue was not pursued.

Case

The patient (15/m) was diagnosed with Marfan syndrome at the age of 8, due to scoliosis and an extreme manifestation of a pectus excavatum (Figs. 1, 2). Progressive scoliosis, severe back pain and a loss of spinal mobility after a growth spurt confirmed the indication for the posterior spinal fusion. A preoperative CT scan showed the scoliosis and pectus excavatum with a clinical irrelevant compression of the vena cava inferior (Figs. 3, 4). A dorsal instrumentation from T4 to L4 vertebrae was carried out (Fig. 5). During the surgical reduction of the lumbar spine for relordosation, a significant drop in blood pressure occurred, requiring major fluids. Intraabdominal blood loss appeared to be the cause of this complication. The reposition was ceased, and the circulation

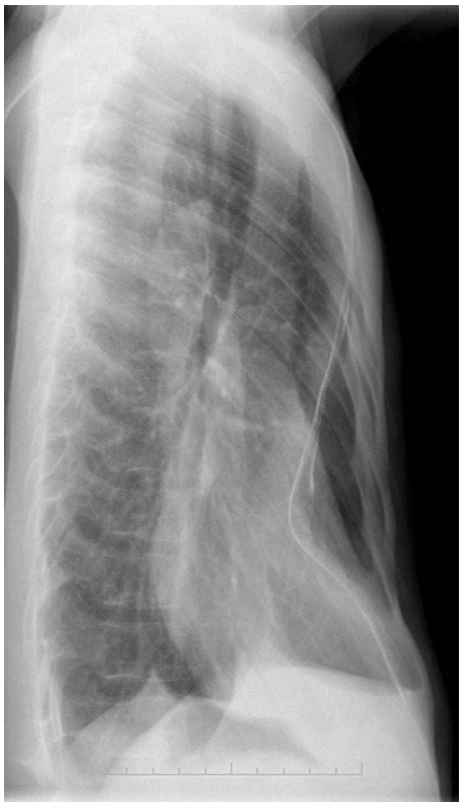

Fig. 1 X-ray showing the thorax preoperatively with obvious signs of a funnel chest

Fig. 2 X-ray showing the spine preoperatively with obvious scoliosis

was stabilized by extensive transfusion of 800 ml cell-saver-blood, 4 red cell concentrates, 1 platelet concentrate, 6 plasmas and 2000IE PCC (prothrombin complex concentrate). Following the transfusions, the dorsal reduction was performed, and the surgical procedures were completed with no further complications. The patient was transferred, intubated and ventilated, to the pediatric intensive care unit.

Following sufficient circulatory resuscitation, the patient was extubated. Due to increasing cardiac distress and a large right pleural effusion, a thoracic drainage was placed with an initial discharge of 1000 ml fluid. On the second postoperative day, the abdomen was distended with ascites, and compressed organs (e.g., liver) and diaphragmatic elevation were detected. Negative fluid balance and substitution of albumin showed a positive effect on the patient's clinical condition, and the thoracic drainage was removed. On the fourth postoperative day, the patient's clinical condition deteriorated rapidly, with large pleural effusion in the right lung and an increasing amount of free intraabdominal fluid. The pleural effusion was again treated with a thoracic drain.

Fig. 3 Preoperatively visible constriction of the inferior vena cava; CT sagittal image

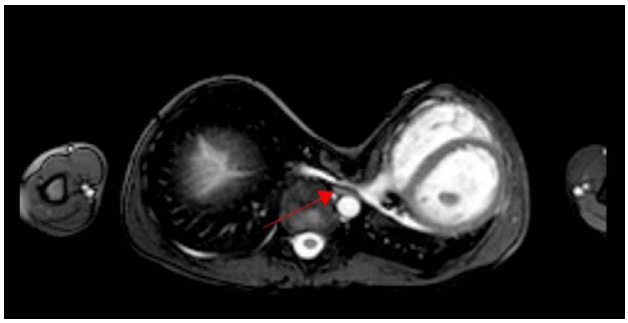

Fig. 4 Preoperatively visible constriction of the inferior vena cava; CT transversal image

The postoperative CT scan of scoliosis surgery suggested a subtotal compression of the vena cava inferior in proximity to the right ventricle, between the sternum and the spine. Furthermore, the scan showed pleural effusions in both lungs and a compression atelectasis of the left basal lung.

Then, all the patients showed severe cardiovascular depression due to severe vena cava compression syndrome. Postoperatively, the patients developed additional symptoms including right pleural effusion, inferior inflow congestion, congested gastritis and a congested liver ascites and swelling

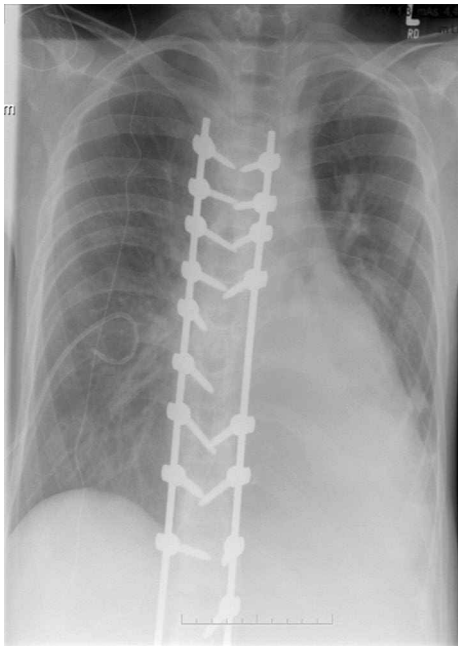

Fig. 5 X-ray showing the postoperative position after posterior spinal fusion. Cardiomegaly, uncertain pulmonary edema

of the lower limbs. Subsequently, the patient was transferred to the pediatric intensive care unit.

Therefore, the Nuss procedure was elected to solve the problems by achieving a sternal elevation by a sub-sternal bar used as an internal brace [6] to increase venous flow (Figs. 6, 7, 8, 9, 10).

The Nuss procedure was performed and a postoperative transthoracic echocardiography after showed an increased filling of the right ventricle and a regular flow of the inferior vena cava. During the clinical course, the volume status improved due to removed compression of the inferior vena cava with distinctive inferior inflow congestion. No complications occurred following the second surgical procedure, and the initial symptoms improved significantly during the clinical course. 3 weeks after the Nuss surgery, the patient was discharged with minimal residual pleural effusions and an oral diuretic therapy.

Discussion

Marfan syndrome is a congenital disorder of the connective tissue. It is an autosomal-dominant defect in microfibrils caused by mutations in the fibrillin-1 gene. This defect results in a weakness of elastic fibers. Marfan syndrome is a rare disease that affects both genders, with a prevalence of 1.5–17.2 per 100,000. Marfan syndrome is characterized by a wide variability in phenotypical appearances. In most patients, the cardiovascular, skeletal and ocular systems are

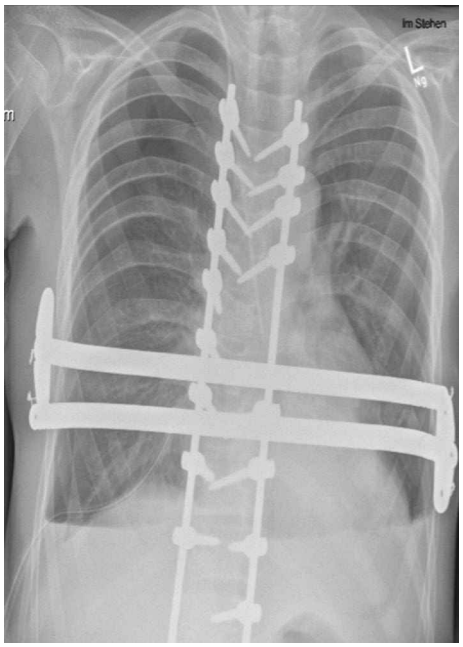

Fig. 6 X-ray showing the postoperative position after the Nuss procedure. Pleural effusions both sides. Thoracic drain right side

Fig. 7 Thoracic deformity prior to the Nuss procedure

affected by the disease. The diagnosis is on the basis of the wide variability of symptoms very complex [7, 8].

Inferior vena cava compression syndrome describes the clinical picture of reduced venous flow to the heart, which is also known as inferior inflow congestion. Pathophysiologic reasons can be the venous system itself, for instance, thrombosis or compression of the lower vena

Fig. 8 Thoracic deformity prior to the Nuss procedure

Fig. 9 Thorax after the Nuss procedure

Fig. 10 Thorax after the Nuss procedure

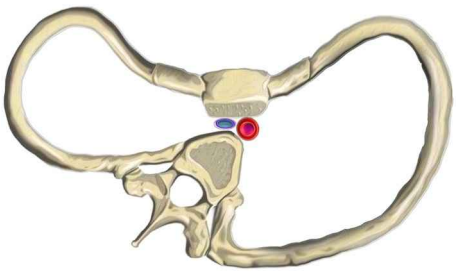

Fig. 11 Schematic illustration preoperatively

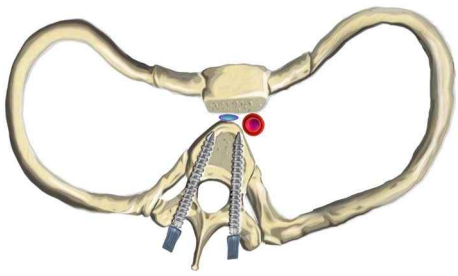

Fig. 12 Schematic illustration after posterior spinal fusion

cava by surrounding structures [9–11]. A clinical pertinent inferior vena cava compression syndrome, due to combined scoliosis and an extreme funnel chest, has not yet been described in the literature. Furthermore, no reference to a clinically pertinent inferior vena cava compression syndrome, among the wide range of cardiovascular symptoms in Marfan syndrome, can be found in the specialist literature. Ghazal et al. [12] described for the first time a congenital stenosis of the inferior vena cava in Marfan syndrome in their 2015 case report. Overall, congenital stenosis or aberrations of the inferior vena cava are very rare. Most commonly, stenosis of the inferior vena cava is observed in the area of the diaphragm or the liver [13].

In the present case, the preoperative cross-sectional imaging showed a significant constriction of the inferior vena cava close to the caval opening of the diaphragm (Figs. 2, 3); however, this was clinically asymptomatic. The correction of scoliosis resulted in a clinically relevant compression of the inferior vena cava against the distinctive funnel chest. Intraoperatively, a relevant cardiovascular depression was caused by the vena cava compression that was stabilized by mitigation of the reposition maneuver and intraoperative mass transfusion. During the clinical course, however, the symptoms of the inferior inflow congestion persisted, resulting in the urgent indication of a surgical correction of the distinctive funnel chest.

A treatment algorithm for the surgical procedure in distinctive scoliosis in the context of Marfan syndrome has not yet been described in the literature. The presented case shows that stenosis of the inferior vena cava already existed preoperatively; however, the clinical relevance concerning scoliosis correction is not yet apparent. The schematic illustrations show the compression of the inferior vena cava before and after each surgery (Figs. 11, 12, 13). MRI or multi-detector CT scans are used to detect this type of stenosis, although there are no data in the literature regarding the degree of restriction at which a clinically relevant inferior cava syndrome is expected. This is mainly due to the fact that the problem of congenital stenosis of the inferior vena cava in Marfan syndrome has not yet been sufficiently investigated.

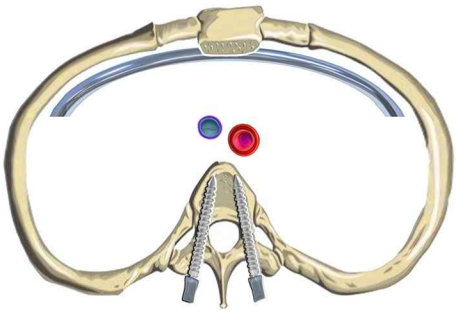

Fig. 13 Schematic illustration after Nuss procedure

Conclusion

When surgical scoliosis correction is indicated and planned in a patient with Marfan syndrome, scoliosis and funnel chest MRI or thoracic/abdominal CT should be performed preoperatively. When there is stenosis of the inferior vena cava, a multidisciplinary preoperative discussion including pediatric cardiologists, cardiothoracic surgeons, radiologists and orthopedic surgeons is recommended to evaluate the relevance of the stenosis. When a risk of further constriction of the inferior vena cava by surgery exists, it should be discussed whether a correction of the funnel chest should be performed first to prevent a clinically relevant compression syndrome. A standardized measurement of the diameter of the inferior vena cava should be carried out in all Marfan patients in order to detect individual risk.

Conflict of interest None of the authors has any potential conflict of interest.

References

1. Brochhausen C, Turial S, Müller FK et al (2012) Pectus excavatum: history, hypotheses and treatment options. Interact CardioVasc Thorac Surg 14:801–806
2. Cobben JM, Oostra RJ, van Dijk FS (2014) Pectus excavatum and carinatum. Eur J Med Genet 57:414–417

3. Nuss D, Kelly RE Jr, Croitoru DP et al (1998) A 10-year review of a minimally invasive technique for the correction of pectus excavatum. J Pediatr Surg 33:545–552
4. Coln D, Gunning T, Ramsay M et al (2002) Early experience with the Nuss minimally invasive correction of pectus excavatum in adults. World J Surg 26:1217
5. Park HJ, Lee SY, Lee CS, Youm W, Lee KR (2004) The Nuss procedure for pectus excavatum: evolution of techniques and early results on 322 patients. Ann Thorac Surg 77:289–295
6. Nuss D, Obermeyer RJ, Kelly RE (2016) Nuss bar procedure: past, present and future. Ann Cardiothorac Surg 5:422–433
7. Mueller GC, Stark VC, Steiner K, von Kodolitsch Y, Rybczynski M, Weil J, Mir TS (2013) Impact of age and gender on cardiac pathology in children and adolescents with marfan syndrome. Pediatr Cardiol 34(4):991–998
8. Loeys BL, Dietz HC, Braverman AC et al (2010) The revised Ghent nosology for the Marfan syndrome. J Med Genet 47:476–485
9. Palladino E, Nsenda J, Siboni R et al (2014) A giant mesenteric desmoid tumor revealed by acute pulmonary embolism due to compression of the inferior vena cava. Am J Case Rep 15:374–377
10. Serdar A, Ufuk C, Dilek K et al (2013) Neonatal neuroblastoma with inferior vena cava syndrome. APSP J Case Rep 4:10
11. Krywko DM, Bhimji SS (2017) Aortocaval compression syndrome. StatPearls Publishing, Treasure Islan
12. Ghazal SN, Ouf SG (2015) Inferior vena cava stenosis: echocardiographic diagnosis in Marfan syndrome. Glob Cardiol Sci Pract 2015:50
13. Koc Z, Oguzkurt L (2007) Interruption or congenital stenosis of the inferior vena cava: prevalence, imaging, and clinical findings. Eur J Radiol 62:257–266

European Spine Journal (2019) 28 (Suppl 2):S37–S40
https://doi.org/10.1007/s00586-018-5823-6

CASE REPORT

Posterior atlantoaxial dislocation without fracture or neurological symptoms treated by transoral–posterior approach surgery: a case report and literature review

Shenghua Ning[1] · Sidong Yang[2] · Wenyuan Ding[2] · Tianxiao Ma[1] · Zhanyong Wu[1]

Received: 30 June 2018 / Accepted: 6 November 2018 / Published online: 17 November 2018

Abstract

Background Atlantoaxial dislocation usually results from hyperextension trauma and is almost always accompanied by odontoid fracture and neurological symptoms. In most cases, patients with atlantoaxial dislocation die instantly. This is a rare report of posterior atlantoaxial dislocation without fracture and neurological symptoms effectively treated by transoral–posterior approach surgery, and only eleven similar cases have been previously reported.

Objective To describe the very rare case of an adult posterior atlantoaxial dislocation patient without fracture who was neurologically treated using transoral–posterior approach surgery and to review the relevant literature.

Method A 52-year-old man riding a motorcycle was rear-ended by a car. Using X-ray, computed tomography (CT) scan and magnetic resonance imaging (MRI), he was diagnosed with posterior atlantoaxial dislocation without a related fracture or a significant change in spinal cord signal. Transoral–posterior approach surgery with sustained skull traction was used after failed closed reduction.

Result During a 6-month follow-up observation, the lateral cervical spine radiography and sagittal reconstructions of CT scans demonstrated no instability of the atlantoaxial complex. Few patients experience posterior atlantoaxial dislocation without a related fracture or spinal cord deficit. For a patient who experiences trauma with hyperextension, such as in rear-end collisions, X-ray, CT scan and MRI should be performed to ensure that this injury is diagnosed. It is necessary to perform surgery to recover atlantoaxial stability, even in the absence of fracture or neurological symptoms.

Conclusion Transoral–posterior approach surgery is a safe and effective way to manage irreducible posterior atlantoaxial dislocation.

Keywords Atlantoaxial dislocation · Transoral–posterior · Skull traction

Introduction

Posterior atlantoaxial dislocation resulting from traffic accidents usually causes death immediately regardless of odontoid fracture, and very few patients have survived, both with and without neurological symptoms. Related reports describing treatments for posterior atlantoaxial dislocation in the absence of fracture or neurological deficit are very rare. By using conservative traction, most dislocations have been reduced. Posterior or anterior internal fixation and fusion should be supplemented to increase atlantoaxial complex stability. Although a few similar cases have been reported subsequently, the choice of ideal treatment strategy remains controversial and the prognosis is not fully clear. Here, we present a new case which was treated effectively through a combined anterior–posterior approach. The patient was informed that data concerning the case would be submitted for publication and he consented to publish the data.

✉ Zhanyong Wu
540339280@qq.com

[1] Department of Orthopedic Surgery, Orthopedic Hospital of Xingtai, Xingtai 054000, Hebei, China

[2] Department of Spinal Surgery, The Third Hospital of Hebei Medical University, Shijiazhuang 050051, China

Case report

A 52-year-old male patient riding a motorcycle was struck by a car and brought to the local county hospital immediately. He was diagnosed as atlantoaxial dislocation, multiple

soft tissue laceration and dislocation of the left ankle joint. According to the county hospital medical record, the conscious and vital parameters of this patient were normal, and he complained about pain in his neck and throat. After 2 days of treatment, including reduction in the ankle joint, debridement of soft tissue laceration and immobilization with a neck collar, the patient was transferred to our hospital for further diagnosis and treatment. Physical examination immediately upon arrival in our hospital showed that motion of his neck was obviously limited, but movements of his limbs were normal with grade IV–V force. Neurological function was defined as E according to the American Spinal Injury Association's (ASIA) standardized neurological classification of spinal cord injury.

Neither severe brain nor abdominal–thoracic injury was found by the initial CT scan. Anteroposterior, lateral and open-mouth X-ray of the patient's cervical vertebrae demonstrated a retro-positioned atlas and total atlantoaxial dislocation (Fig. 1). CT scanning and MRI confirmed the X-ray findings (Fig. 2). There was no cord compression or significant change in the spinal cord signal (Fig. 3).

Four kilograms of skull traction was applied to this patient. Intraoperative real-time fluoroscopy showed that the distance between the atlas and axis was enlarged but was still suitable for reduction. We did not increase the traction strength to avoid causing severe spinal cord injury. The preoperative plan was partial odontoidectomy to reduce

Fig. 1 Lateral radiography of the cervical spine shows posterior dislocation of the atlas with respect to the axis

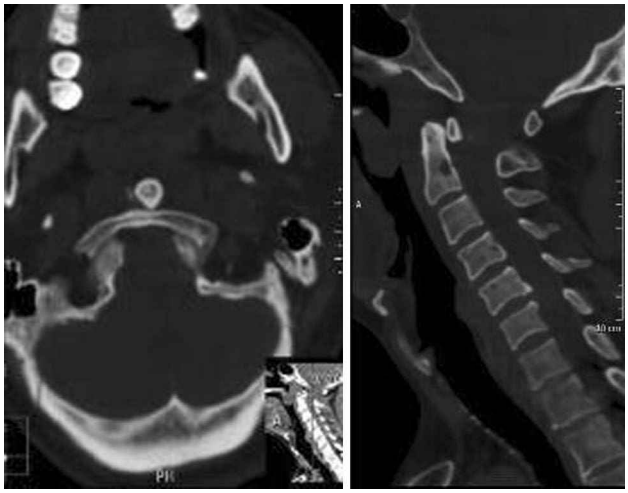

Fig. 2 Axial CT scans confirmed that the odontoid peg was ventral to the anterior arch of the atlas (**a**). Sagittal reconstructions verified lack of rotation or fractures of the odontoid

dislocation. We exposed the axis and atlas by a transoral and retropharynx approach [1] with oral tracheal intubation instead of nasal tracheal intubation anesthesia for convenient nasal disinfection. We performed intraoperative real-time X-ray after anterior atlantoaxial release, which indicated a reduction in atlantoaxial dislocation (Fig. 4). Then, we performed closure in anatomical layers and without grafting in the anterior procedure. Keeping the tracheal cannula and skull traction, we changed the position of the patient for posterior approach surgery. We fixed C1–C2 by an implant

Fig. 3 MRI demonstrated no cord compression or intramedullary cord signal abnormality at the level of the atlantoaxial dislocation

pedicle screw system under lateral fluoroscopy autografted with the morselized iliac crest bone. We did not use any spinal cord monitoring, except a wake-up test.

After the operation, we removed the oral tracheal cannula immediately and moved the patient back to the ward with cardiac monitoring. This patient did not experience complex complications, iatrogenic neurological deficits or postoperative infection. Postoperative lateral radiography and CT scans of the cervical spine showed that there was no instability of the atlantoaxial complex (Fig. 5) and neck and throat symptoms disappeared gradually. His postoperative recovery was very favorable. Three months after the operation, the patient was instructed to remove his neck collar. He has returned to normal life, goes to work and is self-sufficient.

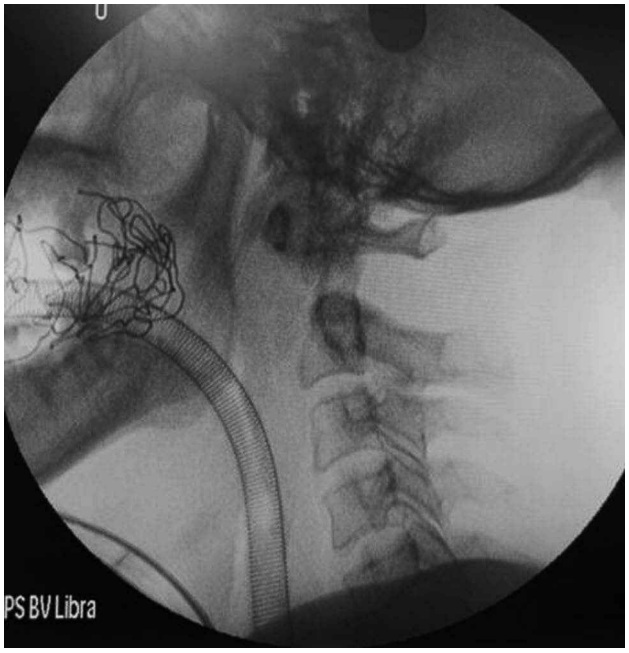

Fig. 4 After anterior atlantoaxial release, intraoperative real-time fluoroscopy showed that the atlantoaxial dislocation had been reduced

Discussion

According to the anatomical structure of C1–C2, the anterior arch of the atlas and the transverse ligament form an osteo-ligamentous ring to create an interlocking odontoid process that combines with interlocking articular processes to provide the main stability of the atlantoaxial complex. Odontoid fracture and ligament rupture characterize most atlantoaxial dislocations. Severe trauma from extension and slack ligaments always results in the odontoid slipping out of the osteo-ligamentous ring and the atlas with respect to the axis, which is called posterior atlantoaxial dislocation. Only 11 cases similar to the present case have been reported in the English-language literature [1–11]. Based upon past experience, cervical spine injury with hyperextension that produces posterior atlantoaxial dislocation like this generally causes immediate and lethal spinal cord damage. However, in the emergency room, this dislocation might be missed due to a lack of symptoms related to neurological deficit and odontoid fracture. Therefore, the incidence of this type of dislocation is likely much higher than previously reported. Haralson et al. [4] believed that posterior atlantoaxial dislocation may be caused by hyperextension with variable amounts of distraction. The neural canal at the atlantoaxial level can be roughly divided into three parts: the odontoid, the spinal fluid and the spinal cord [12]. In some cases, the spinal cord will not be compromised because the neural canal provides adequate space. Tucker and Taylor

Fig. 5 Lateral cervical spine radiography and sagittal reconstructions of CT scans demonstrated stability of the atlantoaxial complex 3 months after the operation

corroborated this idea, finding that canal area decreased to 36% in a skeletal study of simulated posterior atlantoaxial dislocation [13].

Regarding posterior atlantoaxial dislocation diagnosis in the absence of neurological symptoms or odontoid fracture, the atlas and axis are not clearly observed using plain radiography of the cervical spine because the cranial bones overlap and some patients compulsively adopt head or neck positions that obscure the view. Therefore, we guess the misdiagnosis of atlantoaxial dislocation is not infrequent during routine anteroposterior and lateral radiography of the cervical spine. With regard to patients who suffer trauma with hyperextension, such as in a rear-end collision, we should be mindful of this situation and conduct additional examinations, such as tomography and open-mouth X-ray. Despite the low resolution for soft tissues, CT scan shows the bony structures of the atlas and axis clearly. In this case, the structures of the C1–C2 complex were clearly visualized by CT axial scanning. The odontoid peg had slipped from the dorsal to the ventral side of the anterior arch of the atlas, and there was no sign of odontoid fracture. MRI has the advantage of high resolution of soft tissues. In this case, the curve of the cervical spinal cord was changed, as shown by MRI, but there were no abnormal signals or cord compression at the level of C1–C2. Hence, we should use MRI, CT scan and CT three-dimensional reconstruction for a patient with a history of hyperextension trauma.

There are two major methods for treating posterior atlantoaxial dislocation, including closed reduction through traction and open reduction by operation. Closed reduction for this kind of case is effective but dangerous due to the risk of neurological deficit and immediate death caused by overdistraction of the C1–C2 complex. High technical skill and a suitable traction weight are required. Some authors managed this type of dislocation by closed reduction using the three-phase method described by Wong et al. [2, 15, 16]. Some cases have been reduced successfully with 7–10 kg of traction [2, 14, 15]. After the dislocation is reduced, these patients should wear a cervical collar for 3 months in case of instability [2]. Two reported cases required posterior fusion of C1–C2 after closed reduction to treat persistent instability [14, 15].

Posterior atlantoaxial dislocation without odontoid fracture or neurological symptoms is very rare, and there is not a standard operation technique for this kind of dislocation. Jiang et al. [11] reported a similar case treated via an anterior retropharyngeal approach with partial odontoidectomy. In our case, after anterior atlantoaxial release, the atlantoaxial dislocation was reduced. Therefore, we do not believe that partial odontoidectomy is necessary for all cases of posterior atlantoaxial dislocation. Although this surgery was successful, some questions remain. For example, we do not know whether the closed reduction failure was caused by insufficient time or weight of traction or whether changing traction posture favors reduction, but this operation is associated with a very high risk of spinal cord injury and immediate death. Therefore, we suggest applying spinal cord monitoring to closed reduction when choosing the time and weight of traction.

Compliance with ethical standards

Conflict of interest None of the authors has any potential conflict of interest.

References

1. DeAndrade JR, MacNab I (1969) Anterior occipito-cervical fusion using an extra-pharyngeal exposure. J Bone Jt Surg Am 51:1621–1626
2. Chaudhary R, Chaudhary K, Metkar U, Rathod A, Raut A, Sanghvi D (2008) Posterior atlantoaxial dislocation without odontoid fracture. Skelet Radiol 37:361–366
3. Fox JL, Jerez A (1977) An unusual atlanto-axial dislocation. Case report. J Neurosurg 47:115–118
4. Haralson RH III, Boyd HB (1969) Posterior dislocation of the atlas on the axis without fracture. Report of a case. J Bone Jt Surg Am 51:561–566
5. Jamshidi S, Dennis MW, Azzam C, Karim N (1983) Traumatic posterior atlantoaxial dislocation without neurological deficit: case report. Neurosurgery 12:211–213
6. Patzakis MJ, Knopf A, Elfering M, Hoffer M, Harvey JP Jr (1974) Posterior dislocation of the atlas on the axis: a case report. J Bone Jt Surg Am 56:1260–1262
7. Sassard WR, Heinig CF, Pitts WR (1974) Posterior atlanto-axial dislocation without fracture. Case report with successful conservative treatment. J Bone Jt Surg Am 56:625–628
8. Sud S, Chaturvedi S, Buxi TB, Singh S (2002) Posterior atlantoaxial dislocation without associated fracture. Skelet Radiol 31:529–531
9. Wong DA, Mack RP, Craigmile TK (1991) Traumatic atlantoaxial dislocation without fracture of the odontoid. Spine 16:587–589
10. Yoon DH, Yang KH, Kim KN, Oh SH (2003) Posterior atlantoaxial dislocation without fracture: case report. J Neurosurg 98:73–76
11. Jiang LS, Shen L, Wang W, Wu H, Dai LY (2010) Posterior atlantoaxial dislocation without fracture and neurologic deficit: a case report and the review of literature. Eur Spine J 19:S118–S123
12. Steel HH (1968) Anatomical and mechanical consideration of the atlantoaxial articulation. J Bone Jt Surg Am 50:1481–1482
13. Tucker SK, Taylor BA (1998) Spinal canal capacity in simulated displacements of the atlantoaxial segment: a skeletal study. J Bone Jt Surg Br 80:1073–1078
14. Jain VK (2012) Atlantoaxial dislocation. Neurol India 60:9–17
15. Neumann U, Urbanski H, Riedel K (2003) Posterior atlantoaxial dislocation without fracture of the odontoid. A case report. J Bone Jt Surg Am 85-A:1343–1346
16. Lapsiwala SB, Anderson PA, Oza A (2006) Biomechanical comparison of four C1–C2 rigid fixative techniques: anterior transarticular, posterior transarticular, C1–C2 pedicle, and C1–C2 intralaminar screws. Neurosurgery 58:516–521

European Spine Journal (2019) 28 (Suppl 2):S41–S50
https://doi.org/10.1007/s00586-018-5831-6

CASE REPORT

Lung metastases regression with increased CD8+ T lymphocyte infiltration following preoperative spinal embolization and total en bloc spondylectomy using tumor-bearing frozen autograft in a patient with spinal metastatic leiomyosarcoma

Noritaka Yonezawa[1] · Hideki Murakami[1] · Apiruk Sangsin[1] · Eishiro Mizukoshi[2] · Hiroyuki Tsuchiya[1]

Received: 14 April 2018 / Accepted: 12 November 2018 / Published online: 21 November 2018

Abstract

Purpose To report systemic immunological enhancement following preoperative spinal embolization and total en bloc spondylectomy (TES) using tumor-bearing frozen autograft in a patient with spinal metastatic leiomyosarcoma.

Methods A 44-year-old woman with metastatic uterine leiomyosarcoma of the lung and L1 vertebra underwent TES following bilateral three-level preoperative segmental artery embolization. Resected tumor-bearing lamina was frozen using liquid nitrogen and used as tumor-bearing bone graft for spinal reconstruction.

Results Tumor necrosis and obstructing material used in preoperative embolization were detected in the resected specimen of L1. Five days after TES, chest computed tomography scan demonstrated decreased solitary lung mass size without adjuvant treatment. Lobectomy was performed for the lung metastasis 42 days after TES. Infiltration of CD8+ T lymphocyte into tumor tissue significantly increased in shrunk lung metastasis. On the other hand, slight infiltration in both the resected L1 and primary uterine lesion was observed. Six months after TES, activities of daily living were normal with no evidence of local recurrence or distant metastasis. One year after TES, however, lung CT revealed occurrence of another lung metastasis, and molecular-targeting therapy (pazopanib) was initiated.

Conclusions There were no reports demonstrating metastasis regression with CD8+ T lymphocyte infiltration after TES. This case demonstrated that preoperative tumor embolization combined with TES using tumor-bearing autograft provided both a local radical cure and systemic antitumor immunological enhancement, although the long-term effect can be limited.

Keywords Frozen autograft · Embolization · CD8 · Leiomyosarcoma · Spondylectomy

Introduction

Leiomyosarcoma is a malignant soft tissue sarcoma rarely arising in the uterus. Uterine leiomyosarcoma comprises only 1% of all uterus malignancies [1], but has high recurrence rates (45–73%) [2] even with aggressive management. Distant metastasis indicates late-stage disease and has limited treatment options with a 10–35.8% 5-year survival rate [3–5]. Skeletal metastasis occurs in 13.8% of cases [5]. The spine is one of the more common skeletal sites and can be highly morbid and deadly. The surgical options for spinal metastatic leiomyosarcoma range from spinal decompression to en bloc excision. Postoperative radiation and chemotherapy have been used, but no definitive guidelines exist due to their controversial efficacy. Herein, we present a case of metastatic uterine leiomyosarcoma of the lung and L1 vertebra that was successfully treated with total en bloc spondylectomy (TES) using tumor-bearing frozen autograft for reconstruction. After surgery, solitary lung metastasis regression was observed. CD8+ T lymphocyte infiltration into tumor tissue significantly increased in shrunk lung

Electronic supplementary material available on
http://collections.medengine.com/orthopedics/world-spine-day/

✉ Hideki Murakami
hmuraka@med.kanazawa-u.ac.jp

[1] Department of Orthopedic Surgery, Kanazawa University School of Medicine, 13-1 Takara-machi, Kanazawa 920-8641, Japan

[2] Department of Gastroenterology, Kanazawa University Hospital, 13-1 Takara-machi, Kanazawa 920-8641, Japan

metastasis with slight infiltration in both L1 and the primary lesion, suggesting systemic immunological enhancement.

Case report

History and clinical evaluation

A 44-year-old woman was diagnosed with a malignant tumor of the uterus. Three months later, she underwent total hysterectomy at another institution. Histopathological evaluation revealed uterine leiomyosarcoma. She complained of low back pain 2 years later. Lumbar anteroposterior and lateral plain radiographs revealed cortical erosion of the superior and inferior endplates of L1 vertebral body, while the other lumbar vertebrae appeared normal (Fig. 1). Computed tomography (CT) scan and T2-weighted magnetic resonance imaging revealed extensive destruction of L1 vertebral body, causing pathological fracture and extracompartmental invasion of the tumor into the spinal canal and left side of the vertebral body (Figs. 2, 3). Chest CT scan revealed 20 × 21 mm solitary left lung mass suspected of lung metastasis (Fig. 4a).

Treatment

Preoperative embolization of bilateral segmental arteries at three levels was performed 3 days before TES (Fig. 5). Combined left anterolateral retroperitoneal and posterior approach TES was performed without preoperative chemotherapy or radiation. Left anterolateral retroperitoneal approach was initially performed to dissect the segmental arteries from the left lateral aspect of the vertebral body due to extra-compartmental invasion of the tumor on the left side of the vertebral body. The left psoas major muscle was cut to expose the adjacent disks, and the bilateral segmental vessels of L1 were cut (Fig. 6a, b). The posterior approach was subsequently performed. The lower half of T12 lamina was removed to expose the L1 superior articular facet. L1 posterior elements were removed using flexible multifilament thread wire (T-saw; Pro Medical, Kanazawa, Japan) [6], and bilateral L1 nerve roots were ligated and cut. Blunt dissection was performed around the affected vertebra and adjacent disk level. Bilateral pedicle screws were inserted and affixed with a rod on the right side. T12/L1 and L1/2 intervertebral disks were then cut using an L-shaped chisel. L1 vertebral body was then removed en bloc posteriorly (Fig. 6c). After removal of surrounding musculoligamentous tissues, the excised tumor-bearing lamina was frozen by immersing in liquid nitrogen for 20 min. For spinal reconstruction, the frozen lamina was crushed and packed into a titanium mesh cage that was inserted into the anterior defect. A large amount of excess frozen autograft was placed around the cage. The posterior instrumentation was adjusted to slightly compress the inserted cage.

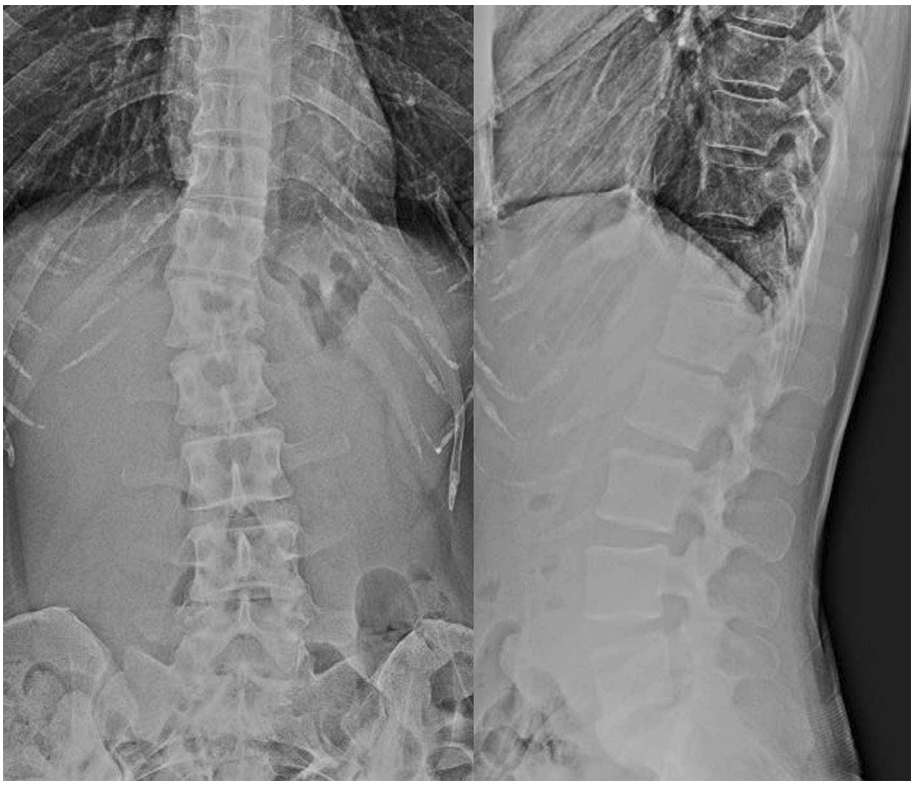

Fig. 1 Preoperative radiograph of the lumbar spine. A radiograph revealed cortical erosion at the superior and inferior endplates of L1 with pathological fracture

Fig. 2 Preoperative computed tomography images of the lumbar spine. Computed tomography image revealed osteolytic tumor involving the L1 vertebral body

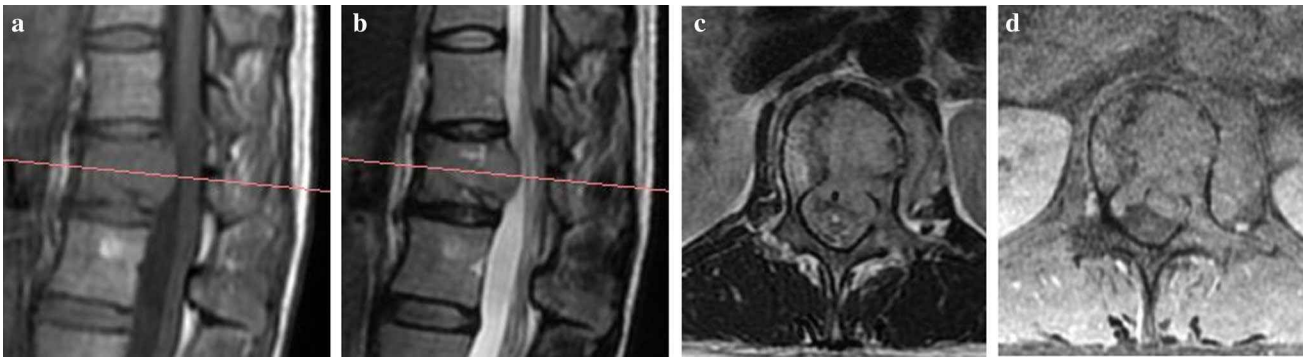

Fig. 3 Preoperative magnetic resonance imaging of the lumbar spine. T1- (**a**) and T2-weighted (**b** and **c**) images. Tumor enhancement was observed with gadolinium contrast (**d**)

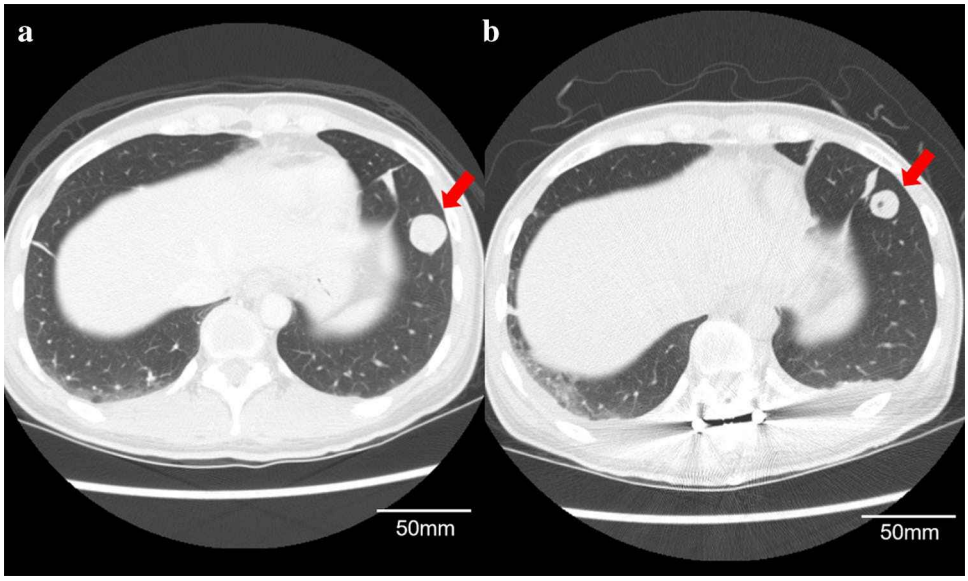

Fig. 4 Pre- and postoperative chest computed tomography images. Before surgery (**a**) and 5 days after total en bloc spondylectomy (**b**). Chest computed tomography scan demonstrated decreased solitary lung mass size to 16 × 18 mm without receiving any adjuvant treatment

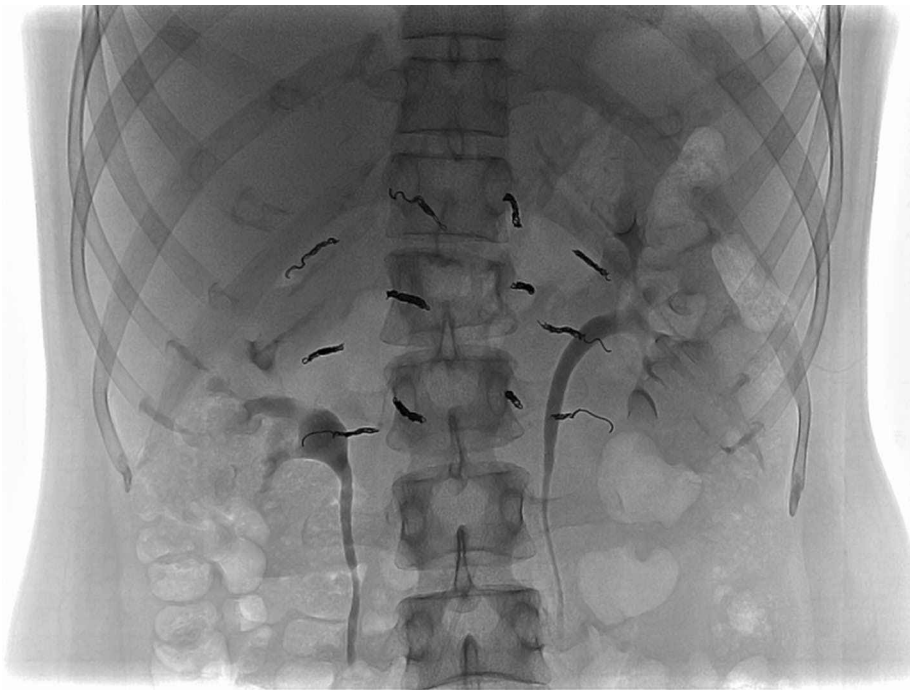

Fig. 5 Preoperative tumor embolization. Preoperative embolization of bilateral segmental arteries at three levels was performed 3 days before total en bloc spondylectomy

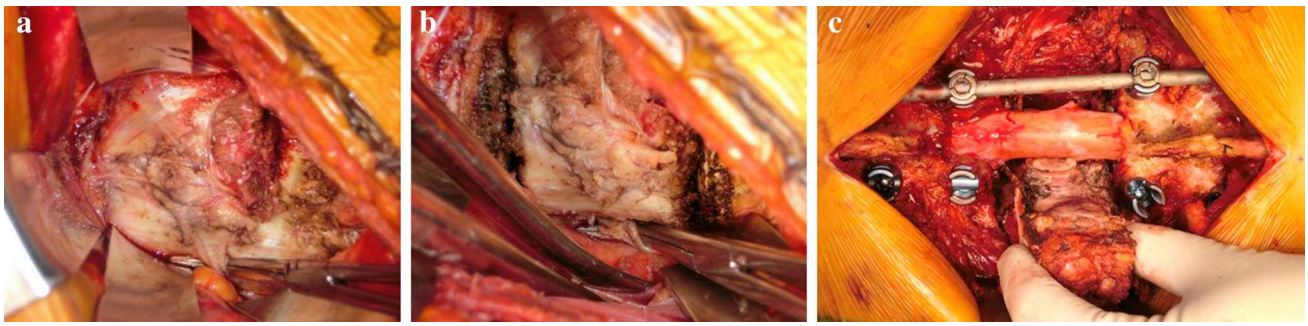

Fig. 6 Intraoperative photographs. Left anterolateral retroperitoneal approach to dissect segmental arteries from the left lateral aspect of the vertebral body. Bilateral segmental vessels of L1 were cut and ligated through this approach: left (**a**) and right (**b**) segmental artery. L1 vertebral body was removed en bloc posteriorly (**c**)

Pathological findings of resected L1

Histological analysis of L1 body sections was performed. Pathological analysis revealed metastasis of uterine leiomyosarcoma. Immunohistochemistry showed that the majority of cells were αSMA-, caldesmon-, desmin-, ER-, and PgR-positive, but negative for CD34, S-100, and EMA. Partial tumor necrosis and obstructing material used in preoperative embolization were detected in the resected specimen (Fig. 7).

Postoperative course

No postoperative complications occurred, and she walked independently 2 weeks after surgery. Five days after TES, chest CT scan demonstrated decreased solitary lung mass size to 16 × 18 mm without receiving any adjuvant treatment (Fig. 4b). Forty-two days after TES, lobectomy of solitary lung metastases was performed. Tumor necrosis was detected in resected lung metastasis, and the ratio of tumor necrosis compared to the whole area of the tumor was approximately 18% (Figs. 8, 9a). Infiltration of CD8+ T lymphocyte into tumor tissue for L1, lung metastasis, and uterus as primary lesion was histologically evaluated (Fig. 9a, b). A rabbit polyclonal antibody against CD8 (1:100, ab101500; Abcam, Cambridge, UK) was used as the primary antibody. Antimouse or rabbit IgG conjugated with peroxidase-labeled polymers (EnVision; Dako, Carpinteria, CA, USA) was used as the secondary antibody. Immunological study revealed

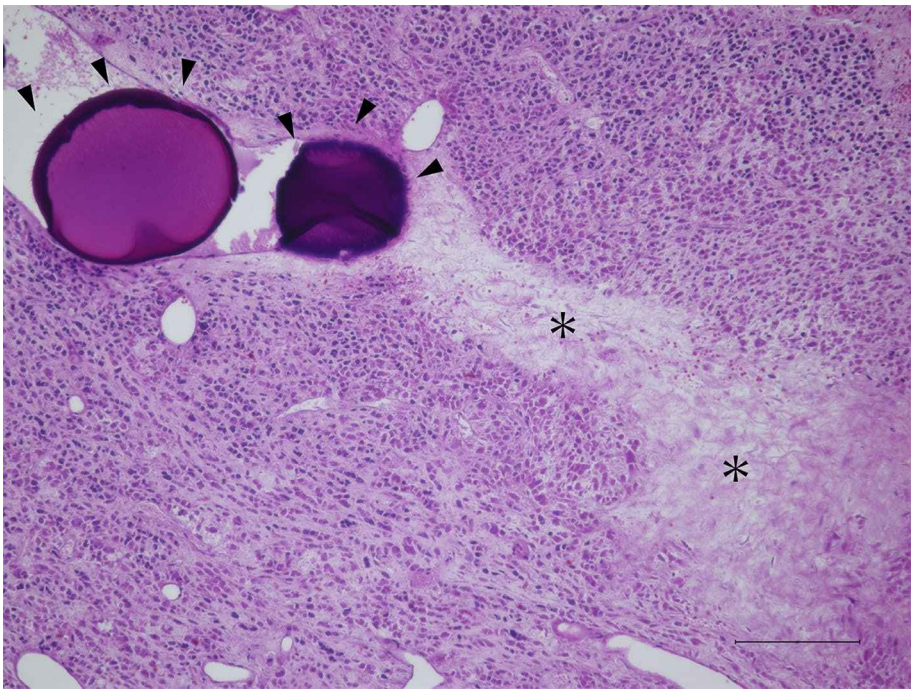

Fig. 7 Pathological findings of the resected tumor (hematoxylin and eosin staining). Tumor necrosis and obstructing material were detected in the resected specimen. Black arrowhead indicates obstructing material. Asterisk indicates tumor necrosis. Scale bar corresponds to 200 µm

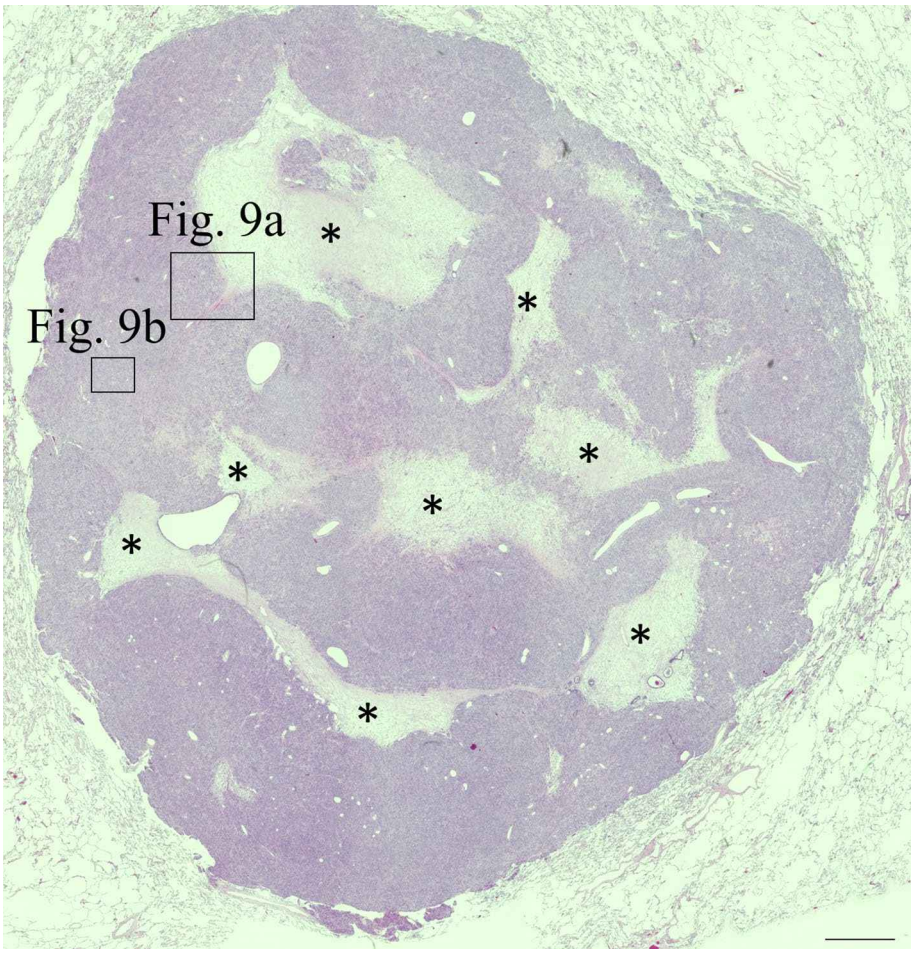

Fig. 8 Histological analysis of resected shrunk lung metastasis (hematoxylin and eosin staining). The asterisk indicates tumor necrosis. The ratio of tumor necrosis compared to the whole area of the tumor was approximately 18%. Scale bar corresponds to 1000 µm

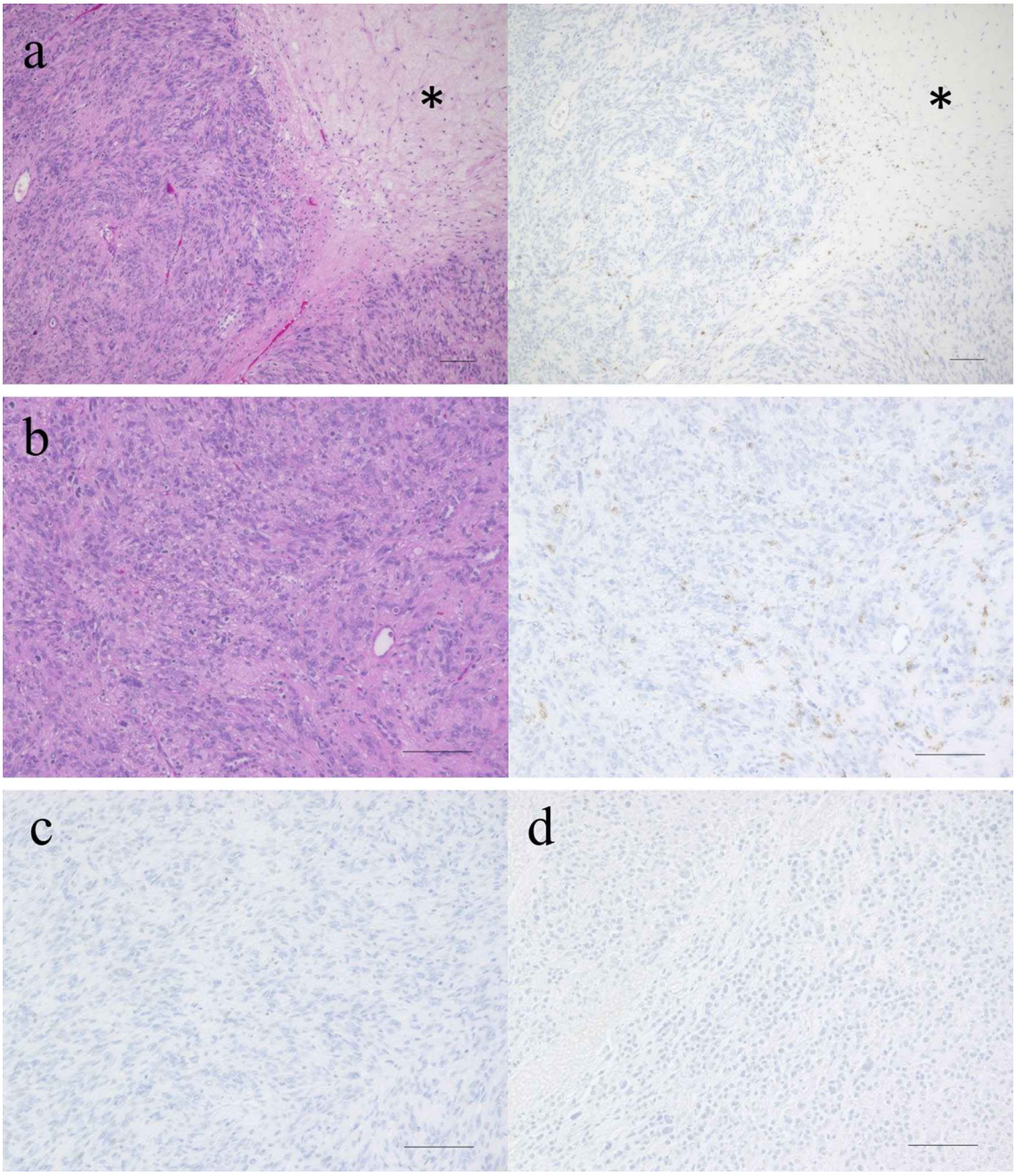

Fig. 9 Histological analysis of resected shrunk lung metastasis (**a**, **b**), primary legion of uterus (**c**), and L1 vertebral body (**d**) (hematoxylin and eosin staining and CD8 immunostaining). The asterisk indicates tumor necrosis. Histologically evaluated determined significantly increased infiltration of CD8+ T lymphocyte in shrunk lung metastasis (**a**, **b**), and no infiltration in both primary uterine lesion (**c**) and L1 vertebral body (**d**). Scale bar corresponds to 100 µm

significantly increased CD8+ T lymphocyte infiltration into tumor tissue in shrunk lung metastasis. On the other hand, slight infiltration in L1 or primary uterine lesion was observed (Fig. 9c, d). Total number of CD8+ cells per ten high power fields was 347 cells (lung metastasis), 9 cells (L1), and 15 cells (primary uterine lesion). Six months after TES, activities of daily living were normal with no evidence of local recurrence or distant metastasis. One year after TES, however, lung CT revealed occurrence of another lung metastasis, and molecular-targeting therapy (pazopanib) was initiated. Postoperative radiography and CT demonstrated that the reconstructed spine was well-maintained (Fig. 10).

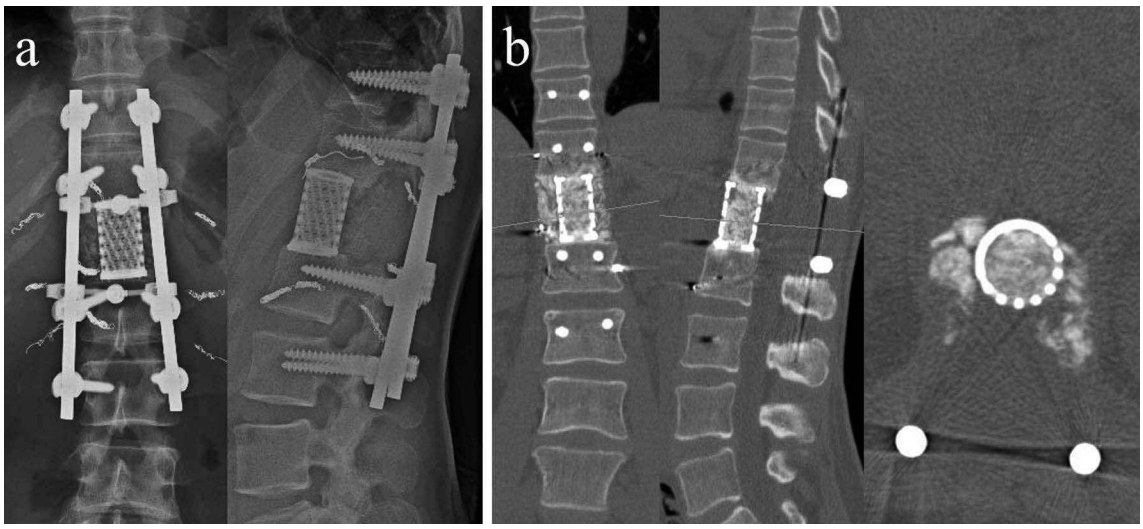

Fig. 10 Postoperative radiological findings 1 year after total spondylectomy. Postoperative radiography and computed tomography demonstrated that the reconstructed spine was well-maintained. A large amount of excess frozen autograft was placed around the cage

Discussion

Spinal metastatic leiomyosarcoma is rare, with only three case series and few case reports published [7–9]. Due to its rarity, disease management is based on clinical case reports, clinical status, and patient survival, which are considered for palliative purposes. There are no current recommendations for adjuvant therapies; however, most spinal metastatic leiomyosarcoma cases received radiation or chemotherapy [7–9]. Radiation in spinal metastasis controls local symptoms and preserves neurological function; however, radioresistant and infiltrative growth pattern of the sarcoma, and difficulty in delivering optimal doses, causes high recurrence rate. For example, stereotactic radiosurgery has a local control rate of 84–88% in metastatic spinal sarcomas [10, 11]; however, failure in metastatic leiomyosarcoma yielded high recurrence rate (32%) compared to other sarcoma types overall (21%) [12]. While efficacy of radiation in spinal metastatic leiomyosarcoma is limited, chemotherapy efficacy still lacks evidence; thus, surgeries are the best treatment, when feasible. Survival from spinal metastatic leiomyosarcoma varies from weeks to up to 13 years [7, 8]. We expected long survival in this patient because she had single-level spinal involvement and single lung metastasis that suited the metastasectomy. Thus, aggressive approaches, including TES of L1 and lobectomy of solitary lung metastases, were performed.

Reconstruction using tumor-bearing autograft treated with liquid nitrogen in patients with malignant bone tumor is safe and effective [13] with no reported local recurrences. Advantages of frozen autografts include: low cost; osteoinductive and osteoconductive properties; good fit between graft and host bone; no disease transmission, immunological rejection, or harmful denatured substances; early revitalization; and cryoimmunological effects [14–16]. Possible induction of systemic antitumor immune response from reimplantation of destroyed tumor tissue treated with liquid nitrogen was observed in a murine model [17] and patient with osteosarcoma who was concurrently treated with dendritic cell therapy [18].

This reconstruction technique has been concurrently performed in TES at our institute since 2010. This technique eliminates graft harvest-site morbidity, decreases blood loss, and shortens surgical time [19]. Our institute previously reported three cases of carcinoma with regression of lung or lymph node metastasis following TES using tumor-bearing frozen autograft for reconstruction, combined with preoperative spinal embolization [20–22]. The present study is the first case of sarcoma showing clinical response of cryoimmunology using this reconstruction technique in TES, combined with preoperative embolization. Further, in 60 TES cases that used this combined reconstruction technique and preoperative embolization, mean IL-12 and IFN-γ relative concentrations significantly increased after TES [23].

Metastatic tumor regression with infiltration of CD8+ T cells in the metastatic tumor tissue is considered as enhancement of immune response. CD8+ T lymphocytes play a central role in immunity to cancer through their capacity to kill malignant cells upon recognition by T cell receptor (TCR) of specific antigenic peptides [24]. To our knowledge, this is the first report to demonstrate lung metastases regression with increased CD8+ T lymphocyte infiltration into tumor tissue following the combined treatment method. Many studies reported immunologic effect resulting in the rejection of secondary tumor challenges following cryoablation in animal model [25–28]. However, CD8 infiltration into the

metastatic tumor was not observed after cryotreatment alone. Cryotreatment-induced metastatic antitumor activity with CD8 infiltration into the metastatic tumor was observed after cryotreatment combined with CTLA-4-blocking antibodies such as ipilimumab in the mouse prostate cancer model [29]; however, the results of their cryoablation study indicate that in their system, cryoablation alone had no effect on secondary tumor growth or T cell infiltration into secondary tumors [29].

The contribution of preoperative embolization in reducing intraoperative blood loss and its clinical importance are reported in palliative surgery for spinal metastasis, which violates the tumor vessels in such a highly vascular condition [30]. However, the contribution of preoperative embolization in reducing intraoperative blood loss in free margin excision such as total en bloc spondylectomy is unclear. In general, surgeons do not need to reduce the tumor vascularity in free margin excision surgery. To our knowledge, there have been no reports suggesting the efficacy of preoperative embolization prior to free margin excision for spinal metastasis. In our institution, spinal embolization is routinely performed 1–3 days before total en bloc spondylectomy, to reduce the risk of unexpected intraoperative bleeding due to the injury of segmental arteries and vein, and to prepare for unexpected intralesional tumor resection.

Preoperative embolization of spinal metastatic tumor can also enhance antitumor immune response. The efficacy of embolization-stimulated antitumor immunological response was mainly reported in transcatheter arterial embolization for hepatocellular carcinoma and renal embolization for renal cell carcinoma. To our knowledge, there have been no reports presenting the efficacy of embolization-stimulated antitumor immunological response for spinal metastasis. This case report is the first report indicating the potential of embolization-stimulated antitumor immunological effect for spinal metastasis. In patients with renal cell carcinoma, preoperative renal artery embolization significantly enhanced systematic antitumor response [31] and elongated survival compared to nephrectomy alone [31, 32]. They concluded that embolization may lead to stimulation of the immune system in the following mechanism: close off blood supply to the tumor leads to necrosis which gives a chance to enhance antigenicity of cancer cells and evoke the potential amplification of the immune system. In hepatocellular carcinoma, transcatheter arterial embolization also enhanced antitumor immune response via the same mechanism [33, 34]. Duan et al. reported that transcatheter arterial embolization combined with radiofrequency ablation activates CD8+ T cell infiltration surrounding residual tumors in the rabbit liver tumors. They concluded that in the rabbit liver tumor model, TAE + RFA activated the highest number of CD8+ T cells surrounding residual tumors [34]. In the present case, partial tumor necrosis was observed in resected L1 tumor after preoperative tumor embolization, potentially indicating embolization-stimulated antitumor immunological response. The combination of preoperative tumor embolization with TES using tumor-bearing frozen autograft caused necrosis and collapse of a large quantity of tumor cells, thereby releasing a large amount of tumor-related antigens, which may have stimulated the antitumor immune response. Li et al. reported that transcatheter renal arterial embolization combined with cryoablation enhances systematic immune response. In the reports, transcatheter renal arterial embolization combined with cryoablation contributes to reduce the percentage of Treg cells and improve the immune situation of patients with renal cell carcinoma, which consequently increase tumor necrosis rate and prolong the patients' survival duration [35]. As shown in our case, this combined treatment for spinal metastasis can improve short-term outcome for the patients with spinal metastasis. However, the long-term effect can be limited. Further investigation of this combined therapy as a new therapy for spinal metastasis is warranted.

Conclusion

The combination of preoperative spinal tumor embolization and TES using tumor-bearing frozen autograft provided both a local radical cure and systemic antitumor immunological enhancement in this case, although the long-term effect can be limited.

Acknowledgements We are grateful to Dr. Takayuki Nojima and Dr. Hiroko Ikeda for their assistance with pathological examinations. We would also like to express my gratitude to Dr. Isao Matsumoto for resection of pulmonary metastasis. We would like to thank Editage (www.editage.jp) for English language editing. We thank Dr. Satoshi Kato and Norihiro Oku for providing clinical data and their help.

Compliance with ethical standards

Conflict of interest The authors declare that they have no conflict of interest.

Ethical approval All procedures performed in studies involving human participants were in accordance with the ethical standards of the institutional and/or national research committee and with the 1964 Declaration of Helsinki and its later amendments or comparable ethical standards.

Informed consent Informed consent was obtained from the patient described in the study.

References

1. Major FJ, Blessing JA, Silverberg SG, Morrow CP, Creasman WT, Currie JL, Yordan E, Brady MF (1993) Prognostic factors in

early-stage uterine sarcoma. A gynecologic oncology group study. Cancer 71:1702–1709
2. Giuntoli RL, Metzinger DS, DiMarco CS, Cha SS, Sloan JA, Keeney GL, Gostout BS (2003) Retrospective review of 208 patients with leiomyosarcoma of the uterus: prognostic indicators, surgical management, and adjuvant therapy. Gynecol Oncol 89:460–469. https://doi.org/10.1016/s0090-8258(03)00137-9
3. Seagle B-LL, Sobecki-Rausch J, Strohl AE, Shilpi A, Grace A, Shahabi S (2017) Prognosis and treatment of uterine leiomyosarcoma: a national cancer database study. Gynecol Oncol 145:61–70
4. Abeler VM, Royne O, Thoresen S, Danielsen HE, Nesland JM, Kristensen GB (2009) Uterine sarcomas in Norway. A histopathological and prognostic survey of a total population from 1970 to 2000 including 419 patients. Histopathology 54:64–355
5. Bartosch C, Afonso M, Pires-Luis AS, Galaghar A, Guimaraes M, Antunes L, Lopes JM (2017) Distant Metastases in Uterine Leiomyosarcomas: the wide variety of body sites and time intervals to metastatic relapse. Int J Gynecol Pathol 36:31–41. https://doi.org/10.1097/PGP.0000000000000284
6. Tomita K, Kawahara N (1996) The threadwire saw: a new device for cutting bone. J Bone Jt Surg Am 78:1915–1917
7. Elhammady MS, Manzano GR, Lebwohl N, Levi AD (2007) Leiomyosarcoma metastases to the spine. Case series and review of the literature. J Neurosurg Spine 6:178–183. https://doi.org/10.3171/spi.2007.6.2.178
8. Ziewacz JE, Lau D, La Marca F, Park P (2012) Outcomes after surgery for spinal metastatic leiomyosarcoma. J Neurosurg Spine 17:432–437. https://doi.org/10.3171/2012.8.SPINE12331
9. Liu A, Sankey EW, Goodwin CR, Kosztowski TA, Elder BD, Bydon A, Witham TF, Wolinsky JP, Gokaslan ZL, Sciubba DM (2016) Postoperative survival and functional outcomes for patients with metastatic gynecological cancer to the spine: case series and review of the literature. J Neurosurg Spine 24:131–144. https://doi.org/10.3171/2015.3.SPINE15145
10. Folkert MR, Bilsky MH, Tom AK, Oh JH, Alektiar KM, Laufer I, Tap WD, Yamada Y (2014) Outcomes and toxicity for hypofractionated and single-fraction image-guided stereotactic radiosurgery for sarcomas metastasizing to the spine. Int J Radiat Oncol Biol Phys 88:1085–1091. https://doi.org/10.1016/j.ijrobp.2013.12.042
11. Laufer I, Iorgulescu JB, Chapman T, Lis E, Shi W, Zhang Z, Cox BW, Yamada Y, Bilsky MH (2013) Local disease control for spinal metastases following "separation surgery" and adjuvant hypofractionated or high-dose single-fraction stereotactic radiosurgery: outcome analysis in 186 patients. J Neurosurg Spine 18:207–214. https://doi.org/10.3171/2012.11.SPINE12111
12. Bishop AJ, Tao R, Guadagnolo BA, Allen PK, Rebueno NC, Wang XA, Amini B, Tatsui CE, Rhines LD, Li J, Chang EL, Brown PD, Ghia AJ (2017) Spine stereotactic radiosurgery for metastatic sarcoma: patterns of failure and radiation treatment volume considerations. J Neurosurg Spine 27:303–311. https://doi.org/10.3171/2017.1.SPINE161045
13. Tsuchiya H, Wan SL, Sakayama K, Yamamoto N, Nishida H, Tomita K (2005) Reconstruction using an autograft containing tumour treated by liquid nitrogen. J Bone Jt Surg Br 87:218–225
14. Yamamoto N, Tsuchiya H, Tomita K (2003) Effects of liquid nitrogen treatment on the proliferation of osteosarcoma and the biomechanical properties of normal bone. J Orthop Sci 8:374–380. https://doi.org/10.1007/s10776-002-0626-3
15. Takata M, Sugimoto N, Yamamoto N, Shirai T, Hayashi K, Nishida H, Tanzawa Y, Kimura H, Miwa S, Takeuchi A, Tsuchiya H (2011) Activity of bone morphogenetic protein-7 after treatment at various temperatures: freezing vs. pasteurization vs. allograft. Cryobiology 63:235–239. https://doi.org/10.1016/j.cryobiol.2011.09.001
16. Igarashi K, Yamamoto N, Shirai T, Hayashi K, Nishida H, Kimura H, Takeuchi A, Tsuchiya H (2014) The long-term outcome following the use of frozen autograft treated with liquid nitrogen in the management of bone and soft-tissue sarcomas. Bone Jt J 96-B:555–561. https://doi.org/10.1302/0301-620X.96B4.32629
17. Nishida H, Tsuchiya H, Tomita K (2008) Re-implantation of tumour tissue treated by cryotreatment with liquid nitrogen induces anti-tumour activity against murine osteosarcoma. J Bone Jt Surg Br 90:1249–1255. https://doi.org/10.1302/0301-620X.90B9.20671
18. Nishida H, Yamamoto N, Tanzawa Y, Tsuchiya H (2011) Cryoimmunology for malignant bone and soft-tissue tumors. Int J Clin Oncol 16:109–117. https://doi.org/10.1007/s10147-011-0218-2
19. Ishii T, Murakami H, Demura S, Kato S, Yoshioka K, Fujii M, Igarashi T, Tsuchiya H (2016) Invasiveness reduction of recent total En Bloc Spondylectomy: assessment of the learning curve. Asian Spine J 10:522–527. https://doi.org/10.4184/asj.2016.10.3.522
20. Murakami H, Demura S, Kato S, Nishida H, Yoshioka K, Hayashi H, Inoue K, Ota T, Shinmura K, Yokogawa N, Fang X, Tsuchiya H (2013) Increase of IL-12 following reconstruction for total en bloc spondylectomy using frozen autografts treated with liquid nitrogen. PLoS ONE 8:e64818. https://doi.org/10.1371/journal.pone.0064818
21. Murakami H, Kato S, Ueda Y, Fujimaki Y, Tsuchiya H (2014) Reconstruction using a frozen tumor-bearing vertebra in total en bloc spondylectomy can enhance antitumor immunity. Eur Spine J 23(Suppl 2):222–227. https://doi.org/10.1007/s00586-013-3056-2
22. Sugita S, Murakami H, Kato S, Tanaka S, Tsuchiya H (2016) Disappearance of lung adenocarcinoma after total en bloc spondylectomy using frozen tumor-bearing vertebra for reconstruction. Eur Spine J 25(Suppl 1):53–57. https://doi.org/10.1007/s00586-015-4077-9
23. Murakami H, Demura S, Kato S, Yoshioka K, Hayashi H, Inoue K, Ota T, Shinmura K, Yokogawa N, Fang X, Tsuchiya H (2014) Systemic antitumor immune response following reconstruction using frozen autografts for total en bloc spondylectomy. Spine J 14:1567–1571. https://doi.org/10.1016/j.spinee.2013.09.030
24. Durgeau A, Virk Y, Corgnac S, Mami-Chouaib F (2018) Recent advances in targeting CD8 T-Cell immunity for more effective cancer immunotherapy. Front Immunol 9:14. https://doi.org/10.3389/fimmu.2018.00014
25. Joosten JJ, Muijen GN, Wobbes T, Ruers TJ (2001) In vivo destruction of tumor tissue by cryoablation can induce inhibition of secondary tumor growth: an experimental study. Cryobiology 42:49–58. https://doi.org/10.1006/cryo.2001.2302
26. Sabel MS, Arora A, Su G, Chang AE (2006) Adoptive immunotherapy of breast cancer with lymph node cells primed by cryoablation of the primary tumor. Cryobiology 53:360–366. https://doi.org/10.1016/j.cryobiol.2006.07.004
27. Sabel MS, Nehs MA, Su G, Lowler KP, Ferrara JL, Chang AE (2005) Immunologic response to cryoablation of breast cancer. Breast Cancer Res Treat 90:97–104. https://doi.org/10.1007/s10549-004-3289-1
28. Urano M, Tanaka C, Sugiyama Y, Miya K, Saji S (2003) Antitumor effects of residual tumor after cryoablation: the combined effect of residual tumor and a protein-bound polysaccharide on multiple liver metastases in a murine model. Cryobiology 46:238–245
29. Waitz R, Solomon SB, Petre EN, Trumble AE, Fasso M, Norton L, Allison JP (2012) Potent induction of tumor immunity by combining tumor cryoablation with anti-CTLA-4 therapy. Cancer Res 72:430–439. https://doi.org/10.1158/0008-5472.CAN-11-1782
30. Hong CG, Cho JH, Suh DC, Hwang CJ, Lee DH, Lee CS (2017) Preoperative embolization in patients with metastatic spinal cord compression: mandatory or optional? World J Surg Oncol 15:45

31. Zielinski H, Syrylo T, Szmigielski S (2013) Renal Artery embolization in treatment of renal cancer with emphasis on response of immune system. In: Chen J (ed) Renal tumor, chap 6. InTech, pp 95–108
32. Zielinski H, Szmigielski S, Petrovich Z (2000) Comparison of preoperative embolization followed by radical nephrectomy with radical nephrectomy alone for renal cell carcinoma. Am J Clin Oncol 23:6–12
33. Mizukoshi E, Nakamoto Y, Arai K, Yamashita T, Mukaida N, Matsushima K, Matsui O, Kaneko S (2010) Enhancement of tumor-specific T-cell responses by transcatheter arterial embolization with dendritic cell infusion for hepatocellular carcinoma. Int J Cancer 126:2164–2174. https://doi.org/10.1002/ijc.24882
34. Duan XH, Li TF, Zhou GF, Han XW, Zheng CS, Chen PF, Feng GS (2016) Transcatheter arterial embolization combined with radiofrequency ablation activates CD8(+) T-cell infiltration surrounding residual tumors in the rabbit VX2 liver tumors. Onco Targets Ther 9:2835–2844. https://doi.org/10.2147/OTT.S95973
35. Li Y, Guo Z, Liu CF, Xing WG, Si TG, Liu F, Guo XY, Xing JZ (2012) Effect of transcatheter renal arterial embolization combined with cryoablation on regulatory CD4 + CD25 + T lymphocytes in the peripheral blood of patients with advanced renal carcinoma. Cryobiology 65:56–59

European Spine Journal (2019) 28 (Suppl 2):S51–S55
https://doi.org/10.1007/s00586-019-05914-5

CASE REPORT

Neurological impairment in a patient with concurrent cervical disc herniation and POEMS syndrome

Tingxian Ling[1] · Limin Liu[1] · Yueming Song[1] · Shilian Zhou[1] · Chunguang Zhou[1]

Received: 24 July 2018 / Revised: 16 December 2018 / Accepted: 9 February 2019 / Published online: 13 February 2019

Abstract

Purpose POEMS syndrome is a rare clonal plasma cell disease characterized by polyneuropathy, organomegaly, endocrinopathy, M protein, and skin changes. We report a rare case of neurological impairment in patients with concurrent cervical disc herniation and POEMS syndrome.

Methods A patient presented to a local hospital with C3/4 and C4/5 disc herniation, apparent spinal cord compression concomitant with neurological signs, and concurrent POEMS syndrome. Anterior cervical discectomy and fusion was performed.

Results The limb numbness was only slightly alleviated, and 10 days postoperatively the patient complained of muscle weakness of the extremities and was referred to our hospital. The patients exhibited non-typical neurological signs and an enlarged liver and spleen that could not be explained. Electroneuromyography and immunofixation electrophoresis produced abnormal results. We diagnosed concurrent POEMS syndrome, for which drug therapy was prescribed. The patient's symptoms receded.

Conclusion Patients presenting with cervical spondylopathy and non-typical neurological signs and symptoms or other systemic problems should be evaluated for the presence of concurrent disease and ruled out differential diagnoses.

Keywords Neurological impairment · POMES syndrome · Cervical disc herniation · Cervical spondylosis

Introduction

Cervical disc herniation is a common spinal disorder that can lead to radiculopathy and myelopathy. If conservative treatments for cervical disc herniation fail, anterior cervical discectomy and fusion (ACDF) is standard treatment. The clinical presentation of cervical spondylotic myelopathy includes numbness, paresthesias, sensory deficits, muscle weakness of extremities, gait disturbances, and/or bladder or bowel dysfunction [1]. The Hoffmann sign is usually positive. The symptoms are likely to be relieved by decompression surgery.

Some patients with cervical spondylotic myelopathy, however, may have a concurrent disease that affects the central nervous system. Multiple sclerosis (MS), for example, is a chronic demyelinating autoimmune disease that has symptoms similar to those associated with myelopathy: spasticity, sensory disturbances, gait ataxia, weakness. It is thus difficult to differentiate neurological signs due to cervical spondylosis from those of demyelinating autoimmune disease. Their treatments are also different and thus complicated for patients with multiple myelopathic pathologies. Lubelski et al. [1] reported the surgical results of patients who had both MS and cervical stenosis. They found that the modified Japanese Orthopaedic Association scores that had improved at the short-term postoperative follow-up worsened at the long-term follow-up.

POEMS syndrome is a rare clonal plasma cell disease characterized by polyneuropathy, organomegaly, endocrinopathy, M protein, and skin changes [2]. Because of demyelinating polyneuropathy with multiorgan involvement, POEMS syndrome often presents as peripheral neuropathy [3]. We found that neurological impairment in patients with concurrent cervical disc herniation and POEMS syndrome is rarely reported. Therefore, we report a case of C3/4 and C4/5 disc herniation with neurological signs that was diagnosed as POEMS syndrome after decompression surgery.

✉ Chunguang Zhou
zhouchunguang@aliyun.com

Tingxian Ling
lingtingxian@126.com

[1] Department of Orthopedics, West China Hospital of Sichuan University, Guoxuexiang No. 37, Wuhouqu, Chengdu 610041, Sichuan, China

Case report

A 39-year-old man presented at a local hospital with a 3 month history of leg numbness and gait disturbances and 1 month of upper limb numbness. On physical examination, the limb muscle strength and muscular tension were normal. He had upper limb tendon reflex weakness, no lower extremity tendon reflex, and hypesthesia of both hands and feet. Hoffmann sign and Babinski reflex were negative. Deep sensation was normal. Magnetic resonance imaging revealed C3/C4 and C4/C5 dural sac and spinal cord compression. The cervical spinal canal behind C3/4 and C4/5 disc showed a herniated disc at the centre and left side on the T2-weighted axial image (Fig. 1a). However, the spinal cord signal was normal. Three-dimensional computed tomography (CT) of the cervical spine showed no calcification of the posterior longitudinal ligament or ligamentum flavum (Fig. 1b).

Routine blood examination (RBE) showed white blood cells at 13.44×109/L (neutrophils 86.2%). Erythrocyte sedimentation rate (ESR) and C-reactive protein (CRP) were elevated. Nevertheless, C3–C5 ACDF was performed at local hospital (Fig. 2). The limb numbness was slightly diminished and the other symptoms unchanged. Ten days postoperatively, his muscle weakness increased accompanied by hyperpyrexia. He was referred to our hospital.

A comprehensive examination was performed. Urine tests demonstrated proteinuria. Abdominal ultrasonography showed enlarged liver and spleen. The neurologist suggested electroneuromyography, immunofixation electrophoresis, and a urine kappa (κ) light chain test. Electroneuromyography showed upper and lower limb peripheral neuropathy. Immunofixation electrophoresis showed a low blood κ light chain level (5.31 g/L, reference value 6.89–13.00), elevated blood lambda (λ) light chain level (11.7 g/L, reference value 3.80–6.50), and low κ/λ light chain ratio. The urine κ light chain concentration had apparently elevated (0.157 g/L, reference value < 0.02). In addition, the patient appeared emaciated with swarthy skin.

The 2003 diagnostic criteria for POEMS included two major criteria (polyneuropathy and monoclonal plasma proliferative disorder) and seven minor criteria (bone lesion, Castleman disease, organomegaly, oedema, endocrinopathy, skin changes, papilledema) [4]. Two major criteria and at least one minor criterion were necessary for diagnosis. According to our comprehensive analysis of symptoms, physical signs, and anomaly indexes, the diagnosis was POEMS syndrome. The rising blood λ light chain and abnormal blood κ/λ light chain ratio indicated the presence of M protein. Therefore, with the neuropathy and the presence of some minor criteria, the diagnosis of POEMS syndrome was confirmed. The patient underwent comprehensive medical therapy including rehabilitation exercise and drug therapy (melphalan combined with dexamethasone). The symptoms of limb numbness and muscle weakness were improved after the treatment. Then, this patient was followed up by neurologist.

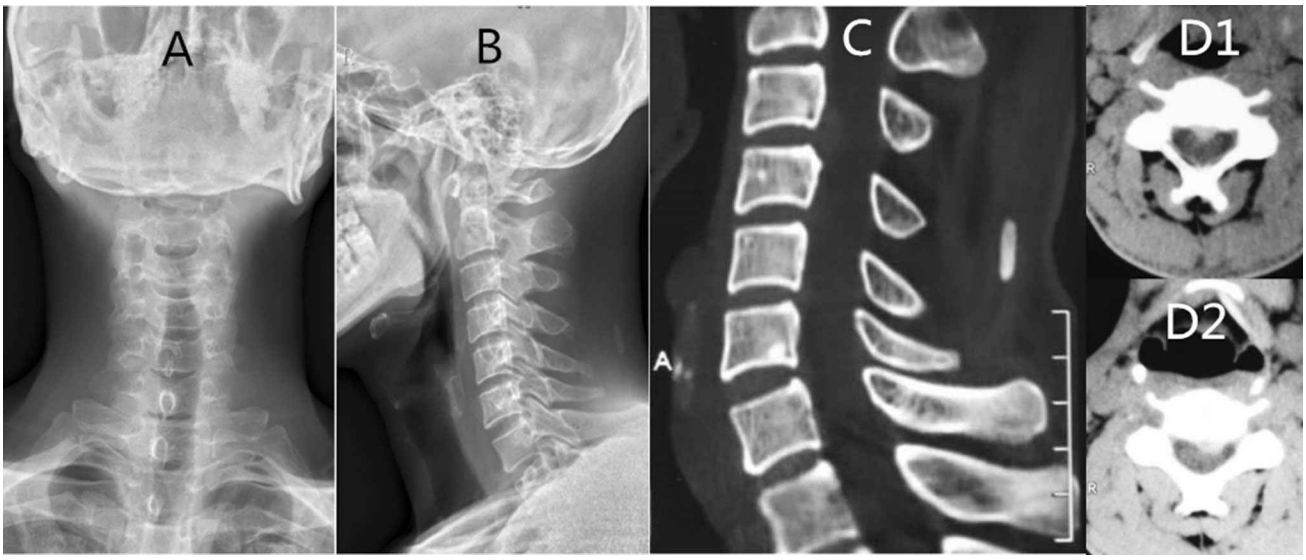

Fig. 1 **a**, **b** Cervical radiography shows normal alignment. **c** Sagittal three-dimensional computed tomography (CT) shows no calcification of the posterior longitudinal ligament or the ligamentum flavum. **d** Transverse sections of cervical CT show an intraspinal soft tissue shadow at the centre at the C3/4 level (**d1**) and on the left side of the C4/5 level (**d2**)

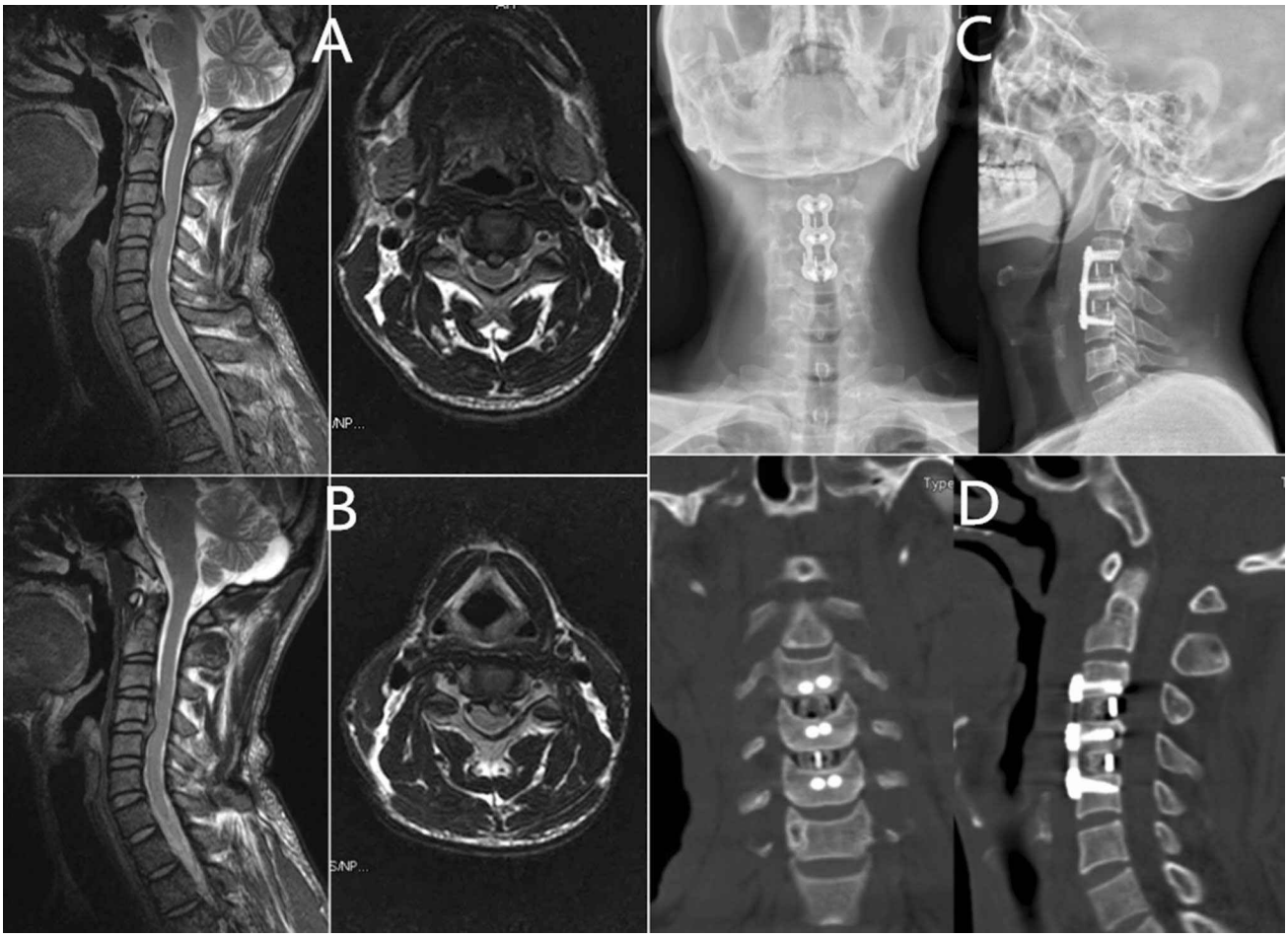

Fig. 2 **a**, **b** Magnetic resonance imaging reveals C3/C4 and C4/C5 dural sacs and spinal cord with apparent compression. The cervical spinal canal behind C3/4 (**a**) and C4/5 (**b**) discs has a herniated disc at the centre and left side on this T2-weighted axial image. **c**, **d** Anterior cervical discectomy and fusion was performed at C3–C5. Postoperative imaging shows good internal fixation. Herniated discs were completely resected

Discussion

Because of the rarity and complicated clinical manifestations of POEMS syndrome, its diagnosis may be missed. POEMS syndrome involves many organs and bodily systems [2]. Misdiagnoses may include other peripheral neuropathies, tuberculosis, diabetes, chronic nephritis, various skin diseases, and multiple myeloma [5]. Dispenzieri et al. [4] reported that polyneuropathy was an essential element for diagnosing POEMS syndrome. Therefore, neurological symptoms are among the most important clinical manifestations. Li et al. [2] found 100% of the patients with POEMS syndrome had peripheral neuropathy. Other specific features of POEMS syndrome include the high level of serum vascular endothelial growth factor, extravascular volume overload, organomegaly, endocrinopathy, monoclonal plasma cell dyscrasia, skin changes, papilledema, bone lesions, and hemangioma [6, 7].

After reviewing the preoperative clinical manifestations and examination results of this patient, we identified several abnormalities different from those of cervical spondylotic myelopathy due to intervertebral disc herniation. First, the neurological signs were different. Polyneuropathy, one of the essential manifestations of POEMS syndrome, may include polyneuropathy, peripheral neuropathy, segmental demyelination alone, axonal loss alone, or a mixture of axonal loss and segmental demyelination [2]. Adams et al. [3] speculated that the neural pathological change is due to immune-mediated nerve injury. The neuropathy of POEMS syndrome is symmetrical and ascending, with either insidious or rapidly progressing onset. Patients often describe numbness and dysesthesias followed by a progressively ascending weakness that overshadows the sensory impairment [4]. In contrast, cervical spondylotic myelopathy is due to spinal cord compression. Reflexes at the biceps, triceps, patellar, and Achilles tendons are usually hyperactive. Pathological

reflexes, including the Hoffman sign and Babinski sign, are usually positive. The patient often presents with asymmetrical extremity weakness and numbness and feels that his/her legs are stepping in cotton (as did our patient). The neurological signs of our patient—symmetrical distal extremity numbness, normal muscle strength, muscular tension—and negative pathological signs were different from those of cervical spondylotic myelopathy alone. Second, our patient showed an unexplained enlarged liver and spleen as well as abnormal electroneuromyography and immunofixation electrophoresis results, which could not be explained by simple cervical spondylotic myelopathy.

Cervical spondylopathy may be accompanied by a disease that affects the nervous system (e.g. MS, Castleman disease, POEMS syndrome) [1, 8, 9]. The overlapping symptoms make identification difficult. When these pathologies converge, the diagnosis and treatment are complicated as the natural histories and therapies are vastly different. Therefore, when the differential diagnosis is cervical spondylopathy but the patient presents with non-typical neurological signs and symptoms, the diagnosing physician should be vigilant for other possibilities.

Lubelski et al. [1] found that preoperative MRI findings were associated with postoperative outcomes in cohorts of either MS or cervical stenosis patients but not with those having *concurrent* MS and cervical stenosis. (The postoperative outcomes in concurrent MS and cervical stenosis patients worsened at the long-term follow-up, possibly related to MS progression.) MS is a chronic demyelinating autoimmune disease with neurological symptoms similar to those of myelopathy, thereby leading to an incorrect diagnosis and treatment.

Castleman disease is a rare lymphoproliferative disorder that may be associated with peripheral neuropathy [10]. Naddaf et al. reported 105 patients with Castleman disease, 27 (27.5%) of whom had peripheral neuropathy [8]. They found that Castleman disease was an additional cause of a demyelinating neuropathy and characteristically presented with mild, predominantly sensory deficits in a duration-dependent pattern, involving mainly the distal lower limbs, but rarely with motor deficits. Therefore, the neurological signs of cervical spondylopathy must be distinguished with those of Castleman disease. If a patient with cervical disc herniation or spinal stenosis has neurological signs and presents with unexplained lymphadenectasis, Castleman disease should be considered. In addition, some haematological disorders (e.g. monoclonal gammopathy of undetermined significance, Waldenström macroglobulinemia) may also be associated with peripheral neuropathy with demyelinating features [11, 12]. The related similarity should be noted.

Reports of neurological impairment concurrent with cervical disc herniation and POEMS syndrome are rare. Because of the aggravated neurological signs postoperatively in our patient, he was referred to our hospital, where POEMS syndrome was finally diagnosed. Because limb numbness only slightly diminished postoperatively, we thought that the neurological symptoms in this case were mainly derived from POEMS syndrome. Thus, spinal cord compression might have explained some of his symptoms but was not the main cause. Although severe disc herniation caused spinal cord compression, the spinal cord signal of this patient shown in MRI was normal (Fig. 1a). In this situation, the diagnosis of cervical spondylotic myelopathy is mainly based on symptoms, neurological examination, and laboratory. However, neurological symptoms and pathological signs of this patient were non-typical for the diagnosis of cervical spondylotic myelopathy. In addition, RBE, ESR, and CRP showed obvious signs of inflammation. Therefore, it was mandatory to perform extensive examination in order to rule out frequent differential diagnoses. The surgery should not be performed without extensive tests for standard differential diagnoses. The preoperative management in this patient was not proper. Medical treatment for POEMS syndrome should be prioritized. If the neurological symptoms are relieved after medical treatment, surgery probably can be avoided. In conclusion, when a cervical spondylopathy patient presents with non-typical neurological signs and symptoms or other systemic problems, concurrent disease may be present and differential diagnoses must be ruled out.

Compliance with ethical standards

Conflict of interest The authors declare that they have no conflict of interest.

References

1. Lubelski D, Healy AT, Silverstein MP, Alvin MD, Abdullah KG, Benzel EC, Mroz TE (2015) Association of postoperative outcomes with preoperative magnetic resonance imaging for patients with concurrent multiple sclerosis and cervical stenosis. Spine J 15(1):18–24. https://doi.org/10.1016/j.spinee.2014.06.013
2. Li J, Zhou DB, Huang Z, Jiao L, Duan MH, Zhang W, Zhao YQ, Shen T (2011) Clinical characteristics and long-term outcome of patients with POEMS syndrome in China. Ann Hematol 90(7):819–826. https://doi.org/10.1007/s00277-010-1149-0
3. Adams D, Said G (1998) Ultrastructural characterisation of the M protein in nerve biopsy of patients with POEMS syndrome. J Neurol Neurosurg Psychiatry 64(6):809–812
4. Dispenzieri A, Kyle RA, Lacy MQ, Rajkumar SV, Therneau TM, Larson DR, Greipp PR, Witzig TE, Basu R, Suarez GA, Fonseca R, Lust JA, Gertz MA (2003) POEMS syndrome: definitions and long-term outcome. Blood 101(7):2496–2506. https://doi.org/10.1182/blood-2002-07-2299
5. Gertz MA, Comenzo R, Falk RH, Fermand JP, Hazenberg BP, Hawkins PN, Merlini G, Moreau P, Ronco P, Sanchorawala V, Sezer O, Solomon A, Grateau G (2005) Definition of organ involvement and treatment response in immunoglobulin light

chain amyloidosis (AL): a consensus opinion from the 10th international symposium on amyloid and amyloidosis, Tours, France, 18–22 April 2004. Am J Hematol 79 (4):319–328. https://doi.org/10.1002/ajh.20381
6. Watanabe O, Arimura K, Kitajima I, Osame M, Maruyama I (1996) Greatly raised vascular endothelial growth factor (VEGF) in POEMS syndrome. Lancet 347(9002):702
7. Zhang B, Song X, Liang B, Hou Q, Pu S, Ying JR, Gao C (2010) The clinical study of POEMS syndrome in China. Neuro Endocrinol Lett 31(2):229–237
8. Naddaf E, Dispenzieri A, Mandrekar J, Mauermann ML (2016) Clinical spectrum of Castleman disease-associated neuropathy. Neurology 87(23):2457–2462. https://doi.org/10.1212/wnl.0000000000003405
9. Hu X, Chen Z, Wang Y (2017) A rare case of concomitant cervical disc herniation and intradural meningioma treated with one-stage posterior surgery. Eur Spine J. https://doi.org/10.1007/s00586-017-5414-y
10. Yu GS, Carson JW (1976) Giant lymph-node hyperplasia, plasma-cell type, of the mediastinum, with peripheral neuropathy. Am J Clin Pathol 66(1):46–53
11. Klein CJ, Moon JS, Mauermann ML, Zeldenrust SR, Wu Y, Dispenzieri A, Dyck PJ (2011) The neuropathies of Waldenstrom's macroglobulinemia (WM) and IgM-MGUS. Can J Neurol Sci (Le journal canadien des sciences neurologiques) 38(2):289–295
12. Mauermann ML (2014) Paraproteinemic neuropathies. Continuum (Minneapolis, Minn) 20(5 Peripheral Nervous System Disorders):1307–1322. https://doi.org/10.1212/01.con.0000455879.99050.26

European Spine Journal (2019) 28 (Suppl 2):S56–S60
https://doi.org/10.1007/s00586-019-05915-4

CASE REPORT

A novel fixation technique using anterior C1 screw in a pediatric solitary cervical spinal juvenile xanthogranuloma

Rekhapalli Rajasekhar[1] · Madhivanan Karthigeyan[1] · Pravin Salunke[1] · Kirti Gupta[2]

Received: 25 September 2018 / Revised: 22 December 2018 / Accepted: 9 February 2019 / Published online: 15 February 2019

Abstract

Purpose Juvenile xanthogranuloma (JXG) presenting as solitary vertebral body lesion is infrequently seen and usually limited to one or two levels. We report a case of an isolated JXG with extensive cervical spinal (bony and extradural) involvement in a 6-year-old child. There was a diagnostic dilemma as the radiologic and intraoperative picture resembled tuberculosis. The spinal reconstruction was also challenging due to involvement of multiple vertebral levels and necessitated an anterior C1 screw.

Methods The lytic lesion was multicompartmental, involving the craniovertebral junction and the subaxial spine (till C6 vertebral body) and extending into the retropharyngeal space. Noticeably, an associated thoracic syringomyelia was also present. Near-total excision of the lesion and 360° spinal fixation was performed using fibular strut graft. The graft was cranially anchored to the C1 anterior arch, thereby sharing the load with the posterior occipito-cervical instrumentation in order to avoid a construct failure due to cantilever effect.

Results At 12-month follow-up, the patient had good clinico-radiologic outcome with evidence of bony fusion and resolution of syrinx.

Conclusion The report highlights the diagnostic dilemma of JXG lesion on both the radiology and surgery and discusses the challenges in the management and the relevant literature. The described technique can be a viable option in pediatric tumors with extensive C2 vertebral body involvement. Occasionally, extradural compression can have associated syrinx formation and the primary treatment per se could tackle the underlying syringomyelia.

Keywords Juvenile xanthogranuloma · Non-Langerhans cell histiocytosis · Craniovertebral junction · Cervical spine · Fibular graft · Vertebral body · C1 screw

Introduction

Juvenile xanthogranuloma (JXG) is a rare, benign, non-Langerhans cell histiocytic proliferative disorder and represents 0.5% of pediatric tumors [1]. It commonly presents as a self-limiting, isolated skin lesion. Occasionally, the disorder can affect subcutaneous tissue, eye, viscera, central nervous system and bones. Such an extracutaneous involvement is seen in approximately 5–10% of cases [2–4].

Spine is an unusual site for JXG. Very few reports describe JXG which presented as isolated vertebral body lesions, mostly confined to one or two vertebral bodies [3–6]. We hereby report a case of pediatric solitary JXG with extensive involvement of the cervical spine along with spread into the retropharyngeal space. The relevant differential diagnosis and the management issues have been discussed.

Case report

A 6-year-old boy who is a diagnosed case of Klippel–Feil syndrome presented with 2-year history of neck tilt and recent-onset dysphagia. He also had complaint of mild neck pain. General physical examination showed pectus excavatum. His neurology was normal. Computed tomography

✉ Madhivanan Karthigeyan
karthigeyanm82@gmail.com

[1] Department of Neurosurgery, Postgraduate Institute of Medical Education & Research (PGIMER), Sector 12, Chandigarh 160012, India

[2] Department of Histopathology, PGIMER, Chandigarh, India

(CT) of the cervical spine showed an osteolytic destruction involving the C2, fused C3–C5 and C6 vertebral bodies (Fig. 1). The C1 arch and uppermost portion of dens were intact. Magnetic resonance imaging (MRI) demonstrated a contrast-enhancing extradural soft tissue lesion intending the cord and bulging out anteriorly into the retropharyngeal space. An associated thoracic syringomyelia was noted.

A CT-guided biopsy of the lesion was inconclusive. In view of the spinal compression and indefinite biopsy report, an excision of the lesion was planned (by senior author PS). The child underwent excision of the mass through an anterior approach along with posterior stabilization that included the occiput, C1 lateral mass, C7 and T1 pedicle screws. During surgery, it was seen that the prevertebral fascia was plastered. On incising it, a dirty-white, flaky material was noted within the lesion. The mass was near-completely excised leaving the portion adjacent to the vertebral arteries. An autologous fibular graft was then fashioned to bridge the bony defect and fixed with cortico-cancellous screws, the cranial one extending from the graft into the C1 anterior arch, and the caudal screw into the C7 body.

Intraoperative frozen sections showed histiocytic collection and occasional multinucleated giant cells. Considering the high endemicity of tuberculosis in our area, the child was discharged on antituberculous therapy. The final histopathological examination of the paraffin-embedded sections, however, turned out to be JXG (Fig. 2).

The child was on Philadelphia collar for 3 months. At 12-month follow-up, he was doing well without any evidence of recurrence. Repeat imaging showed resolution of the syrinx and good bony fusion (Fig. 1).

Discussion

According to the recent classification, the histiocytic disorders consist of five groups such as Langerhans-related (L group), cutaneous and mucocutaneous (C group), malignant histiocytoses (M group), Rosai–Dorfman disease (R group), and hemophagocytic lymphohistiocytosis and macrophage activation syndrome (H group) [7]. JXG is the most common form of cutaneous histiocytosis (C group). The extracutaneous variety is biologically different from cutaneous JXG and is classified in L group [7]. Histologically, JXG is composed of characteristic Touton giant cells in a background of mononuclear cells which are seen in about 85% of cases [2]. These giant cells may be less pronounced in extracutaneous lesions [2]. It is important to distinguish JXG from Langerhans cell histiocytosis, as the latter shows more aggressive clinical

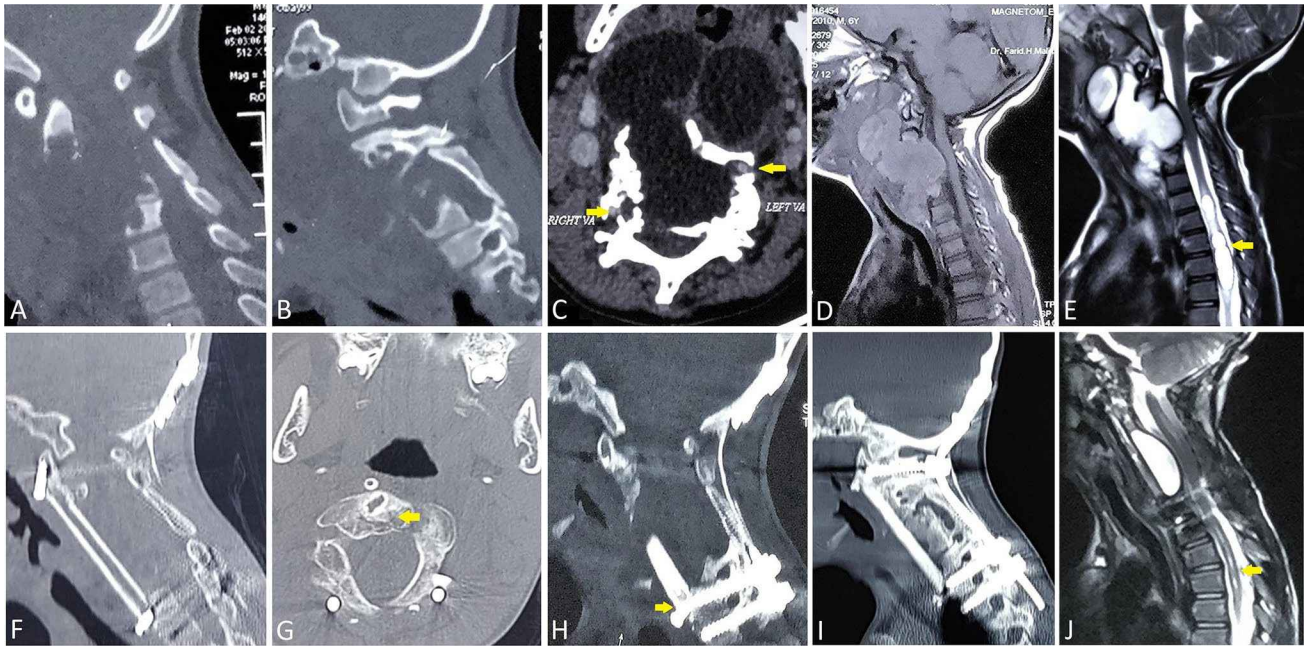

Fig. 1 Preoperative images (**a**–**e**): sagittal (**a**) and parasagittal (**b**) reconstruction of computed tomography (CT) scan show extensive osteolysis of the C2, fused C3–C5 and C6 vertebral bodies. **c** Axial CT section of subaxial spine (C3 level) shows vertebral body destruction; vertebral artery (VA) indicated with arrow. **d**, **e** On magnetic resonance imaging (MRI), the lesion is T1-isointense and T2-hyperintense and extends into retropharyngeal space. Syringomyelia is seen in the thoracic spine (arrow in **e**). **f**–**h** Postoperative CT at 1-year follow-up. Sagittal section (**f**) shows anterior column reconstruction using fibular strut graft with screws placed in the C1 anterior arch and C7; fusion is seen at graft–C1 interface (arrow in **g**) and at the caudal end (arrow in **h**). **i** Posterior occipito-cervical fusion was performed using occipital, C1 lateral mass, C7 and T1 pedicle screws). **j** Follow-up MRI shows resolution of syrinx (arrow)

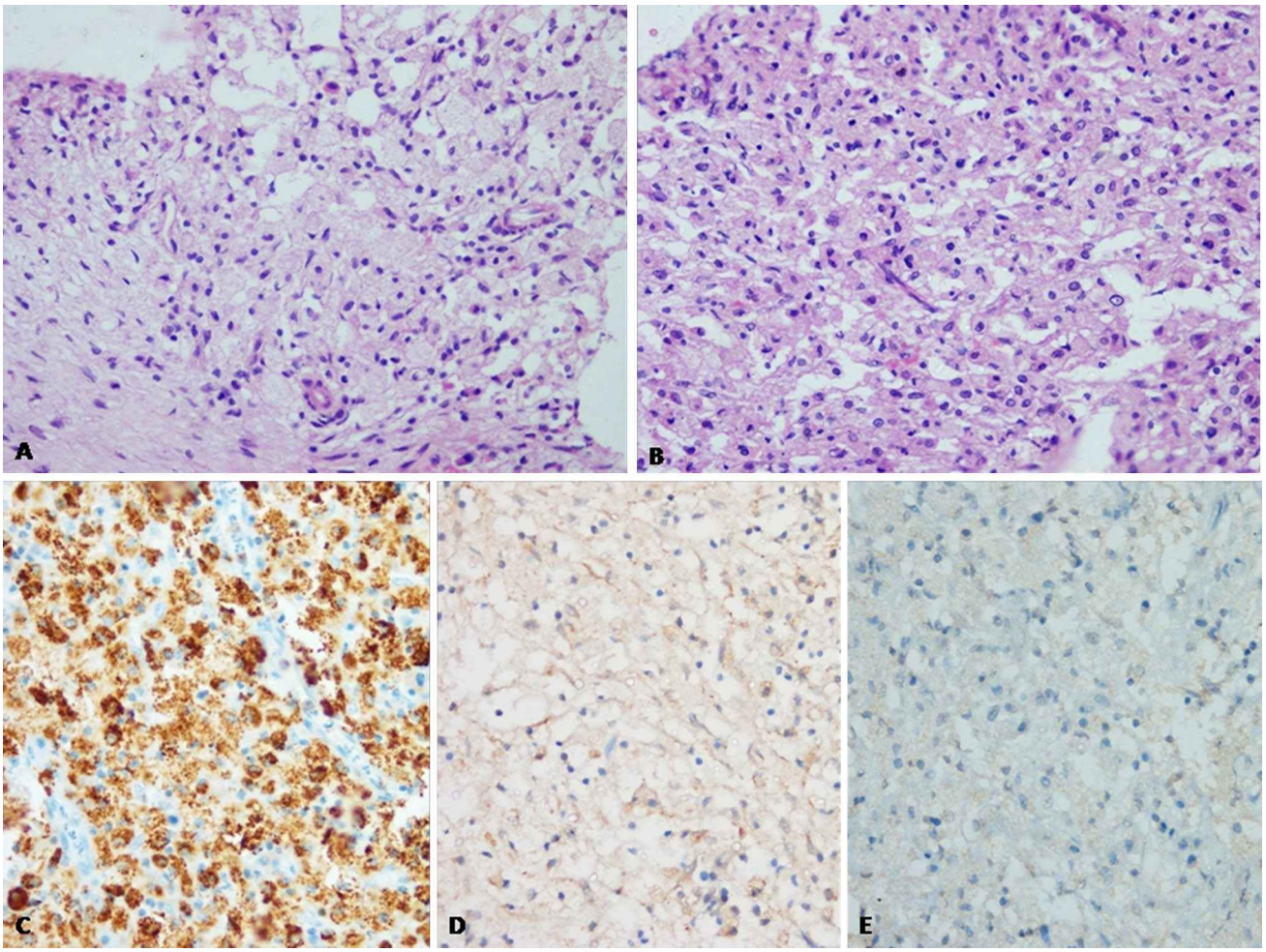

Fig. 2 **a** High magnification showing collection of foamy histiocytes and few lymphomononuclear cells. The infiltrate comprised chiefly of macrophages (H&E×400). **b–e** Foamy histiocytes and macrophages show strong and diffuse positivity with vimentin (**b**), CD68 (**c**) and are negative for S-100 (**d**) and CD1a (**e**) (**b–e**, immunoperoxidase ×400)

course [7]. The immunohistochemistry helps in this regard [1, 2].

JXG occurs primarily in the first two decades of life and most commonly (45–70%) within first 12 months of age. The most common presentation is a solitary dermal lesion (67%). Other less common presentations include solitary subcutaneous or deep soft tissue mass (16%), multiple cutaneous lesions (7%), solitary extracutaneous lesions (5%) and systemic disease (5%) [1, 2].

Solitary JXG involving the spine is unusual and can present in various forms such as an osteolytic lesion of the vertebral body, intradural or epidural mass, spinal nerve root lesion and rarely as an intramedullary tumor [3–6, 8]. Any part of the vertebral column can be involved. The MRI appearance varies from iso-hypointense in T1 and hypo-hyperintense in T2 sequence; the lesions usually show homogenous enhancement with contrast. Those lesions presenting as intradural extramedullary masses resemble meningioma on imaging, and the spinal nerve root involvement may mimic schwannoma [5]. In our patient, an extensive osteolytic lesion along with paraspinal and epidural spread made us think of possibilities such as spinal tuberculosis, aneurysmal bone cyst or osteolytic vertebral neoplasms.

The present case has certain unique characteristics. Firstly, the occurrence of solitary JXG in the region of craniovertebral junction (CVJ) is unusual. It was an extensive lesion involving almost the entire cervical spine (C2–C6) causing CVJ instability, and extending into the retropharyngeal space. Such long segmental disease involving multiple vertebral levels has not been reported. Secondly, there was a dilemma in the diagnosis because of its similarity to tuberculosis on imaging, intraoperative appearance and frozen sections. The presence of syringomyelia which was thought to be due to spinal arachnoiditis also supported a diagnosis of tuberculosis. Next interesting feature is the

association of the syrinx with an extradural lesion such as JXG. Though the reasons are unclear, it could be secondary to alteration of cerebrospinal fluid flow as in any other cervico-medullary lesion or due to an occult asymptomatic spinal arachnoiditis [9]. The syrinx resolution on follow-up MRI suggests that no additional procedures are necessary for the underlying syringomyelia in an extradural lesion.

Lastly, the extensive osteolysis caused by the tumor mandated a staged 360° fusion. In subaxial cervical spinal tumors with associated instability, the tumor excision is usually performed by an anterior approach, supplemented by mesh cage or strut graft. An additional posterior fusion may be required if the tumors extend to the lateral masses. In cases of solitary C2 body involvement, an anterior removal of the mass followed by an occipito-cervical fusion would suffice [10]. As the weight of the head is transmitted from the occipital condyle through C1–C2 lateral mass to the body of subaxial vertebrae, an additional anterior graft placement may not be necessary. However, in the event of associated destruction of C2 lateral mass or the body of subaxial spine, the major weight transmission would be borne by the posterior construct alone. This posterior construct is likely to fail over a period (cantilever effect), unless it is augmented by a load-sharing anterior strut (Fig. 3) [11].

Usually, an anterior extrapharyngeal approach is required to access the lesions that involve the C2 body along with multiple subaxial vertebrae. Reaching up to the clivus and obtaining its anchorage would be difficult through this approach and requires extensive dissection. In such cases, a strut graft can be placed between the intact C1 anterior arch and the uninvolved lower cervical spine, as described in the present report. We believe that ending the construct at C1 would provide an equally stable construct, thus obviating the need for an extensive dissection in a child. The autologous graft can be fashioned with ledges on the ends such that the body of the graft bears the weight, and also its cortical surfaces abut the anterior surface of C1 and the lower cervical spine (Fig. 3). A cortico-cancellous screw would firmly hold the graft until fusion occurs. Posteriorly, fusing the occipital squama to the C1 lateral mass and the subaxial spine is also necessary to prevent movement in between the occipito-atlantal joints that could dislodge the graft. Additionally, the C1 and the occiput act as a single unit, thereby sharing the weight transmission between the anterior strut graft and posterior construct.

A mesh cage or autologous graft is useful for an anterior column reconstruction. In our patient, a bone graft was preferred over a metallic cage as the latter could cause excessive sinking/subsidence in an immature bone; also a bone graft would allow some gain in the height of the vertebral column with time. Commonly, a rib graft is utilized in children for single- or two-level corpectomy [10]. This was not suitable in the present case due to a long-segment bony defect. Hence, we resorted to a fibular strut graft for the anterior column support. The upper screw was inserted through the fibular graft into the C1 anterior arch to stabilize the construct and prevent possible graft dislodgement. Such a technique can be a viable procedure to anchor the graft in cases with extensive C2 destruction. Although this has been occasionally described after C2 spondylectomy in adults, an insertion of tricortical screw anchored to the C1 arch in an immature spine has not been described to the best of our knowledge [12]. Furthermore, this technique is technically demanding in a pediatric spine due to a limited availability of C1 bone mass for screw purchase.

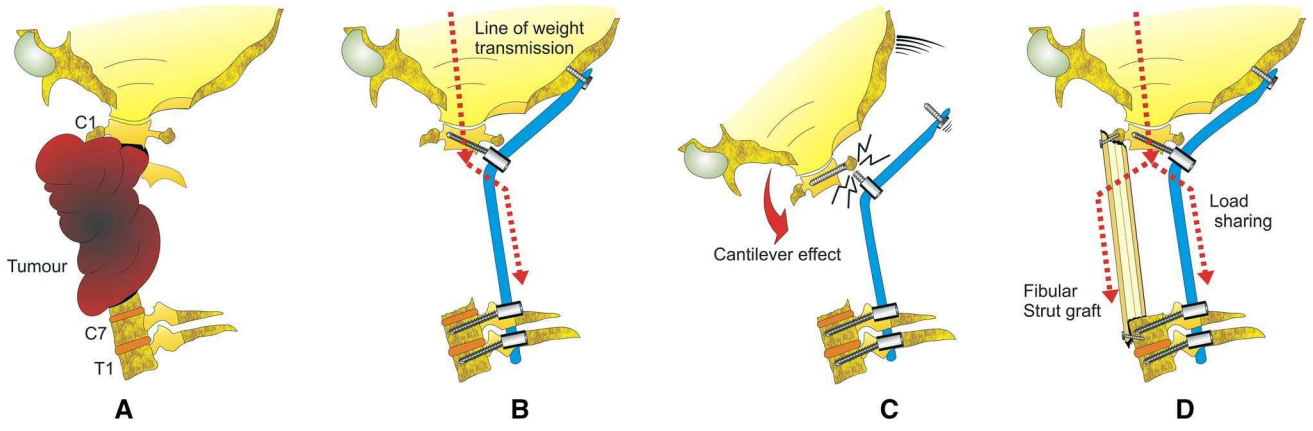

Fig. 3 Schematic diagram demonstrating the surgical technique and cantilever effect. **a** Osteolytic lesion extending from C2 to C6 vertebral bodies. **b** In the absence of an anterior graft, the entire weight of head is borne by the posterior occipito-cervical construct alone. The axis of weight transmission is indicated by dotted line. **c** Eventually, the posterior construct tends to fail due to cantilever mechanism (arrow). **d** The anterior strut graft allows load sharing between the anterior and posterior constructs and provides stable fixation. The fibular graft is fashioned with ledges on the ends such that the cortical surfaces abut the anterior surface of C1 and the lower cervical spine. The upper and lower screws are inserted through the graft into the anterior arch of C1 and the C7 vertebral body, respectively

Occasionally, cutaneous JXG has been reported in the context of neurofibromatosis type 1 [2]. The present case had an association with Klippel–Feil anomaly.

As far as the management of JXG is concerned, the majority of the classical skin lesions show spontaneous regression [2, 13]. In patients with systemic involvement, chemotherapy (steroids, vinblastine and methotrexate) is administered [1, 4, 13]. Owing to the rarity, no definitive treatment protocol exists for isolated spinal JXG. Total excision appears to be curative [3–6]. After partial excision, few have undergone adjuvant radiotherapy/chemotherapy [4, 14, 15]. Recently, neoadjuvant therapy using denosumab has been attempted in a pediatric patient [16]. A review of the reported cases with spinal involvement has shown an overall favorable clinical outcome with no recurrent disease [6]. Hence, we decided for an expectant treatment, considering the possible adverse effects of radiotherapy in young age.

Conclusion

Though uncommon, JXG should be thought of, in the differential diagnosis of solitary osteolytic lesions of vertebral bodies. They can simulate a tuberculous etiology on imaging and at surgery. At times, the lesions tend to be extensive and the management can be challenging. The described technique can be utilized for anterior column reconstruction in children with C2 body destruction.

Acknowledgements We thank Mr. Dharamjit singh, medical illustrator at PGIMER, Chandigarh, for his illustrations.

Compliance with ethical standards

Conflict of interest The authors declare that they have no conflict of interest.

Informed consent Informed consent was obtained from the patient.

References

1. Janssen D, Harms D (2005) Juvenile xanthogranuloma in childhood and adolescence: a clinicopathologic study of 129 patients from the kiel pediatric tumor registry. Am J Surg Pathol 29:21–28
2. Dehner LP (2003) Juvenile xanthogranulomas in the first two decades of life: clinicopathologic study of 174 cases with cutaneous and extracutaneous manifestations. Am J Surg Pathol 27:579–593
3. Cao D, Ma J, Yang X, Xiao J (2008) Solitary juvenile xanthogranuloma in the upper cervical spine: case report and review of the literatures. Eur Spine J 17(Suppl 2):S318–S323
4. Inoue H, Seichi A, Yamamuro K, Kojima M, Kimura A, Hoshino Y (2011) Dumbbell-type juvenile xanthogranuloma in the cervical spine of an adult. Eur Spine J 20(Suppl 2):S343–S347
5. Jain A, Mathur K, Khatri S, Kasana S, Jain SK (2011) Rare presentation of juvenile xanthogranuloma in the thoracic spine of an adult patient: case report and literature review. Acta Neurochir (Wien) 153:1813–1818
6. Shenoy A, Singhal SS, Shinde S (2018) Solitary intraspinal juvenile xanthogranuloma in an infant. Asian J Neurosurg 13:172–175
7. Emile JF, Abla O, Fraitag S, Horne A, Haroche J, Donadieu J et al (2016) Histiocyte Society. Revised classification of histiocytoses and neoplasms of the macrophage-dendritic cell lineages. Blood 127:2672–2681
8. Pirillo V, Prontera A, Rizzo P, Cecchi PC, Maffei M, Schwarz A (2017) A rare case of intramedullary solitary juvenile xanthogranuloma of the lumbar spine in the adult: a case report. J Spine Surg 3:504–508
9. Levine DN (2004) The pathogenesis of syringomyelia associated with lesions at the foramen magnum: a critical review of existing theories and proposal of a new hypothesis. J Neurol Sci 220:3–21
10. Menezes AH, Ahmed R (2014) Primary atlantoaxial bone tumors in children: management strategies and long-term follow-up. J Neurosurg Pediatr 13:260–272
11. Salunke P, Sahoo SK, Sood S, Mukherjee KK, Gupta SK (2016) Focusing on the delayed complications of fusing occipital squama to cervical spine for stabilization of congenital atlantoaxial dislocation and basilar invagination. Clin Neurol Neurosurg 145:19–27
12. Štulík J, Kozák J, Šebesta P, Vyskočil T, Kryl J, Klezl Z (2010) Total spondylectomy of C2: report of three cases and review of the literature. J Spinal Disord Tech 23:e53–e58
13. Classen CF, Minkov M, Lehrnbecher T (2016) The non-Langerhans cell histiocytoses (rare histiocytoses)—clinical aspects and therapeutic approaches. Klin Padiatr 228(6–07):294–306
14. Agabegi SS, Iorio TE, Wilson JD, Fischgrund JS (2011) Juvenile xanthogranuloma in an adult lumbar spine: a case report. Spine (Phila Pa 1976) 36:E69–E73
15. Castro-Gago M, Gómez-Lado C, Alvez F, Alonso A, Vieites B (2009) Juvenile xanthogranuloma of the cauda equina. Pediatr Neurol 40:123–125
16. Irmola T, Laitinen MK, Parkkinen J, Engellau J, Neva MH (2018) Solitary juvenile xanthogranuloma in the spine pretreated with neoadjuvant denosumab therapy followed by surgical resection in a 5-year-old child: case report and literature review. Eur Spine J. https://doi.org/10.1007/s00586-018-5651-8

European Spine Journal (2019) 28 (Suppl 2):S61–S67
https://doi.org/10.1007/s00586-019-05929-y

CASE REPORT

Chylous fistula: management of a rare complication following right anterior cervical spine approach

Federica Novegno[1] · Pierluigi Granaroli[1] · Luigi Ciccoritti[2] · Pierpaolo Lunardi[1] · Mario Francesco Fraioli[1]

Received: 6 February 2018 / Revised: 1 February 2019 / Accepted: 21 February 2019 / Published online: 28 February 2019

Abstract

Purpose Chylorrhea resulting from injury of the lymphatic system during neck dissection is a well-known complication. It is an uncommon occurrence in spinal surgery, and only one case after right anterior cervical spine surgery has been described so far. Despite its rarity, chylous leakage deserves a particular attention since it may become a serious and occasionally fatal complication if not detected early and managed appropriately.

Methods We report the case of a 42-year-old man who underwent a standard anterior cervical discectomy and fusion according to Cloward approach for a C6–C7 disk herniation. The patient developed a delayed prevertebral chyle collection on postoperative day 5, presenting with mild breathing and swallowing difficulties.

Results He was managed with conservative care, including bed rest, low-fat diet and drainage pouch positioning, which led to the complete resolution of the fluid collection.

Conclusions Knowledge of the normal anatomy of the lymphatic system and of its variations is essential when planning an anterior spinal procedure, and represents the first measure to be adopted in order to avoid such complication. The prompt identification of a postoperative chylous fistula and the applicability of an individually based management's protocol may help in the majority of the cases to reduce the potential morbidity, without significant long-term effects.

Keywords Cervical spine · Chyle leak · Lymphatic ducts · Discectomy · Surgical complication

Introduction

The anterior cervical discectomy and fusion (ACDF) is one of the most common surgical procedures adopted in the treatment of cervical myeloradiculopathy [1, 2]. The most frequent complications include dysphagia, hoarseness, infections, postoperative hematoma, new neurological deficits and laryngeal injuries [2–5]. In this case report, we describe a patient with a postoperative chylous fistula following a standard right C6–C7 ACDF [6].

✉ Federica Novegno
federicanovegno@hotmail.it

[1] Department of Neurosurgery, Tor Vergata University Medical School, University of Rome "Tor Vergata", V.le Oxford 81, 00133 Rome, Italy

[2] Department of Endocrine and Metabolic Surgery, Fondazione Policlinico Universitario A. Gemelli, IRCCS, Rome, Italy

Case report

A 42-year-old man was admitted with a 6-month history of left cervicobrachialgia associated with paresthesia and hypoesthesia, resembling a severe C7 radiculopathy, that had failed to improve after adequate medical therapies. The cervical magnetic resonance (MR) scans showed a prevalently left C6–C7 disk herniation and uncovertebral joint osteophyte formation.

The patient underwent a right anterior C6–C7 discectomy and fusion with titanium cage, according to a standard Cloward approach.

The immediate postoperative course was uneventful and characterized by a significant improvement in the radicular symptoms; the patient was discharged on the third postoperative day. On the fifth postoperative day, the patient came back with mild breathing and swallowing difficulties, associated with a non-tender mobile mass superior to the skin incision (Fig. 1a).

Cervical computed tomography (CT) scan and ultrasound examination confirmed the presence of a hypodense fluid

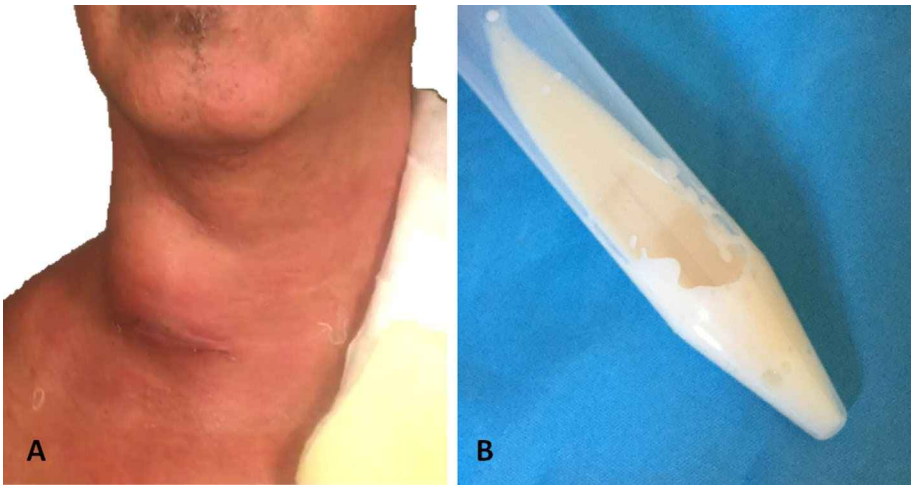

Fig. 1 **a** Photograph of the patient showing the non-tender mobile mass superior to the skin incision observed on the 5th postoperative day, **b** photograph of a test tube containing the white, milky, creamy fluid drained for laboratory examination

collection in the right supraclavicular region; both trachea and esophagus appeared displaced medially (Fig. 2). We drained about 60 cc of fluid with milky appearance (Fig. 1b). The laboratory analysis of the fluid showed: triglyceride (TG) level 2164 mg/dl, LDL cholesterol 25.00 mg/dl, HDL cholesterol 8.00 mg/dl, glucose 151 mg/dl, albumin 2.1 g/dl, LDH 127 UI/l, total proteins, 6.6 g/dl, lipase 1056 U/l and amylase 58 UI/l. Thus, a diagnosis of chylous fistula was made.

During the following 3 days, the patient underwent daily percutaneous drainage and local compression, with no significant improvement in drain output (about 100 cc/day). Therefore, he was put on a low-fat diet. The wound was partially reopened through the previous incision (about 5 mm), and a drainage pouch was positioned. This allowed a spontaneous constant drainage, avoiding patient discomfort, until an inversion of the pressure gradient was obtained. The drainage volume decreased progressively and, eventually, the wound healed spontaneously after 3 more days. Once discharged, the patient underwent periodic clinical–radiological evaluations. Seriated ultrasound examinations demonstrated the progressive reabsorption of the fluid collection (Fig. 3). At 2-year follow-up, the patient presents a complete resolution of the radiculopathy and no evidence of chylous fistula recurrence.

Discussion

The anterior approach to the cervical spine has been widely used with a low rate of major complications (9–20%). The most frequent complications include dysphagia (16.2%), hoarseness (4.8%), epidural hematoma, C5 palsy (2%), CSF leakage (1.9%), infection (0.9%) and implant extrusion (0.8%) [2, 7]. Extremely rare complications include hemothorax, carotid or vertebral artery injury, spinal cord injury, brachial plexopathy, hypoglossal nerve palsy, Horner's

Fig. 2 Postoperative axial (**a**, **b**) computed tomography (CT) images demonstrating the presence of a right prevertebral fluid collection, with hypodense signal, extending up to the hyoid bone level (**a**) and displacing the cervical trachea and esophagus laterally to the left. Some small air bubbles are visible in the contest of the collection. **c** Postoperative sagittal reconstruction of the cervical CT showing the proper position of the interbody cage at C6–C7 level

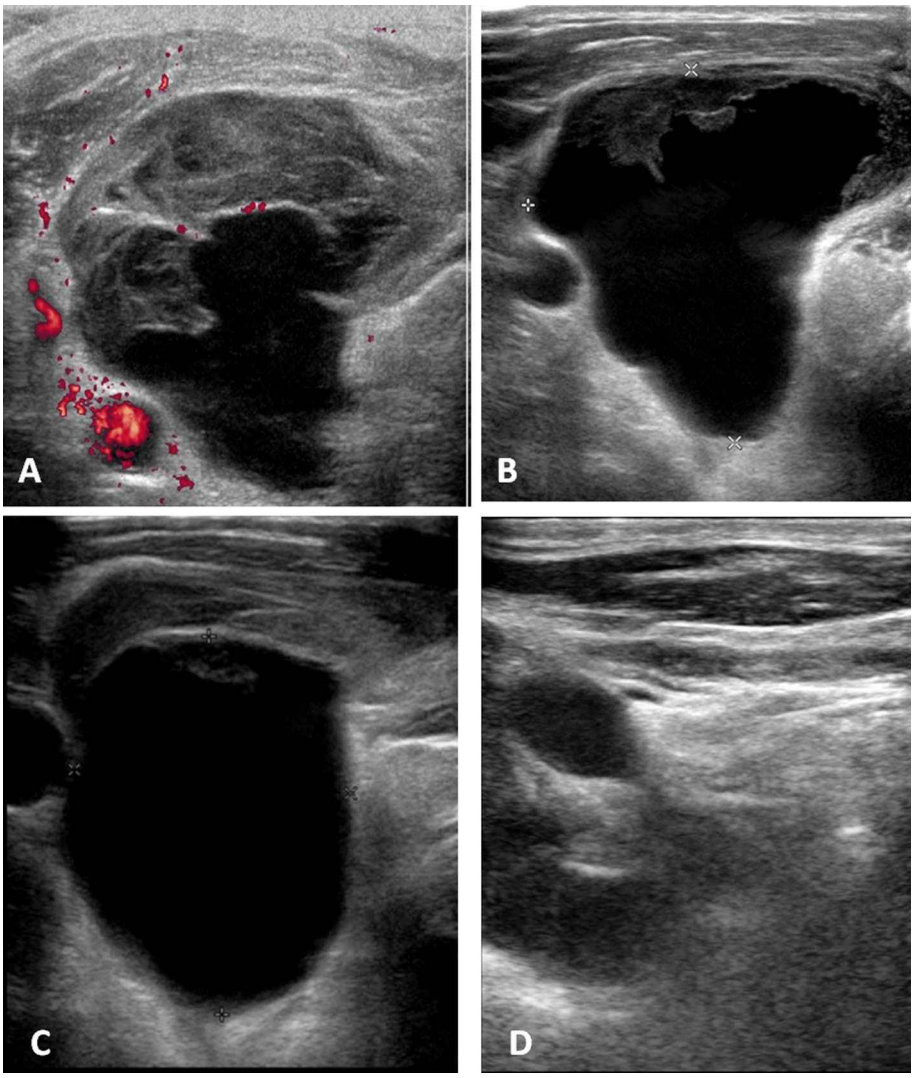

Fig. 3 Axial ultrasonography images **a** depicted on the 6th postoperative day, showing the presence of a anechoic cyst partially organized (48×47 mm) displacing the right thyroid lobe. Doppler examination shows physiological pulsatility index of common carotid artery. Axial ultrasonography images (**b**–**d**) obtained, respectively, at the 10th, 30th and 60th postoperative days demonstrating the progressive reabsorption of the chylous collection

syndrome, vision loss, esophageal perforation and intraoperative death [1, 3, 4, 8–14].

Postoperative chylous fistula represents an even rarer complication in anterior approaches to the cervical spine. Indeed, its prevalence rate has been estimated at 0.02%.

It represents a well-known entity as a serious complication of head and neck surgery that occurs in 0.5–1.4% of thyroidectomies and 2–8% of radical neck dissections [16]. The majority of these cases may be encountered during surgery of the left neck (75–92%), limiting to one-fourth of the cases associated with right neck surgeries [16, 17].

Data from the literature pointed out that this kind of complication has been seldom reported during spinal surgeries, particularly in anterior thoracolumbar approaches, where the anatomical dissection to reach the column involves the biggest lymphatic collectors and the thoracic duct itself [5, 18–21]. Only five cases occurring after anterior cervical surgeries have been described in the literature so far, among which only one was a right side approach (Table 1) [15, 22–24].

Despite its rarity, chylous leakage deserves a particular attention since, without an early detection and appropriate management, it may become a serious and occasionally fatal complication. Delayed wound healing, wound breakdown with fistula formation and infection may result as a consequence of the disruption of the normal biochemical environment [16, 25]. The chyle fluid, indeed, presents erosive properties on the surrounding tissues, leading to possible injuries of the neighboring vessels. Furthermore, the pressure of a chyle collection may decrease tissue perfusion, resulting in flap necrosis [25]. Systemic problems are related to dehydration, nutritional deficiencies (depletion of electrolytes, hypoproteinemia, low blood lipid levels and deficiencies of the fat-soluble vitamins), hypovolemia, respiratory dysfunction and immunosuppression. Chyle leak is burdened by a mortality rate of 50% without supportive therapy [5].

Table 1 Summary of the cases with chylous leakage after anterior cervical spine procedures reported in the literature

Authors	Sex/age	Clinical history	Surgical procedure	Chyle leak complication	Treatment	FU
Hart et al. [22]	M/37	C7 radiculopathy	Left C6–C7 ACDF	Intraoperative occurrence	Intraoperative closure of thoracic duct with sutures	No recurrence at 1 year
Warren et al. [24]	F/58	Advanced cervical degenerative disease	Right multilevel C3–C7 ACDF (plates and screws)	1 week PO: chyloptysis, dysphagia, respiratory distress. Huge prevertebral fluid collection	First attempt: urgent percutaneous aspiration under US and positioning of drainage Second attempt: sclerotherapy Third attempt: percutaneous embolization	No recurrence at 6 months
Derakhshan et al. [15]	M/NR	Radicular pain	Left C5–C6 ACDF	Intraoperative occurrence	Intraoperative closure of thoracic duct with clips	No recurrence at 80 days
	F/NR	Radiculopathy	Left C5–C6 ACDF	After 2 months fluid collection superior to the incision	Needle aspiration	No recurrence at 3.5 years
Mueller et al. [23]	F/59	Bilateral cervicobrachialgia, already C4–C5 ACDF	Left C5–C6 ACDF and C7 corpectomy	On 1st PO day chyle into the drain	Low-fat diet Octreotide	No recurrence after several years
Present case	M/42	Left C7 radiculopathy	Right C6–C7 ACDF	On 5th PO fluid collection superior to the incision with dysphagia and respiratory distress	Low-fat diet Drainage pouch positioned	No recurrence at 2 years

ACDF anterior cervical discectomy and fusion, *NR* not reported, *PO* postoperative, *yr* year, *US* ultrasound

Relevant anatomy and variations: surgical nuances

The lymphatic system is accessory to the circulatory system: It transports the products of fat digestion, drains excess fluids from the body back to the blood and filters them through lymph nodes [21, 26]. The thoracic duct drains three quarters of the lymph into the venous blood stream, including that originating from the lower body and the left head and arm. It originates from the cisterna chyli, usually located on the anterior surface of the first and second lumbar vertebral body [22]. Ascending to the thorax, at T7 it deviates obliquely behind the esophagus and crosses the midline to the left at the level of T5–T6 vertebrae. It then passes behind the aorta and to the left of the esophagus, emptying into the confluence of the left internal jugular and subclavian veins, about 2–3 cm above the clavicle [26, 27]. The remaining third of the lymph, originating from the right thorax, arm, neck and head, flows into the adult right lymphatic duct. This duct is 1–2 cm long, closely related to the anterior scalene muscle, and usually empties into a corresponding location on the right, at the level of the junction between the right subclavian and internal jugular veins [27, 28].

There is a wide variation in lymphatic system anatomy due to deviations in normal embryologic development; if present, developmental anomalies of the lymphatic system can provide surgical challenges [28]. Several anatomical variants have been described so far: a complete left-sided thoracic duct, a complete right-sided thoracic duct, a proximal and distal partial duplication of the thoracic duct, a plexiform variation of the thoracic duct or absence of the cisterna chyli [27]. The greatest variation in thoracic duct anatomy is seen in proximity to its termination, with multiple branching in about 40% of cases, thus explaining why the most common site of injury to the ducts during neck dissection is lateral to the inferior portion of the carotid sheath on either side [28]. In 5% of cases, the main thoracic duct may terminate on the right side of the neck. This is the reason that although most injuries of the thoracic duct are in the left cervical area, a smaller percentage of injuries may occur in the right side of the neck [17].

The right lymphatic duct may present likewise anatomical variations (1–5%). Its most frequent origin is from the right jugular, bronchomediastinal and subclavian lymphatic trunks, although these vessels may terminate individually so that the main duct results absent [28].

Diagnosis

The diagnosis of chylous fistula can be made intraoperatively or postoperatively [16, 29]. In general, some authors recommend a careful inspection of the surgical field after a head and neck procedure, especially in those cases involving the dissection low in the neck; the occurrence of creamy or milky fluid is highly suspicious for a lymphatic system trauma. Intraoperative diagnosis may be challenging because patients are usually in a fasting state before surgery, slowing down significant lymph production [15]. Thus, maneuvers that increase intrathoracic and/or intraabdominal pressure may improve the visibility of the chyle leakage. However, the presence of variant terminations may compromise the efficacy of the ligation resulting in persistent chylous fistula [16].

The majority of cases (about 86%) are diagnosed during the first three postoperative days, owing to the resumption of foods that contain fat, which induce an increment in chyle production and flow [16, 17]. The patient may exhibit a sudden increase in drain output, with a typical milky appearance, and volumes between 300 and 500 ml/day [25]. Nevertheless, low-volume leakages may be underestimated because it was mixed with blood and mistaken as purulent secretions. On inspection, the skin may present a bulge at the level of the supraclavicular fossa, associated with induration, edema, erythema [16, 25].

The drain fluid can be analyzed: The fat content of chyle ranges from 0.4 to 4%, and the main lipid component is triglyceride (greater than 100–200 mg/dl) [16, 17]. Other biochemical elements include percentage of chylomicrons greater than 4% and total protein level greater than 3 g/dl [17]. Leukocytes normally range from 1000 to 20,000/mm^3 in thoracic duct lymph [25].

Lymphoscintigraphy with technetium 99 has been proposed in unclear cases with low-volume leakages; data from the literature do not report a consensus on its actual efficacy, and the majority of authors do not utilize this technique routinely [17, 29].

Treatment

The chylous leakage should be repaired immediately once identified intraoperatively. The thoracic duct may be ligated using either non-absorbable 3-0 or 4-0 sutures or surgical clips [16, 29]. Locoregional myofascial flap may be added to perform a coverage of the area, using the clavicular head of the sternocleidomastoid or the pectoralis major [16, 30]. In addition, the region can be sealed with fibrin, polyglactin or collagen [29].

Since 30–80% of patients treated with conservative therapies healed definitively, the general attitude in these cases is to maintain a non-surgical approach, especially when dealing with low-volume output fistulae [16, 17]. Thus, the first step is to evaluate the amount of drain output per day: It can be categorized as low output (less than 500 ml/day) or high output (more than 500 ml/day) [16].

Non-surgical management

As a general disposition, the patient should take bed rest, with elevation of the head (30°–40°), in order to reduce chyle flow; stool softeners can be employed to lessen intraabdominal pressure [16].

Dietary modifications play a crucial role in non-surgical approach, aiming at both decreasing chyle production and flow and replenishing fluid and electrolytes. Diets can include nonfat, low-fat or medium-chain fatty acids (for low output) [16, 30]. Octreotide therapy may represent another step of conservative management: It acts directly on vascular somatostatin receptors to minimize the chyle production [16, 30]. Several authors are reporting encouraging results on its efficacy, but no consensus guidelines are available yet: Its dosage ranges in different reports from 100 to 200 mcg, two or three times per day, with a duration variable between 3 and 24 days [16, 31].

A pressure dressing is generally not recommended because the supraclavicular region has no solid basis to support it and there is a potential risk of damaging the skin flap perfusion [16]. Suction drainage is generally employed to evacuate the chyle collection while monitoring drain output. Negative wound pressure medications have also been used in some cases. However, the application of a permanent negative pressure to the entire wound bed may prevent the closure of the chyle fistula, with significant collateral risks, namely major bleeding and infections [16, 32].

Invasive procedures

Surgical re-exploration is generally recommended once conservative approach fails. In particular, surgery should be performed in high output volumes (> 1000 ml/day) lasting for more than 5 days, when low output leakage continues after more than 10 days, or when there are serious complications [29, 30]. The main goal is to identify the leakage site and isolate the lymphatic duct to perform a definitive ligation; however, given the poor state of tissues, this may result extremely difficult even for expert surgeons. Hence, some authors recommend to apply automatically fibrin sealant, followed by a layer of muscle and fascia [29].

Further options of treatment include minimally invasive techniques, often employed as second-line procedures, namely thoracic duct embolization and therapeutic lymphangiography [30]. Despite its promising results, these techniques are both time-consuming and technically challenging, requiring often several attempts [24, 30]. In patients who underwent failed

surgery, ligation of the thoracic duct by means of a thoracoscopic approach can be an effective salvage procedure, avoiding the significant morbidity of major thoracic access [16, 30].

Chylous fistula after anterior cervical spine surgery: lesson learned

According to the literature review, there are only five cases describing lymphatic duct injuries during cervical spine surgery reported so far (Table 1) [15, 22–24]. All but one was left-approached surgical procedures; the only right-approached case was a right multilevel C3–C7 ACDF [24], which required an extensive neck exposure. Indeed, despite being more easily comprehensible, the left laterality cannot alone explain the occurrence of such a complication in cervical spine surgery. The possible anomalous locations or anatomical variations of the terminal branches of the thoracic duct may have contributed to the inadvertent injury, most likely in our case, which was a standard single-level C6–C7 ACDF, requiring minimal neck dissection [22, 24]. In particular, we hypothesized that a damage of the right cervical duct may have resulted in either excessive traction or improper coagulation of redundant fat in proximity of the esophagus during the soft tissues dissection. Fortunately, in our case the leakage resolved in a relatively short time with conservative treatments, so that we excluded a major laceration of the main thoracic duct (even suspecting its anomalous right side termination) not requiring further invasive diagnostic procedures.

In order to avoid the lymphatic system's injury, a sound understanding of its anatomy and an intraoperative awareness of the potential interpatient variations are, therefore, advisable (Fig. 4) [15]. With concern to anterior cervical approaches, this knowledge is important for spinal surgeons, since preoperative radiographic methods (namely sonography, CT, MR lymphography and MRI) are considered neither determinant nor useful in clinical practice [18].

In two cases, the chyle leakage occurred intraoperatively and required an immediate surgical repair [15, 22]. In these two cases, the fistula presented with a mild amount [15, 23] and, as in our case, a conservative approach resulted effective. The last case required several procedures, including positioning of a drainage, catheter-based sclerotherapy treatments and percutaneous thoracic duct embolization [24]. In conclusion, all the patients had a good prognosis, with no recurrences at the last follow-up.

Conclusions

Complications involving the lymphatic system are rarely encountered in anterior cervical spine surgery; however, a prompt identification and use of an individually based protocol of management may help reduce potential morbidity without significant long-term effects, achieving the complete resolution of symptoms [23].

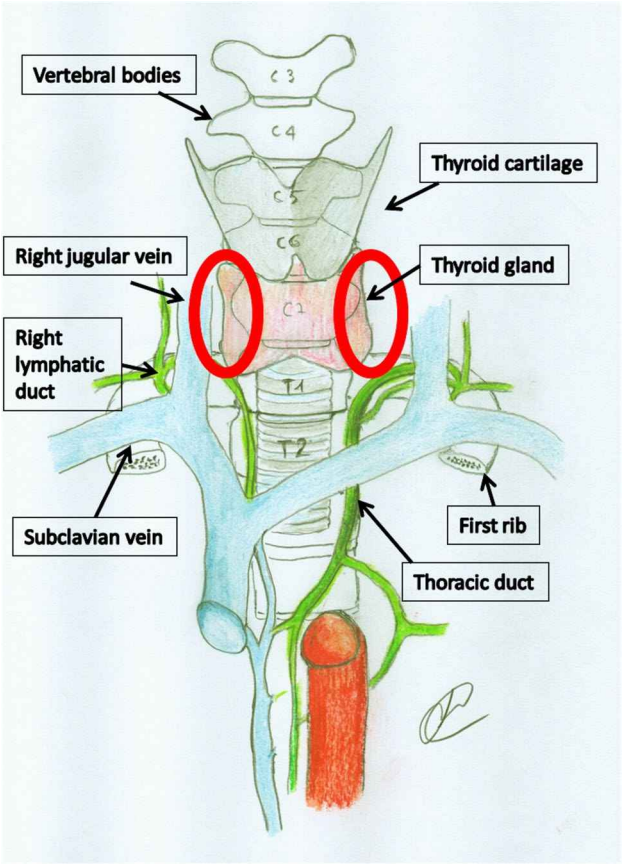

Fig. 4 Schematic drawing showing the relevant anatomy of the neck. The ellipses indicate the likely region of most lymphatic system injuries on both sides, given the anatomical variability of the ducts pathways in the cervical area described in the text

Acknowledgements We thank Dr. Elena Jane Mason for editing the manuscript.

Compliance with ethical standards

Conflict of interest The authors report no conflict of interest concerning the materials or methods used in this study or the findings specified in this paper.

References

1. Harhangi BS, Menovsky T, Wurzer HA (2005) Hemothorax as a complication after anterior cervical discectomy: case report. Neurosurgery 56(4):E871
2. Wang T, Tian XM, Liu SK, Wang H, Zhang YZ, Ding WY (2017) Prevalence of complications after surgery in treatment for cervical compressive myelopathy: a meta-analysis for last decade. Medicine (Baltimore) 96(12):e6421

3. Ames CP, Clark AJ, Kanter AS et al (2017) Hypoglossal nerve palsy after cervical spine surgery. Glob Spine J 7(1 Suppl):37S–39S
4. Daniels AH, Hart RA, Hilibrand AS et al (2017) Iatrogenic spinal cord injury resulting from cervical spine surgery. Glob Spine J 7(1 Suppl):84S–90S
5. Denaro L, Longo UG, Papalia R, Denaro V (2010) Complications related to antero-lateral approaches. In: Denaro L, D'Avella D, Denaro V (eds) Pitfalls in cervical spine surgery. Springer, Berlin, pp 91–108
6. Cloward RB (1958) The anterior approach for removal of ruptured cervical disks. J Neurosurg 15(6):602–617
7. Smith GA, Pace J, Corriveau M et al (2017) Incidence and outcomes of acute implant extrusion following anterior cervical spine surgery. Glob Spine J 7(1 Suppl):40S–45S
8. Gabel BC, Lam A, Chapman JR et al (2017) Perioperative vision loss in cervical spinal surgery. Glob Spine J 7(1 Suppl):91S–95S
9. Härtl R, Alimi M, Abdelatif Boukebir M et al (2017) Carotid artery injury in anterior cervical spine surgery: multicenter cohort study and literature review. Glob Spine J 7(1 Suppl):71S–75S
10. Hilibrand AS, Nassr A, Arnold PM et al (2017) Epidemiology and outcomes of vertebral artery injury in 16 582 cervical spine surgery patients: an AOSpine North America Multicenter Study. Glob Spine J 7(1 Suppl):21S–27S
11. Hsu WK, Kannan A, Mai HT et al (2012) Chyloretroperitoneum following anterior spinal surgery. J Neurosurg Spine 17(5):415–421
12. Than KD, Mummaneni PV, Smith ZA et al (2017) Brachial plexopathy after cervical spine surgery. Glob Spine J 7(1 Suppl):17S–20S
13. Traynelis VC, Malone HR, Smith ZA et al (2017) Rare complications of cervical spine surgery: Horner's syndrome. Glob Spine J 7(1 Suppl):103S–108S
14. Wang JC, Buser Z, Fish DE et al (2017) Intraoperative death during cervical spinal surgery: a retrospective multicenter study. Glob Spine J 7(1 Suppl):127S–131S
15. Derakhshan A, Lubelski D, Steinmetz MP et al (2017) Thoracic duct injury following cervical spine surgery: a multicenter retrospective review. Glob Spine J 7(1 Suppl):115S–119S
16. Delaney SW, Shi H, Shokrani A, Sinha UK (2017) Management of chyle leak after head and neck surgery: review of current treatment strategies. Int J Otolaryngol. https://doi.org/10.1155/2017/8362874
17. Priego Jiménez P, Collado Guirao MV et al (2008) Chyle fistula in right cervical area after thyroid surgery. Clin Transl Oncol 10(9):593–596
18. Akcali O, Kiray A, Ergur I, Tetik S, Alici E (2006) Thoracic duct variations may complicate the anterior spine procedures. Eur Spine J 15(9):1347–1351
19. Bhat AL, Lowery GL (1997) Chylous injury following anterior spinal surgery: case reports. Eur Spine J 6(4):270–272
20. Su IC, Chen CM (2007) Spontaneous healing of retroperitoneal chylous leakage following anterior lumbar spinal surgery: a case report and literature review. Eur Spine J 16(Suppl 3):332–337
21. Upadhyaya CD, Park P, La Marca F (2007) Chyloretroperitoneum following anterior spinal deformity correction. Case report. J Neurosurg Spine 7(5):562–565
22. Hart AK, Greinwald JH Jr, Shaffrey CI, Postma GN (1998) Thoracic duct injury during anterior cervical discectomy: a rare complication. Case report. J Neurosurg 88(1):151–154
23. Mueller K, Syed HR, Rhee JW, Nair MN (2017) Delayed chyle leak following anterior cervical spinal surgery: a case report and management algorithm. Cureus 9(5):e1231. https://doi.org/10.7759/cureus.1231
24. Warren PS, Hogan MJ, Shiels WE (2013) Percutaneous transcervical thoracic duct embolization for treatment of a cervical lymphocele following anterior spinal fusion: a case report. J Vasc Interv Radiol 24(12):1901–1905
25. Erisen L, Coskun H, Basut O (2002) Objective and early diagnosis of chylous fistula in the postoperative period. Otolaryngol Head Neck Surg 126(2):172–175
26. Phang K, Bowman M, Phillips A, Windsor J (2014) Review of thoracic duct anatomical variations and clinical implications. Clin Anat 27(4):637–644
27. Johnson OW, Chick JF, Chauhan NR et al (2016) The thoracic duct: clinical importance, anatomic variation, imaging, and embolization. Eur Radiol 26(8):2482–2493
28. Smith ME, Riffat F, Jani P (2013) The surgical anatomy and clinical relevance of the neglected right lymphatic duct: review. J Laryngol Otol 127(2):128–133
29. Santaolalla F, Anta JA, Zabala A et al (2010) Management of chylous fistula as a complication of neck dissection: a 10-year retrospective review. Eur J Cancer Care (Engl) 19(4):510–515
30. Campisi CC, Boccardo F, Piazza C, Campisi C (2013) Evolution of chylous fistula management after neck dissection. Curr Opin Otolaryngol Head Neck Surg 21(2):150–156
31. Prabhu S, Thomas S (2015) Octreotide for conservative management of intractable high output post operative chylous fistula: a case report. J Maxillofac Oral Surg 14(Suppl 1):21–24
32. Kadota H, Kakiuchi Y, Yoshida T (2012) Management of chylous fistula after neck dissection using negative-pressure wound therapy: a preliminary report. Laryngoscope 122(5):997–999

European Spine Journal (2019) 28 (Suppl 2):S68–S72
https://doi.org/10.1007/s00586-019-06005-1

CASE REPORT

Delayed presentation of infected common iliac artery pseudoaneurysm caused by malpositioned pedicle screw after minimally invasive scoliosis surgery

Seung-Woo Suh[1] · Gang-Un Kim[2] · Hoon-Nyun Lee[1] · Jae Hyuk Yang[1] · Dong-Gune Chang[2]

Received: 12 November 2018 / Accepted: 9 May 2019 / Published online: 14 May 2019

Abstract

Purpose To report delayed onset common iliac artery perforation and infected pseudoaneurysm caused by malpositioned pedicle screw after minimally invasive scoliosis surgery (MISS).

Methods A 21-year-old female was referred to our hospital with a 1-week history of abrupt right-sided low back pain, lower abdominal pain, and fever with a history of MISS using cannulated pedicle screws 18 months earlier. Paravertebral arterial erosion with pseudoaneurysm and retroperitoneal and paraspinal abscess were suspected.

Results We performed resection of the pseudoaneurysm, vascular repair of right common iliac artery by angioplasty with a bovine patch and removal of implant. At 6 months after the last surgery, she had no limitations or problems in her daily activities with no recurrence of low back pain, abdominal pain, or fever as well as without loss of deformity.

Conclusions Our case showed that misplaced pedicle screws can cause potentially fatal complications, such as infected pseudoaneurysm, even in the late postoperative period.

Keywords Abscess · Common iliac artery · Fistula · Pseudoaneurysm · Malpositioned cannulated pedicle screw · Minimally invasive scoliosis surgery

Introduction

Pedicle screw instrumentation has been used to treat various complex spinal disorders, including spinal deformity correction [1]. However, damage to major vessels, including the aorta and iliac arteries, due to pedicle screw fixation has been reported [2–4]. Most acute major vessel injuries cause sudden hemodynamic instability, which may inadvertently lead to a life-threatening condition [5, 6]. More rarely, however, major vessel injuries after pedicle screw misplacement may be found with delayed symptom presentation or incidental findings in asymptomatic patients [7–10].

We experienced delayed onset common iliac artery perforation and infected pseudoaneurysm caused by a malpositioned pedicle screw after minimally invasive scoliosis surgery (MISS). Our report highlights that even posterior instrumentation surgery of the lower lumbar vertebra may cause major arterial injury in the late postoperative period, and a malpositioned cannulated screw could be a facilitating conduit to the spread of infection.

Materials and methods

A 21-year-old female was referred to our hospital with a 1-week history of abrupt right-sided low back pain, lower abdominal pain, and fever. About 18 months previously,

Seung-Woo Suh and Gang-Un Kim equally contributed to this study as the co-first author.

Jae Hyuk Yang and Dong-Gune Chang equally contributed to this study as the co-corresponding author.

IRB Status This study received the approval of the institutional review board of Korea University Guro Hospital (K2018-1903).

✉ Dong-Gune Chang
spine@paik.ac.kr

[1] Department of Orthopaedic Surgery, Korea University Guro Hospital, Guro-Dong, Guro-Gu, Seoul 152-703, Republic of Korea

[2] Department of Orthopaedic Surgery, Sanggye Paik Hospital, College of Medicine, Inje University, 1342, Dongil-Ro, Nowon-Gu, Seoul 01757, Republic of Korea

she had undergone a minimally invasive scoliosis surgery (MISS) for the treatment of adolescent idiopathic scoliosis using a cannulated pedicle screw system from T4 to L4. Abdomino-pelvic computed tomography (AP-CT) revealed about $6.5 \times 11 \times 9$ cm-sized collection of pre- and paravertebral fluid surrounding a rim-like enhancement around L3-5 level, containing more than two lobulated spaces filled with high-density-contrast material (maximum 4.1 cm in size, Fig. 1a) predominantly at the L4–5 level. In addition, a cystic lesion with a similar appearance was observed around the adjacent paraspinal muscle area, more than $3.3 \times 5 \times 10.5$ cm, from T12 to Rt S1 level (Fig. 1b). Subsequent lumbar spine X-ray and CT revealed that the right L4 screw was positioned too far anteriorly with periscrew halo formation, adjacent vertebral body erosion, and detachment of the transverse process (Fig. 2). The medical records and postoperative radiographs of the hospital where the first operation was performed confirmed the surgical information: On medical record examination, there was no specific finding to cause infection on pre- and postoperative period except long operation time (about 10 h). On surgical procedures, deformity was corrected with MISS technique which

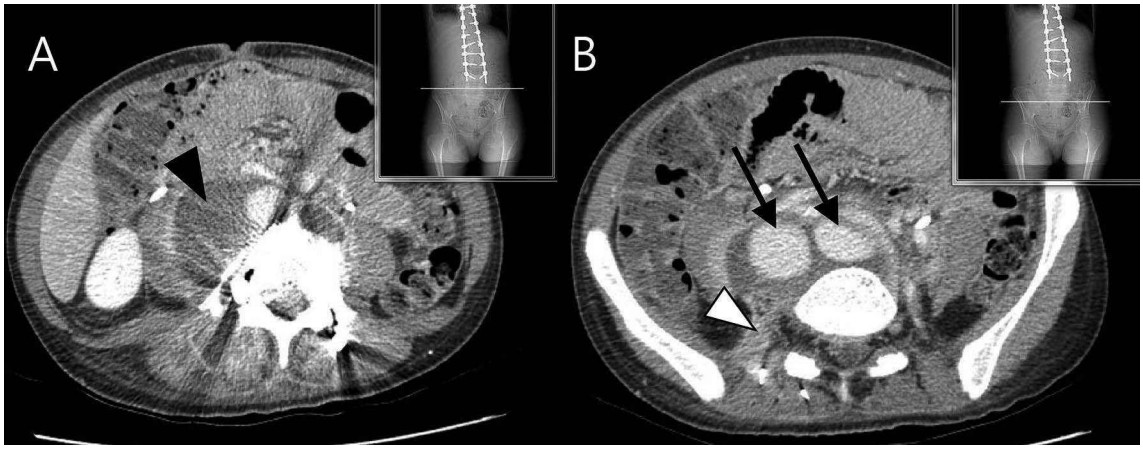

Fig. 1 Abdomino-pelvic computed tomography (AP-CT) revealed a collection of pre- and paravertebral fluid collection (black arrowhead) surrounding a rim-like enhancement around the L3–5 level, containing more than two lobulated spaces filled with high-density-contrast material (black arrow, **a**), predominantly at the L4–5 level. In addition, a cystic lesion with a similar appearance was observed around the adjacent paraspinal muscle area, from T12 to Rt S1 level (white arrowhead, **b**)

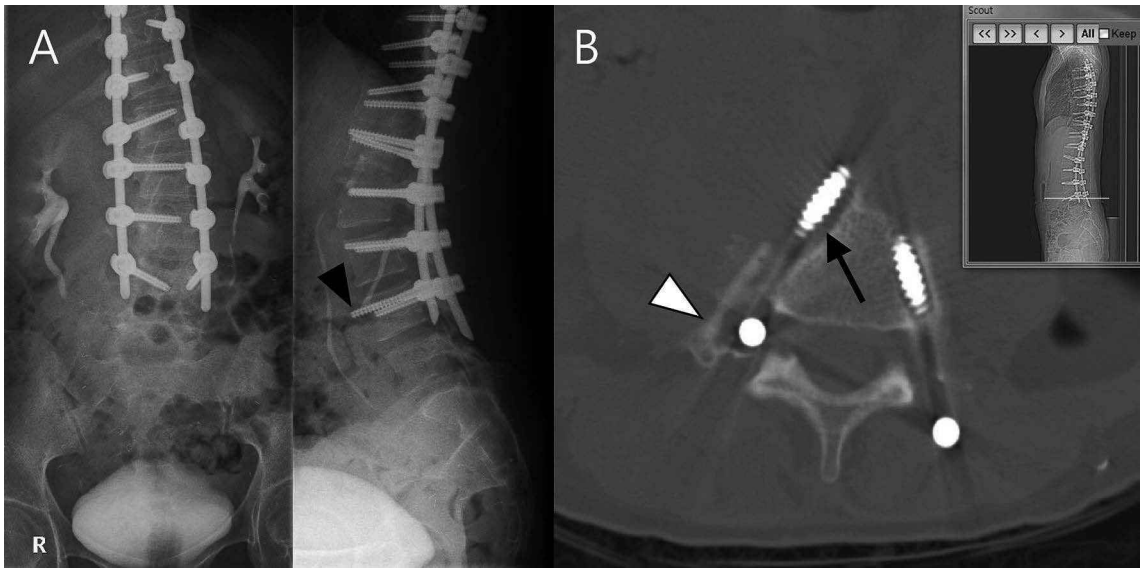

Fig. 2 Lumbar spine X-ray and CT revealed that the right L4 pedicle screw (black arrowhead) was positioned to far anteriorly, with periscrew halo formation (black arrow), adjacent vertebral body erosion, and detachment of the transverse process (white arrowhead)

was made up with free-handed cumulated poly-axial pedicle screw insertion through 2–4 skin incisions each of size 3 cm, pre-contoured rod insertion, thoracoplasty using the same skin incision, arthrodesis by facetal fusion and correction using rod translation and rotation maneuvers [11]. On immediate postoperative radiography at first operation, right L4 pedicle screw malposition was seen without a screw halo.

Clinically, paravertebral arterial erosion with pseudoaneurysm and retroperitoneal and paraspinal abscess were suspected, and surgical treatment was inevitable. Our operating strategy was an interdisciplinary single-session two-step approach, with a vascular surgery team. The first step of surgery was retroperitoneal exploration through the anterior midline abdominal incision. Intraoperatively, a 3-mm perforation at the posterior wall of the right common iliac artery (just below the aortic bifurcation) and pseudoaneurysm behind the artery with surrounding abscess were identified (Fig. 3). After drainage of the abscess, vascular repair of the right common iliac artery was performed with a bovine patch angioplasty. Common iliac artery perforation was treated with primary suture repair. The second step included removal of the right-sided instrument and paravertebral abscess drainage. There was dark-black mucoid fluid with abundant granulation tissues around the right-sided implant at T12–L5 level. Also, a fistula from the right L4 pedicle screw insertion site to the cavity to the retroperitoneal abscess was identified. Left-sided instrumentation was not removed because there was no evidence or sign of infection.

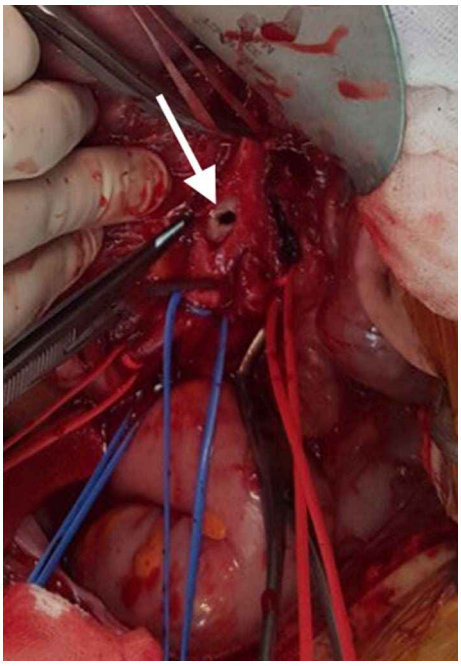

Fig. 3 A 3-mm-sized perforation at the posterior wall of the right common iliac artery, just below the aortic bifurcation (white arrow) was identified and was connected to the fistula from the pedicle screw insertion site

Postoperatively, methicillin-resistant Staphylococcus aureus (MRSA) was identified in the tissue culture from the abscess from the operation field and the patient was treated with intravenous ciprofloxacin according to the antibiotics susceptibility results. At postoperative day seven, the patient recovered to ambulation without any assistance and was discharged without pain or fever. At the 6-month follow-up after the last surgery, she had no limitations or problems in her daily activities with no recurrence of low back pain, abdominal pain, or fever. On the standing whole spine radiograph taken at the last follow-up that was 6 months later after last operation, there was no progression of the residual deformity despite removal of the right-sided instrumentation (Fig. 4).

Discussion

The rate of pedicle screw misplacement varies from 5 to 41% for the lumbar spine, depending on underlying pathology, surgical technique used, and site of screw fixation [12, 13]. The pedicles of the lumbar spine are larger than the pedicles of the thoracic spine. Therefore, the risk of screw misplacement is lower in the lumbar spine than in the thoracic region [14, 15]. Nevertheless, complications caused by pedicle misplacement of the lumbar spine have been reported consistently.

Major vascular injury is one of the most fatal complications of malpositioned pedicle screws. The overall reported incidence of major vascular injury during spine surgery is less than 0.01% [16, 17]. Major vessel injury can remain undiscovered even in follow-up and can become symptomatic in the late postoperative period. The patient may be asymptomatic for months or years after the initial operation. Delayed presentation is most commonly combined with pseudoaneurysm and arteriovenous fistula [18, 19]. Parker et al. reported the incidence of vascular encroachment (a pedicle screw that was touching or deforming the wall of a major vessel) as 0.22% among 6816 consecutive pedicle screws in the thoracic and lumbosacral spine [20]. Foxx et al. reported that 33 of 680 inserted screws were in contact with a major vessel on routine postoperative imaging after a mean follow-up of 44 months, including the aorta (four cases), the iliac artery (seven cases), and the iliac veins (22 cases), but there were no symptoms or sequelae such as pseudoaneurysms, erosions, or deaths [2].

In this case, the patient presented a sudden symptom about 18 months after MISS. MISS for the treatment of AIS has multiple potential benefits such as less blood loss, shorter hospital stay, earlier mobilization, and relatively less pain, but minimally invasive approach usually needs longer

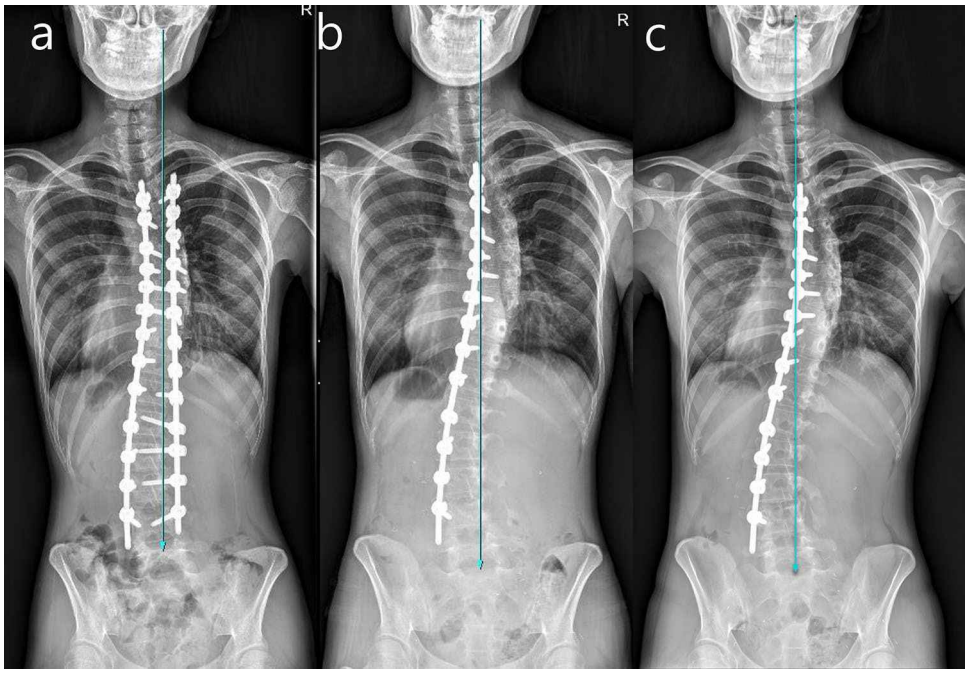

Fig. 4 **a** Standing radiograph at 2 months after initial corrective surgery. Despite removal of right-sided instrumentation (**b**), there was no progression of the residual deformity during the six-month follow-up after the last surgery (**c**)

median operative time and has more potential to make radiologic complications, such as screw loosening or malposition [21–23]. The initial entry point of the misplaced screw was targeted too laterally, and the screw tip was placed too far anteriorly. At this time, the screw tip may have been in contact with the common iliac artery. Screw halo formation, adjacent vertebral body erosion, and detachment of the transverse process indicate that the pedicle screw was not securely fixed to the vertebra. This poor bone-screw anchorage might give less fixation power and finally result in continuous and repetitive motion around the misplaced screw. Scoliosis is one of the most commonly encountered spinal deformities to influence the location of the aorta relative to the vertebral body [24]. Vertebral rotation and angular alterations in scoliosis patients may increase the risk of major vessel injury [14]. In addition, because the misplaced screw was located at the lowest instrumented vertebrae (LIV) of the pedicle screw construct, repetitive toggling motion associated with lumbar spine motion might have occurred on the misplaced screw. This toggling motion of the screw tip was presumed to have caused chronic erosive damage to the adjacent iliac artery and would have contributed to subsequent delayed pseudoaneurysm formation.

In our case, the patient had an infected pseudoaneurysm with abscess formation. Based on a fever episode, complicated infection was presumed to have initiated 1 week before the visit. Paradoxically, the development of this infectious condition helped early detection of late vascular complications in this case. The cause of sudden bacterial infection is presumed to be a hematogenous infection complicated with hematoma around the vessel. In addition, the cannulated pedicle screw used as an instrument for MISS would have contributed to cause increased bleeding and/or spread of infection to the paravertebral muscle layer from the retroperitoneal space where the abscess first occurred.

Our repair strategy for damaged common iliac artery was performed with an open surgical approach, resection of the pseudoaneurysm and an angioplasty with bovine patch. Thanks to effective antibiotic use and relatively young age of the patients, early recovery was achieved without any complications. However, direct repair of the chronic perforation of that vessel seems to be dangerous, especially in the complicated infectious condition. Transient insertion of the vascular stent may also be considered a good alternative technique to consider until the time of infection control.

In summary, we report a rare case of delayed vascular complication following MISS due to malpositioned lumbar pedicle screw, and the cannulated screw could be a facilitating conduit for the spread of infection. Our case showed that misplaced pedicle screws can cause potentially fatal complications even in the late postoperative period, such as infected pseudoaneurysm. In addition, the pedicle screw inserted in the LIV must be inserted in the correct position with sufficient holding strength to prevent delayed complication.

Compliance with ethical standards

Conflict of interest None of the authors has any potential conflict of interest.

References

1. Kim YJ, Lenke LG, Kim J, Bridwell KH, Cho SK, Cheh G, Sides B (2006) Comparative analysis of pedicle screw versus hybrid instrumentation in posterior spinal fusion of adolescent idiopathic scoliosis. Spine (Phila Pa 1976) 31(3):291–298. https://doi.org/10.1097/01.brs.0000197865.20803.d4
2. Foxx KC, Kwak RC, Latzman JM, Samadani U (2010) A retrospective analysis of pedicle screws in contact with the great vessels. J Neurosurg Spine 13(3):403–406. https://doi.org/10.3171/2010.3.spine09657
3. Smythe WR, Carpenter JP (1997) Upper abdominal aortic injury during spinal surgery. J Vasc Surg 25(4):774–777
4. Vanichkachorn JS, Vaccaro AR, Cohen MJ, Cotler JM (1997) Potential large vessel injury during thoracolumbar pedicle screw removal. A case report. Spine (Phila Pa 1976) 22(1):110–113
5. Bierdrager E, Van Rooij WJ, Sluzewski M (2004) Emergency stenting to control massive bleeding of injured iliac artery following lumbar disk surgery. Neuroradiology 46(5):404–406. https://doi.org/10.1007/s00234-004-1198-y
6. Bingol H, Cingoz F, Yilmaz AT, Yasar M, Tatar H (2004) Vascular complications related to lumbar disc surgery. J Neurosurg 100(3 Suppl Spine):249–253
7. Kakkos SK, Shepard AD (2008) Delayed presentation of aortic injury by pedicle screws: report of two cases and review of the literature. J Vasc Surg 47(5):1074–1082. https://doi.org/10.1016/j.jvs.2007.11.005
8. Keerthi I, Dhillon CS, Shetty MB (2012) Late-onset bowel perforation and iliac artery erosion after prominent anterior spinal instrumentation. Spine (Phila Pa 1976) 37(22):E1402–E1405. https://doi.org/10.1097/brs.0b013e318267f813
9. Mirza AK, Alvi MA, Naylor RM, Kerezoudis P, Krauss WE, Clarke MJ, Shepherd DL, Nassr A, DeMartino RR, Bydon M (2017) Management of major vascular injury during pedicle screw instrumentation of thoracolumbar spine. Clin Neurol Neurosurg 163:53–59. https://doi.org/10.1016/j.clineuro.2017.10.011
10. Woo EJ, Ogilvie RA, Krueger VS, Lundin M, Williams DM (2016) Iliac vein compression syndrome from anterior perforation of a pedicle screw. J Surg Case Rep. https://doi.org/10.1093/jscr/rjw003
11. Kim TH, Lee SH, Yang JH, Hong JY, Suh SW (2018) Clinical significance of superior articular process as a reference point for free-hand pedicle screw insertion in thoracic spine. Medicine (Baltimore) 97(7):e9907. https://doi.org/10.1097/md.0000000000009907
12. Gelalis ID, Paschos NK, Pakos EE, Politis AN, Arnaoutoglou CM, Karageorgos AC, Ploumis A, Xenakis TA (2012) Accuracy of pedicle screw placement: a systematic review of prospective in vivo studies comparing free hand, fluoroscopy guidance and navigation techniques. Eur Spine J 21(2):247–255. https://doi.org/10.1007/s00586-011-2011-3
13. Lehman RA Jr, Lenke LG, Keeler KA, Kim YJ, Cheh G (2007) Computed tomography evaluation of pedicle screws placed in the pediatric deformed spine over an 8-year period. Spine (Phila Pa 1976) 32(24):2679–2684. https://doi.org/10.1097/brs.0b013e31815a7f13
14. Qiu XS, Jiang H, Qian BP, Wang WJ, Zhu F, Zhu ZZ, Qiu Y (2014) Influence of prone positioning on potential risk of aorta injury from pedicle screw misplacement in adolescent idiopathic scoliosis patients. J Spinal Disord Tech 27(5):E162–E167. https://doi.org/10.1097/bsd.0000000000000075
15. Sarwahi V, Suggs W, Wollowick AL, Kulkarni PM, Lo Y, Amaral TD, Thornhill B (2014) Pedicle screws adjacent to the great vessels or viscera: a study of 2132 pedicle screws in pediatric spine deformity. J Spinal Disord Tech 27(2):64–69. https://doi.org/10.1097/BSD.0b013e31825bfecd
16. Kopp R, Beisse R, Weidenhagen R, Piltz S, Hauck S, Becker CR, Pieske O, Buhren V, Jauch KW, Lauterjung L (2007) Strategies for prevention and operative treatment of aortic lesions related to spinal interventions. Spine (Phila Pa 1976) 32(25):E753–E760. https://doi.org/10.1097/brs.0b013e31815b657c
17. Papadoulas S, Konstantinou D, Kourea HP, Kritikos N, Haftouras N, Tsolakis JA (2002) Vascular injury complicating lumbar disc surgery. A systematic review. Eur J Vasc Endovasc Surg 24(3):189–195
18. Choi JB, Han JO, Jeong JW (2001) False aneurysm of the thoracic aorta associated with an aorto-chest wall fistula after spinal instrumentation. J Trauma 50(1):140–143
19. Sokolic J, Sosa T, Ugljen R, Biocina B, Simunic S, Slobodnjak Z (1991) Extrinsic erosion of the descending aorta by a vertebral fixator. Tex Heart Inst J 18(2):136–139
20. Parker SL, Amin AG, Santiago-Dieppa D, Liauw JA, Bydon A, Sciubba DM, Wolinsky JP, Gokaslan ZL, Witham TF (2014) Incidence and clinical significance of vascular encroachment resulting from freehand placement of pedicle screws in the thoracic and lumbar spine: analysis of 6816 consecutive screws. Spine (Phila Pa 1976) 39(8):683–687. https://doi.org/10.1097/brs.0000000000000221
21. Than KD, Mummaneni PV, Bridges KJ, Tran S, Park P, Chou D, La Marca F, Uribe JS, Vogel TD, Nunley PD, Eastlack RK, Anand N, Okonkwo DO, Kanter AS, Mundis GM Jr (2017) Complication rates associated with open versus percutaneous pedicle screw instrumentation among patients undergoing minimally invasive interbody fusion for adult spinal deformity. Neurosurg Focus 43(6):E7. https://doi.org/10.3171/2017.8.focus17479
22. Sarwahi V, Wollowick AL, Sugarman EP, Horn JJ, Gambassi M, Amaral TD (2011) Minimally invasive scoliosis surgery: an innovative technique in patients with adolescent idiopathic scoliosis. Scoliosis 6:16. https://doi.org/10.1186/1748-7161-6-16
23. Sarwahi V, Horn JJ, Kulkarni PM, Wollowick AL, Lo Y, Gambassi M, Amaral TD (2016) minimally invasive surgery in patients with adolescent idiopathic scoliosis: is it better than the standard approach? A 2-year follow-up study. Clin Spine Surg 29(8):331–340. https://doi.org/10.1097/bsd.0000000000000106
24. Qiao J, Zhu F, Xu L, Zhu Z, Qian B, Liu Z, Qiu Y (2012) Comparison of the aorta impingement risks between thoracolumbar/lumbar curves with different convexities in adolescent idiopathic scoliosis: a computed tomography study. Eur Spine J 21(10):2043–2049. https://doi.org/10.1007/s00586-012-2315-y

European Spine Journal (2019) 28 (Suppl 1):S1–S2
https://doi.org/10.1007/s00586-018-05863-5

OPEN OPERATING THEATRE (OOT)

Posterior foraminotomy for lateral cervical disc herniation

C. Mehren[1,2] · L. Wanke-Jellinek[1,2]

Keywords Posterior cervical foraminotomy · Keyhole foraminotomy · Lateral cervical disc herniation · Posterior cervical approach

Learning objectives

- Indication for posterior-lateral foraminotomy
- Surgical technique of posterior-lateral foraminotomy

General information

The ideal approach to the treatment of soft cervical disc herniation remains controversial. Although anterior cervical procedures have gained prominence over the past years, posterior cervical foraminotomy has proven benefits. Multiple studies found a relieve of symptoms in 82–97% of patients who have radiculopathy caused by foraminal stenosis or posterolateral herniated discs [1–3].

Furthermore, a posterior approach avoids complications associated with an anterior approach to the cervical spine such as injury of large vessels, esophagus and trachea, postoperative dyspnea and dysphagia, recurrent laryngeal nerve injury as well as accelerated occurrence of adjacent segment disease after fusion.

On the downside, postoperative neck pain and muscular spasm are disadvantages of a posterior cervical approach [3]. An extensive periosteal muscle dissection for adequate visualization can induce neck discomfort, which can result in a slower recovery. Minimally invasive techniques can help to minimize the downsides and allow for fast recoveries and early resumption of normal activities. Summarized, posterior cervical foraminotomy is an effective surgical technique for the treatment of radicular pain caused by foraminal stenosis or posterolateral herniated discs.

Case description/patient history with imaging

A 28-year-old patient presented with brachialgia of the right arm corresponding to dermatome C7. The pain occurred about 2 weeks prior to presentation without any previous trauma. The patient described only minor neck pain. Also, he noticed a weakness of the right arm. No pain was described in the left upper extremity.

The medical examination revealed a 3/5 paresis of the right triceps. The triceps reflex was not provocable. No sensitive deficit could be detected.

The MRI imaging revealed a posterolateral disc herniation C6/7 to the right side with significant compression of the right C7 nerve root.

Surgical strategy

Due to the clinically evident paresis of the triceps together with the radiological findings, we decided to perform posterior cervical foraminotomy C6/7 from the right side along with removal of the sequester.

Prophylactic antibiotics are administered. After nasotracheal intubation, the patient's head is positioned in a

✉ C. Mehren
CMehren@Schoen-Kliniken.de

[1] Spine Center, Schön Clinic Munich Harlaching, Harlachinger Str. 51, 81547 Munich, Germany

[2] Academic Teaching Hospital and Spine Research Institute of the Paracelsus Medical University (PMU), Salzburg, Austria

Watch surgery online

Mayfield three-point pin-holder clamp and log-rolled in a prone position and secured on the operating table. After confirming the correct operative level by fluoroscopy, the microscope is swinged in and a 2 cm skin incision is made slightly right of the posterior midline with the facet joint C6/7 centered on the incision. The paravertebral muscles are stripped subperiosteal on the right side from the spinous process and the lamina of the adjacent vertebra. The tubular system is inserted and the correct level C6/7 fluoroscopically confirmed. This is followed by the preparation of the interlaminar window and medial border of the facet joint C6/7. Using a diamond high-speed burr and Kerrison punches, a small portion of the medial part of the facet joint is removed in a circular—"keyhole"—manner. The partial resection of the ascending facet of C7 is the crucial point for bony decompression of the neuroforamen respectively the nerve root C7. The yellow ligament is identified. The lateral aspect is removed using Kerrison punches to visualize the lateral border of the thecal sack. A large sequester is exposed and carefully resected using the rongeur. Hemostasis is achieved by bipolar pincette. A thorough exploration of the neuroforamen is performed using the dental probe to ensure the complete removal of the sequester. The medial and lateral aspect of both, the cranial and especially caudal pedicle is palpated to ensure a proper decompression. After irrigation the wound is inspected for sources of bleeding. The muscle, fascia and subcutaneous tissue are reapproximated with absorbable sutures. The skin layer is closed with interrupted sutures and bandages are applied.

After log-rolling the patient in a supine position, the Mayfield clamp is carefully removed.

Postoperative information/patient outcome with imaging

The patient experienced a severe improvement of the brachialgia almost immediately after surgery. In the postoperative course, the initially existing 3/5 paresis of the right triceps slowly improved as well. The patient was released from the hospital at 2 days after surgery.

Compliance with ethical standards

Conflict of interest None of the authors has any potential conflict of interest.

References

1. Henderson CM, Hennessy RG, Shuey HM Jr, Shackelford EG (1983) Posterior-lateral foraminotomy as an exclusive operative technique for cervical radiculopathy: a review of 846 consecutively operated cases. Neurosurgery 13:504–512
2. Aldrich F (1990) Posterolateral microdiscectomy for cervical monoradiculopathy caused by posterolateral soft cervical disc sequestration. J Neurosurg 72:370–377
3. Korinth MC, Kruger A, Oertel MF, Gilsbach JM (2006) Posterior foraminotomy or anterior discectomy with polymethyl methacrylate interbody stabilization for cervical soft disc disease: results in 292 patients with monoradiculopathy. Spine 31:1207–1214

European Spine Journal (2019) 28 (Suppl 1):S3–S5
https://doi.org/10.1007/s00586-018-05864-4

OPEN OPERATING THEATRE (OOT)

Thoracoscopic technique of anterior discectomy and interbody fusion (ATIF)

Daniel Sauer[1,2] · Franziska C. Heider[1,2] · Christoph Mehren[1,2] · Christoph J. Siepe[1,2]

Keywords Thoracoscopy · Thoracic spine · Minimally invasive technique · Anterior discectomy · Interbody fusion · MIS surgery

Learning objectives

To describe the technique of anterior discectomy and interbody fusion (ATIF) in the thoracic spine performed via a transthoracic, thoracoscopic approach.

General information

The development of video assisted thoracoscopic surgeries (VATS) has opened the platform to perform an anterior stabilization and fusion of the thoracic spine in a minimally invasive fashion. The technique was developed in the early 1990s, and since then, thoracoscopic procedures have been used on an increasingly widespread scale.

In the beginning of the 1990s, Rosenthal and colleagues from Germany developed the thoracoscopic approaches for the treatment of various spinal pathologies [1]. Likewise, Mack et al. and Regan et al. established the technique of thoracoscopic spine surgery in the United States [2, 3].

As a result of further technical advancements, i.e. the Bozzini light conductor, the thoracoscopic technique has undergone a remarkable evolution since the introduction [4].

✉ Daniel Sauer
DSauer@Schoen-Kliniken.de

[1] Spine Center, Schön Clinic Munich Harlaching, Harlachinger Str. 51, 81547 Munich, Germany

[2] Academic Teaching Hospital and Spine Research Institute of the Paracelus Medical University (PMU), Salzburg, Austria

To date, thoracoscopic interventions have been established as a safe surgical technique in the spine surgeon's armamentarium, which serve to address a wide variety of indications and pathologies from degenerative disc disease to tumor and deformity surgery. Surgical procedures include anterior thoracic interbody fusion (ATIF), (hemi-) corpectomy, and vertebral body replacement, anterior discectomies of thoracic disc herniations or sympathectomies in selected cases.

At the same time, thoracoscopic surgeries follow the principles of minimally invasive, MIS-surgery, with significantly reduced access trauma in comparison to classic open techniques.

Case description/patient history with imaging

The patient is a 65-year old female with adjacent segment degeneration and concomitant spinal stenosis with severe compression of the neural structures at the level T12/L1 following previous fusion of L1 to the sacralized L5 vertebra.

An increasing kyphotic deformity at the thoracolumbar junction led to an additional stable T12 fracture, defined as type A3 according to the AO classification system [5].

Clinically, the patient presented with intractable back pain and signs of cauda equina compression syndrome. The neurological examination revealed an ataxia with broad-based gait, hypoesthesia in both legs and anterior thighs.

Based on the clinical and radiological findings, a combined posterior-anterior fusion procedure was indicated with an extension of the fusion from T10 to L5, including a microsurgical decompression of the neural structures at the affected level T12/L1.

Watch surgery online

In order to achieve a solid support of the anterior column, an additional ATIF was performed via a transthoracic, thoracoscopic approach.

Surgical strategy

The patient is fixed in a stable lateral position with a four-point support at the symphysis, sacrum, scapula and with additional arm-rest. Oxygenation is maintained via a single lung ventilation through a double-lumen intubation. In accordance with the patient's vascular anatomy of the aorta and the V. cava, the patient positioning and single lung ventilation was performed on the right, whilst the surgical approach was performed from the left side.

The preoperative localization of the target area is determined under image intensifier in both ap- and lateral projection. The 4 portals such as the main working portal, portal for light source, for retractor, and for the suction system are placed in a standardized fashion in relation to the main target area. A slightly wider, approx. 25 mm skin incision is chosen for the working portal in order to enable the transthoracic introduction of the implants, whilst an approx. 10 mm skin incision will suffice for the remaining portals and instruments. The surgical procedure routinely starts with the most cranial, intercostal approach and placement of the optical channel following deflation of the lung on the ipsilateral side.

The thoracoscope with its 30° optics is inserted at a shallow angle, aiming in the direction of the second trocar for the retractor system, which is placed on the contralateral side of the ipsilateral thoracic cavity. The transthoracic intercostal insertion of the remaining trocars is performed under direct visualization through the endoscope with an "inside-out" view.

The anterior circumference of the motion segment, the course of the spine as well as the aorta are palpated and identified with a blunt probe. After exposing the target area, two K-wires are inserted into the adjacent vertebral bodies under fluoroscopic guidance. The optimal position of the K-wire is in between the middle to the posterior third of the vertebral body in the lateral plane, in proximity to the disc space in order to avoid a laceration of the segmental vessels. The positioning of the K-wires will serve as landmarks for orientation in the due surgical course and will assist to create a "safety working zone" for the surgeon.

The pleura is detached, starting from posterior into an anterior direction, directly over the disc space T11/12 with the aid of monopolar cauterization. The annulus is incised, and a complete discectomy is performed with meticulous removal of the cartilage from the adjacent endplates. Following the insertion of trial implants, an adequately sized Mesh-Cage is inserted press-fit into the cavity of the disc space. Both cages as well as the remaining disc space are packed with allogenic bone graft substitute (calcium phosphate silicate). Fluoroscopic control confirms adequate implant positioning.

The due surgical course revealed that at the cranially adjacent segment T10/11 the aorta overlapped the access to the targeted disc space to a large extent and it was not possibly to achieve a sufficient mobilization in order to permit an adequate access to the disc space. Thus, an additional ATIF was not performed at this level.

After thorough irrigation of the thoracic cavity and removal of blood clots, the chest tube is inserted in the caudal recess. The instruments and portals are then removed, and the lung is fully re-inflated under visual control to confirm full ventilation and in order to prevent atelectasis and/or the development of effusions during the postoperative course.

The final steps of the surgery are completed with suturing of the subcutaneous tissue and skin closure.

Postoperative information

The patient is extubated after surgery and supervised on the ICU for 24 h. Following removal of the chest tube on the first postoperative day, the patient is mobilized and early pulmonary ventilation training is started.

Postoperative i.v. antibiotics (2nd generation cephalosporine) are administered for a 24-h period on a routine basis.

Fractionated heparin was administered for thromboembolic prophylaxis until full mobilization. A 4-point brace may be prescribed for a 6–12-week period for additional external support depending on the surgeon's preference.

At the first follow-up examination 4 weeks postoperatively, the patient presented in a satisfactory condition with adequate mobility, significant pain reduction (VAS 2) and signs of recovery of the preoperative neurological symptoms.

Discussion and conclusion

The minimally invasive, transthoracic, thoracoscopic surgery of thoracic and thoracolumbar pathologies bears a number of advantages in comparison to "classic" procedures such as open thoracotomies. Benefits include decreased postoperative pain, lesser disruption of the anatomy due to reduced access trauma, outstanding intraoperative visualization of the patient's anatomy, high patient safety due to highly standardized intraoperative surgical steps, reduced postoperative scar tissue, shorter hospitalization as well as immediate mobilization and enhanced recovery of the patients.

Complication rates associated with the thoracoscopic procedure are comparable or even reduced to those that have previously been published for open procedures, whilst maintaining the full range of benefits of MIS surgery [6–8].

Compliance with ethical standards

Conflict of interest The authors declare that they have no conflict of interest.

References

1. Rosenthal D, Rosenthal R, De Simone A (1994) Removal of a protruded thoracic disc using microsurgical endoscopy: a new technique. Spine 19:1087–1091. https://doi.org/10.1097/00007632-199405000-00018
2. Mack MJ, Regan JJ, Bobechko WP, Acuff TE (1993) Application of thoracoscopy for diseases of the spine. Ann Thorac Surg 56:736–738. https://doi.org/10.1016/0003-4975(93)90966-L
3. Regan JJ, Mack MJ, Picetti GD 3rd (1995) A technical report on video-assisted thoracoscopy in thoracic spinal surgery. Preliminary description. Spine (Phila Pa 1976) 20:831–837. https://doi.org/10.1097/00007632-199504000-00018
4. Bush RB, Leonhardt H, Bush VI, Landes RR (1974) Dr. Bozzini's Lichtleiter. A translation of his original article (1806). Urology 3:119–123
5. Vaccaro AR, Oner C, Kepler CK, Dvorak M, Schnake K, Bellabarba C, Reinhold M, Aarabi B, Kandziora F, Chapman J, Shanmuganathan R, Fehlings M, Vialle L (2013) AOSpine thoracolumbar spine injury classification system: Fracture description, neurological status, and key modifiers. Spine 38:2028–2037. https://doi.org/10.1097/BRS.0b013e3182a8a381
6. Sauer D, Heider F (2016) Minimally invasive thoracoscopic partial corpectomy of T12, followed by anterior stabilization and fusion through cage implantation with an anterior plate fixation. Eur Spine J. https://doi.org/10.1007/s00586-016-4466-8
7. Cheung KMC, Al Ghazi S (2008) Approach-related complications of open versus thoracoscopic anterior exposures of the thoracic spine. J Orthop Surg (Hong Kong) 16:343–347. https://doi.org/10.1177/230949900801600315
8. Sauer D, Heider F, D'Agostini Annes R, Haubitz I, Korge A, Mehren C, Mayer HM, Siepe CJ (2015) Incidence of complications and adverse events after video assisted thoracic surgeries (VATS): results of a systematic retrospective analysis of 282 patients. Presented at: annual meeting of the international society for the study of the Lumbar Spine (ISSLS). San Francisco, CA, USA

European Spine Journal (2019) 28 (Suppl 1):S6–S8
https://doi.org/10.1007/s00586-018-05865-3

OPEN OPERATING THEATRE (OOT)

Surgical correction in AIS

Cesare Faldini[1,2] · Fabrizio Perna[1,2] · Alberto Ruffilli[1,2] · Antonio Mazzotti[1,2] · Alessandro Panciera[1,2] · Francesco Traina[1,2,3]

Keywords Double rods · Pedicle screw · High density · Surgical technique · Scoliosis surgery

Learning objectives

- To explain the concept of three-dimensional deformity correction in adolescent idiopathic scoliosis
- To explain the Lenke Classification of AIS
- To explain effects of translation on frontal, sagittal and axial planes
- To explain how direct vertebral rotation works

Introduction

Adolescent idiopathic scoliosis (AIS) is a three-dimensional deformity with coronal, sagittal and axial impairment. These deformities lead to clinical manifestations that include: trunk imbalance, shoulder height difference, rib-hump and thoracic hypokyphosis. The Lenke classification has progressively gained popularity and it is now recognized as the most reliable and complete classification for AIS [1]. The purpose of the surgical treatment is to correct the deformity obtaining a stable balanced spine preserving mobile segments of the lumbar spine when possible with restoration of good clinical alignment on all three planes [2].

✉ Cesare Faldini
cesare.faldini@ior.it

1 IRCCS Istituto Ortopedico Rizzoli, Via Giulio Cesare Pupilli 1, 40136 Bologna, Italy

2 Department of Biomedical and Neuromotor Sciences, University of Bologna, 40123 Bologna, Italy

3 BIOMORF University of Messina, Messina, Italy

The aim of this paper is to schematically describe the concept of differently shaped rods translation and direct vertebral rotation for the surgical treatment of AIS.

Case description

We present two different cases of AIS as representative of the different techniques used for thoracic, such as Lenke type 1 and 2 curves and lumbar curves such as Lenke type 3 to 6.

Surgical strategy

The skin incision is made from one vertebra superiorly and one vertebra inferiorly to the planned fusion area, to allow the entire spine to be exposed. The facets and their articular process in the fusion area, except at the uppermost and the lowermost levels, are removed in order to facilitate the identification of the entry points, promote arthrodesis and allow an easier deformity correction.

Uniplanar pedicle screws are placed at each level on both sides of the curve using drill assisted technique. High-density system helps to distribute the applied forces during the translation and the direct vertebral rotation on more pedicles with lesser risks of screws pull-out or pedicle breakage. All screws should be placed with the same technique in an harmonic way according to the scoliotic curves [3]. The length of the rod is measured and each rod is bent using a rods bender according to the desired sagittal contour. In case of a main thoracic curve, the rod on the concave side is over-shaped, while the rod on the convex side is under-shaped. The apex of the main thoracic scoliotic curve and the apex of the desired thoracic kyphosis should be determined to achieve the desired rods shape.

Watch surgery online

Due to the different position of the desired thoracic kyphotic apex and the main rotated vertebrae at the scoliotic apex, the over-shaped rod on the concave side remains far distant in two parts including: the apex of the thoracic kyphosis and the zone of maximum rotation of the scoliotic curve; while the under-shaped rod on the convex side remains adjacent to the screw heads in the zone of maximum rotation and far distant from the screw heads on the apex of the thoracic kyphosis at the same level of the other rod on the concave side. At the desired kyphotic apex, both rods must be placed far from the screw heads with low height differences with the aim to restore height. On the contrary, at the apex of the scoliosis curve high height differences with low maximum height must be present in order to restore rotation. In this way while the force is applied to reduce the rod on the screws' head on the concave side, vertebral bodies rotate toward the concave side and vertebral rotation on the axial plane is achieved consequently.

In case of double curves at the level of thoracic and lumbar spine including Lenke 3 to 6 scoliosis curve types, the over-shaped rod is applied on the concave side of the thoracic curve, and on the convex side of the lumbar curve; while the under-shaped rod is applied on the convex side of the thoracic spine and concave side of the lumbar spine. The over-shaped rod on the concave thoracic side remains far distant in two parts including: the apex of the thoracic kyphosis and the zone of maximum rotation of the scoliotic curve, and adjacent to the zone of maximum rotation of the lumbar curve. Instead the under-shaped rod on the convex thoracic side remains adjacent to the screw heads in the zone of maximum rotation and far distant from the screw heads on the apex of the thoracic kyphosis and at the apex of the lumbar lordosis. In these cases, the aim should be to restore rotation at the lumbar level without lowering the lumbar lordosis.

For direct vertebral rotation, the neutral vertebrae are kept stable while the other vertebrae are rotated in a clockwise direction applying a downward and lateral force on the convex side and lateral force on the concave side. This maneuver is a critical part of the correction and neurological monitoring should be performed continuously. When the desired axial correction is achieved, the crickets should be reduced completely in order to complete translation and tighten the rods to maintain the correction.

Postoperative information

For the first 6 weeks after surgery we use a brace to restrict spinal movements and allow initial bone graft fusion. The patient is able to leave the hospital 7 days after the surgery and he is then followed-up at 1, 3 and 6 months and then yearly.

Discussion and conclusion

Aim of this study was to present a corrective strategy using differently shaped rods translation and direct vertebral rotation for the two main different categories of AIS curves.

The rib hump deformity caused by the axial rotational of the vertebrae is an important element of AIS because it is strictly related to the patient's self-image. Several techniques such as translation and DVR have been proposed in order to avoid thoracoplasty procedure and its related complications such as prolonged surgical time, haemothorax and pleural effusion [4]. According to the recent literature, the derotation effect obtained using DVR technique only is between 37 and 63% [5, 6]. Clement et al. [7] first described the translation technique using high-density pedicle screws reporting good clinical and radiological results especially on the sagittal plane, however, they did not use differently shaped rods. We believe that the combination of the translation technique with differently shaped rods and DVR allow good three-dimensional correction of the deformity while reducing the risk of screw pullout at the time of DVR due to the wider distribution of forces on more pedicles and in separate surgical steps [2, 8]. In this paper and in its related video, a step-by-step procedure has been presented in order to explain surgical tricks for AIS deformity correction in different scoliosis curve types.

Compliance with ethical standards

Conflict of interest The authors declare no conflicts of interest.

References

1. Lenke LG, Betz RR, Harms J et al (2001) Adolescent Idiopathic Scoliosis: a new classification to determine extent of spinal arthrodesis. J Bone Joint Surg Am 83:1169–1181
2. Faldini C, Perna F, Borghi R et al (2017) Direct vertebral rotation and differently shaped dual rod translation technique in adolescent idiopathic scoliosis. J Biol Regul Homeost Agents 31:91–96
3. Perna F, Borghi R, Pilla F et al (2016) Pedicle screw insertion techniques: an update and review of the literature. Musculoskelet Surg 100:1–5. https://doi.org/10.1007/s12306-016-0438-8
4. Seki S, Kawaguchi Y, Nakano M et al (2016) Rod rotation and differential rod contouring followed by direct vertebral rotation for treatment of adolescent idiopathic scoliosis: effect on thoracic and thoracolumbar or lumbar curves assessed with intraoperative computed tomography. Spine J 16:365–371. https://doi.org/10.1016/j.spinee.2015.11.032

5. Rushton PRP, Grevitt MP (2014) Do vertebral derotation techniques offer better outcomes compared to traditional methods in the surgical treatment of adolescent idiopathic scoliosis? Eur Spine J 23:1166–1176. https://doi.org/10.1007/s00586-014-3242-x
6. Faldini C, Perna F, Chehrassan M et al (2016) Simultaneous double rod and en-bloc direct vertebral rotation technique for correction of main thoracic adolescent idiopathic scoliosis: retrospective analysis of 14 cases. J Biol Regul Homeost Agents 30:181–186
7. Clement J-L, Chau E, Geoffray A, Suisse G (2014) Restoration of thoracic kyphosis by simultaneous translation on two rods for adolescent idiopathic scoliosis. Eur Spine J Off Publ Eur Spine Soc Eur Spinal Deform Soc Eur Sect Cerv Spine Res Soc 23(Suppl 4):S438–445. https://doi.org/10.1007/s00586-014-3340-9
8. Faldini C, Chehrassan M, Borghi R et al (2017) Simultaneous dual-rod correction and direct vertebral rotation technique to correct double major adolescent idiopathic scoliosis curve. JAAOS—J Am Acad Orthop Surg 25:829. https://doi.org/10.5435/JAAOS-D-17-00723

Pfizer Limited: The Capital – A Wing 1802, 18th Floor, Plot No. C-70, G-Block, Bandra – Kurla Complex, Bandra (East), Mumbai - 400051.

For the use only of a Registered Medical Practitioner or a Hospital or a Laboratory.

PP-LYR-IND-0124 dated 30th Sept, 2019